



Durham E-Theses

The exact s-matrices of affine toda field theories

Dorey, Patrick Edward

How to cite:

Dorey, Patrick Edward (1990) *The exact s-matrices of affine toda field theories*, Durham theses, Durham University. Available at Durham E-Theses Online: <http://etheses.dur.ac.uk/6473/>

Use policy

The full-text may be used and/or reproduced, and given to third parties in any format or medium, without prior permission or charge, for personal research or study, educational, or not-for-profit purposes provided that:

- a full bibliographic reference is made to the original source
- a [link](#) is made to the metadata record in Durham E-Theses
- the full-text is not changed in any way

The full-text must not be sold in any format or medium without the formal permission of the copyright holders.

Please consult the [full Durham E-Theses policy](#) for further details.

THE EXACT S-MATRICES OF AFFINE TODA FIELD THEORIES

by

PATRICK EDWARD DOREY

A thesis presented for the degree
of Doctor of Philosophy at the
University of Durham

The copyright of this thesis rests with the author.
No quotation from it should be published without
his prior written consent and information derived
from it should be acknowledged.

Department of Mathematical Sciences
University of Durham
Durham DH1 3LE
England.

September 1990



25 JUN 1991

THE EXACT S-MATRICES OF AFFINE TODA FIELD THEORIES

by

PATRICK EDWARD DOREY

Ph.D. Thesis, 1990

Abstract

This thesis is concerned with exact solutions to various massive field theories in 1+1 dimensions.

Two approaches are described. The first, abstract and non-lagrangian, relies on the considerable understanding that there now is of massless two-dimensional field theories. A perturbative scheme can be developed within which various exact statements may be made. Chapter 1 contains a review of this technique, together with some work applying it in various simple situations. The particular structures studied turn out to have a deep connection with certain Lie algebras, a fact which is discussed in the concluding three sections of the chapter.

A complementary approach is to study specific, classically integrable, lagrangians in the hope that their quantum versions will also permit an exact treatment. Motivated to some extent by the findings of chapter 1, the remainder of the thesis is devoted to a particular class of models known as affine Toda field theories. A mixture of perturbative and non-perturbative ideas are employed. The non-perturbative elements are to be found in analytic S-matrix theory, reviewed in chapter 2, while various features of the classical theory necessary for a perturbative quantum treatment are derived in chapter 3. Making use of this information, chapter 4 proposes exact expressions for the S-matrices for a large subset of the Toda theories, which are then checked in perturbation theory.

Finally, the relevance or otherwise of the Toda S-matrices to the perturbations of massless theories studied in chapter 1 is discussed, and some possible directions for future work are mentioned.

Preface

This thesis is the result of work carried out in the Department of Mathematical Sciences at the University of Durham, between October 1987 and September 1990, under the supervision of Dr. E. Corrigan. No part of it has been previously submitted for any degree, either in this or any other university.

The motivation for the work in chapter 1 came from some papers by Zamolodchikov,^[1, 2] and much of the chapter is a review of his work. The computer algebra calculations and their possible interpretations in terms of W -algebras are original, although similar conclusions were reached by a number of other authors^[3-5] from a variety of starting points.

No claim of originality is made for the review in chapter 2, apart from the connection between S -matrix and conserved charge bootstraps described in the final section, which was included in an article in *Nuclear Physics B*.^[6]

Most of the remainder of the thesis is based on work carried out with Harry Braden, Ed Corrigan and Ryu Sasaki, which can be found in a number of joint papers,^[6-9] although sections 4.1 and 4.5 contain new material. Section 4.1, giving a detailed description of the conserved charges, is due solely to the author, as are the ideas of dualising and higher-pole bootstrap structure contained in section 4.5. However the explicit evaluations of higher pole residues mentioned in that section were carried out by Harry Braden, Ed Corrigan and Ryu Sasaki.

There has been much interest in the S -matrices of affine Toda field theories during the last year,^[10-16] and many results have been obtained by a number of groups, all working to a large extent independently. For this reason there seems to be little point in trying to give detailed credit for every feature to be mentioned below; this paragraph is intended to provide a general reference to all of this material. However one item should perhaps be mentioned separately, namely that the main result of section 4.1 was also noted by Klassen and Melzer, and is published in [14].

I would like to thank Ed Corrigan for all his help, and also Harry Braden and Ryu Sasaki for many interesting discussions during an enjoyable collaboration. In addition I would like to mention with thanks Robert Leese, Paul Fletcher, Hisham Zainuddin, Ian Strachan and Tim Hollowood. Financial support was provided by the Science and Engineering Research Council, whom I acknowledge and thank.

Contents

1. Perturbations of Conformal Field Theories	
1.1 Introduction: The Ising Model	1
1.2 The Renormalization Group	4
1.3 Conformal Field Theory	11
1.4 Perturbing a Conformal Field Theory	18
1.5 Implementing the Counting Argument	22
1.6 General Discussion of the Results	24
1.7 The Rôle of Lie Algebras	28
1.8 The Rôle of Extended Algebras	31
1.9 Discussion and Conclusions	36
2. Exact S-Matrices	
2.1 Introduction	39
2.2 Conserved Charges in 1+1 Dimensions	40
2.3 Factorization	41
2.4 General Properties of the Two-Particle S-Matrix	47
2.5 Purely Elastic S-Matrices and the Bootstrap	52
3. Classical Affine Toda Field Theory	
3.1 Introduction	60
3.2 The Classical Lagrangian	61
3.3 Classical Data for the Simply-Laced Theories	63
3.4 Folding and the Non Simply-Laced Cases	76
4. The Quantum Theory	
4.1 Conserved Charges in Affine Toda Theories	87
4.2 Fundamental S-Matrix Elements	95
4.3 Following Through the Bootstrap	104
4.4 Perturbative Checks of the Proposed S-Matrices	110
4.5 Higher Poles	121
5. Conclusions	142

Appendices

1	REDUCE Listings for Character Calculations	146
2	Block Structure of the $e_8^{(1)}$ S-Matrix	149
3	On-shell Diagrams for Scattering in the $e_8^{(1)}$ Theory	153

Tables

1	Perturbing fields and conserved charges	156
2	Perturbing fields and further conserved charges	159
3	Exponents of the simple Lie algebras	160
4	$g^{(1)} \times g^{(k)} / g^{(k+1)}$ cosets for which $c < 1$	161
5	Untwisted affine Dynkin diagrams	162
6	Twisted affine Dynkin diagrams	164
7	Assignments of masses to Dynkin diagrams	165
8	Cartan matrix eigenvectors	167
9	$e_6^{(1)}$ couplings and Clebsch-Gordon series	168
9a	$e_6^{(1)}$ minimal and full S-matrix elements	169
10	$e_7^{(1)}$ couplings and Clebsch-Gordon series	170
10a	$e_7^{(1)}$ minimal and full S-matrix elements	171
11	$e_8^{(1)}$ couplings and Clebsch-Gordon series	172
11a	$e_8^{(1)}$ minimal and full S-matrix elements	173

References	174
-----------------------------	-----

Chapter 1

Perturbations of Conformal Field Theories

1.1 Introduction: The Ising Model

The Ising model is a particularly simple statistical system, and yet it embodies most of the features that will be relevant in this chapter. Picture a square d -dimensional lattice, on each site of which sits a spin σ taking the values ± 1 ('up' or 'down'). The energy of a configuration $\{\sigma\}$ is given by

$$E(\{\sigma\}) = \sum_{\langle ij \rangle} \sigma_i \sigma_j, \quad (1.1)$$

the summation running over all pairs of nearest neighbour sites $\langle ij \rangle$. (The unit of energy is taken to be one.) A simple generalization with non-trivial consequences is to add a term representing an external magnetic field h , in which case the energy becomes

$$E(\{\sigma\}) = \sum_{\langle ij \rangle} \sigma_i \sigma_j + \sum_i h \sigma_i. \quad (1.2)$$

For the time being this possibility will be ignored, so that the model has a symmetry between spin up and spin down.

The aim is to study this classical system when in statistical equilibrium at some finite temperature T . The relative probabilities of the different configurations are then given by the Boltzmann distribution, and the partition function is simply

$$Z = \sum_{\{\sigma\}} e^{-E(\{\sigma\})/T}. \quad (1.3)$$

Configurations of higher energy are less likely to occur, this suppression becoming weaker as T is increased.

Physically, the Ising model is motivated as an attempt to understand various aspects of magnetism. Each spin variable is to be thought of as a microscopic magnet. The energy function, by penalizing any disagreement between neighbouring spins, captures

the tendency of these small magnets to line up, leading to overall magnetisation of the whole solid. For $d > 1$ this penalty is the dominant effect at low temperatures and the system is said to be in an ordered phase. Note that the magnetisation breaks the up-down symmetry in spin space – an example of spontaneous symmetry breaking.

As T is increased another factor comes into play, in that there are many more available states for the system if the spins do not all agree, and despite their individually smaller probability such configurations eventually come to dominate sums such as (1.3). The system is then in a disordered phase, up-down symmetry has been restored, and it has undergone a phase transition. This lack of long-range order is seen most clearly in the behaviour of correlation functions, which give the expectation values of measurements on the system in equilibrium (as averages over all possible states, weighted by the Boltzman distribution). For example, the correlation function of two Ising spins at sites a and b is

$$\langle \sigma_a \sigma_b \rangle = Z^{-1} \left(\sum_{\{\sigma\}} \sigma_a \sigma_b e^{-E(\{\sigma\})/T} \right). \quad (1.4)$$

For T large enough, an expansion of the exponential in $1/T$ (using the expression (1.1) for the energy) is appropriate.^[17] Each element in this expansion contains a product of terms $\sigma_i \sigma_j$ with i and j neighbouring sites, and so the element may be drawn as a collection of nearest-neighbour links on the lattice. (This representation of an element in the high-temperature expansion should not, of course, be confused with a possible configuration $\{\sigma\}$ of the model, although it is interesting to note that for $d = 2$ this ‘confusion’ forms the basis for the Krammers-Wannier duality of the 2-dimensional Ising model, relating the low and high temperature phases of the theory.^[18]) In the summation over all configurations, only products in which every spin appears to an even power contribute. Pictorially, this means that the links must form a chain between sites a and b (since the right hand side of (1.4) contains the product $\sigma_a \sigma_b$ outside the exponential), along with any number of closed loops. As each link carries with it a factor $1/T$, at high temperatures the most important term will have the smallest number of links possible, and so will be a chain of links connecting a and b by the shortest path. Hence (taking the lattice spacing to be 1 for now),

$$\begin{aligned} \langle \sigma_a \sigma_b \rangle &\approx T^{-|a-b|} Z^{-1} \left(\sum_{\{\sigma\}} \sigma_a (\sigma_a \sigma_i) \dots (\sigma_k \sigma_b) \sigma_b \right) \\ &= T^{-|a-b|} \end{aligned} \quad (1.5)$$

(where $\langle ai \rangle, \dots, \langle kb \rangle$ are all nearest neighbour pairs). So in the high temperature

phase the absence of long range order manifests itself in the exponential decay of correlation functions over distances of the order of $\zeta = (\ln T)^{-1}$. ζ is known as the correlation length, and measures the distance scale over which degrees of freedom are coupled. As T decreases ζ increases and the phase transition is approached, this time from above. Eventually the approximation of only considering the shortest path between a and b breaks down as the factors of $1/T$ become insufficient to overcome the combinatorial fact that many more paths of greater length may be drawn on the lattice. At some temperature $T = T_c$ (the critical temperature) ζ becomes infinite, signalling the transition to the phase discussed earlier, with long range order prevailing.

There are a number of lessons to be drawn from this admittedly crude treatment. The correlation length signals the appearance of a new (temperature-dependent) length scale in the system, in addition to the lattice spacing. If the lattice spacing is a in some physical units, this new scale is ζa . It is this length which governs the decay of correlation functions at large distances, and not the lattice spacing. When T is close to T_c the correlation length is very many times the lattice spacing, and on the scale of this length the fact that the spin variables live on a discrete lattice rather than at every point in space becomes unimportant. Given this, the correlation function defined by (1.5) looks very much like that of a continuum quantum field theory involving particles of mass $1/\zeta$. This should not be too surprising; the definition (1.4) of the correlation function is exactly what would be written for a lattice-regularized definition of a (Euclidean) functional integral, with the action given by the energy function (1.1).

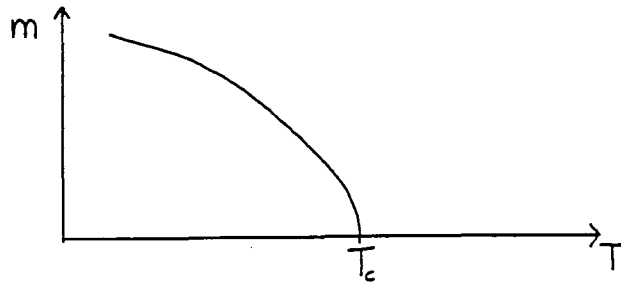
Some of the limitations of the particular high temperature expansion employed above are also clear: for example, if the correlation functions of the Ising model near T_c really are approximated by those of a suitable quantum field theory, then one would expect them to possess approximate rotational invariance, while the approximation involved in (1.5) preserves the special nature of the directions defined by the axes of the lattice. To see the way in which short-distance details such as the precise structure of the lattice are 'lost' as T approaches T_c requires a more sophisticated analysis, and the framework for this is provided by the renormalization group.

1.2 The Renormalization Group ⁽¹⁹⁻²⁴⁾

To generalize the discussion above, this section begins with a few definitions. The two phases of the Ising model were distinguished by the expectation value of the spin variable σ ; if $m = |\langle \sigma \rangle|$, then $m = 0$ in the high temperature (disordered) phase while $m \neq 0$ at low temperatures. The variable σ is called an order parameter. The possible behaviour of the order parameter actually at the transition temperature serves to divide phase transitions into two types. A transition is first order if the order parameter has a discontinuity there, while if the parameter (though not necessarily its derivatives) is a continuous function of T at T_c , then the transition is second order. This is known as Landau's classification.

Near the phase transition one phase is only marginally favoured over the other, so large patches of the 'wrong' phase will tend to persist. For second order transitions these large scale fluctuations come to dominate completely at criticality, and this is reflected in a divergence of the correlation length. First order transitions generally lead to a finite correlation length even at the transition, fluctuations never dominating completely. The classification according to the behaviour of the correlation length is the more directly relevant one in the study of critical phenomena.

Near a second order transition, a plot of the order parameter against T looks like



For T just below T_c , a power law behaviour is commonly found:

$$m \propto (T_c - T)^\beta.$$

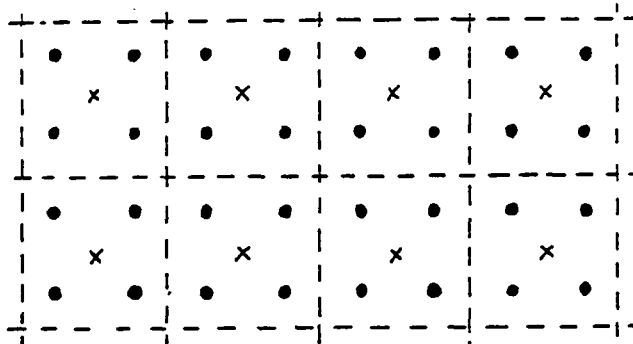
The number β , defined in the vicinity of a critical point, is an example of a critical exponent. While the precise value of T_c depends on the microscopic details of the model, that of β tends not to, being sensitive only to bulk features such as the dimensionality of the system or the symmetry properties of the order parameter. For example, the Ising model in two dimensions can be solved exactly for square or triangular lattices, and in

both cases β has the value $1/8$. This property is known as universality, and reflects the 'washing out' of short distance structure in the fluctuation-dominated regime.

It should be noted that $1/8$ is not an integer, and so the order parameter depends non-analytically on the temperature at the transition. Such behaviour is at first sight unexpected given the simple ('analytic') way in which T appears in expressions for expectation values such as (1.4). Indeed any perturbative treatment to finite order in T or $1/T$ will always give analytic results. The resolution of this puzzle is that the transition is occurring at precisely the point where perturbation methods, seeing only finitely many of the degrees of freedom, cease to apply. At the phase transition the correlation length has diverged, and infinitely many degrees of freedom are coupled together. Even near the phase transition, there are still so many degrees of freedom within one correlation length that an alternative to perturbation theory is needed.

Given the difficulty in these situations of evaluating expressions such as (1.3) or (1.4) directly, some progress might be made by performing the part of the summation involving short-distance degrees of freedom, leaving the longer distance modes for later. This idea, coupled with the observation that the residual summation will be of much the same form as the initial one, is the motivation for the transformations making up the renormalization group.

There are two stages to a renormalization group transformation. In real space, the first step is to 'lose' some short distance structure by the introduction of block variables. For example, on a square lattice form 2×2 blocks as shown:



To each block assign a single 'block spin', representing the net behaviour of all the spins in that block:

$$\sigma'(x') = \sigma_1(x_1) + \sigma_2(x_2) + \sigma_3(x_3) + \sigma_4(x_4)$$

(where $x' = \frac{1}{4}(x_1 + x_2 + x_3 + x_4)$).

Now the sum over all configurations can happen in two stages: first holding the block spins constant, and only then over the block spins. The final sum over the block spins is governed by an ‘effective’ probability distribution induced by that of the original spins. To preserve the form of the equations, this distribution can be written as the exponential of some new energy function, the effective Hamiltonian for the block spins. (It is convenient to treat the temperature as just another parameter in the Hamiltonian, and write $H = E/T$.) Thus

$$Z = \sum_{\{\sigma'\}} e^{-H'(\{\sigma'\})} \quad (1.6)$$

where

$$e^{-H'(\{\sigma'\})} = \sum_{\{\sigma\}} \prod_{\text{blocks}} \delta(\sigma'(x') - \sigma_1(x_1) - \sigma_2(x_2) - \sigma_3(x_3) - \sigma_4(x_4)) e^{-H(\{\sigma\})}. \quad (1.7)$$

Equation (1.6) looks much the same as (1.3), albeit with a modified Hamiltonian. However the lattice spacing has doubled, as the new lattice sites sit in the middle of each 2×2 block. The second stage of the renormalization group transformation consists of rescaling the x' coordinates, in this case by a factor of a half, to restore the lattice spacing to its original value. The whole process is illustrated below.



The new lattice model is equivalent to the old so long as there is no interest in features on scales smaller than the blocks. If the original Hamiltonian involved only short-range couplings, then the same is expected to be true of the new one. It may however contain new short-range couplings, generated by the transformation. It is important to note that, due to the rescaling, this new Hamiltonian has a correlation length half that of the old – a reflection of the work that has been done in evaluating part of the configuration sum.

In momentum space things work in much the same way, the highest momentum modes are summed over, and then a rescaling is performed to restore the momentum cutoff to its original value.

The above can be formalized by considering the space of all possible short-range Hamiltonians defined on the lattice. This is an infinite-dimensional space, spanned by coupling constants for all the (local) interaction terms that can be defined between the basic fields. Thus the point $(\lambda_1, \lambda_2, \dots)$ would label the Hamiltonian

$$H^{\lambda_1 \lambda_2 \dots} = \lambda_1 \sum_i \psi_i^{(1)} + \lambda_2 \sum_i \psi_i^{(2)} + \dots \quad (1.8)$$

where the summations run over all lattice sites, and $\psi_i^{(\alpha)}$ is a possible local interaction term, depending only on the lattice variables in the immediate vicinity of the point i and corresponding to a (perhaps composite) local field in continuum field theory. The term $\sum \psi^{(\alpha)}$ is conjugate to the variable λ_α . As an example, the Hamiltonian for the Ising model of (1.2) and (1.3) would be written as

$$H(\{\sigma\}) = E(\{\sigma\})/T = H^{\frac{1}{T}, \frac{h}{T}, 0, \dots}(\{\sigma\})$$

with

$$\psi_i^{(1)} = \frac{1}{2} \sum_j' \sigma_i \sigma_j, \quad \psi_i^{(2)} = \sigma_i. \quad (1.9)$$

($\psi_i^{(1)}$ is usually written ϵ_i ; the sum over j is restricted to lattice sites adjacent to i .)

It is sufficient to restrict attention to a finite-dimensional submanifold so long as it is large enough to include the interaction terms generated by transformations of the initial Hamiltonian. In this space, the renormalization group transformation acts as a nonlinear operator R :

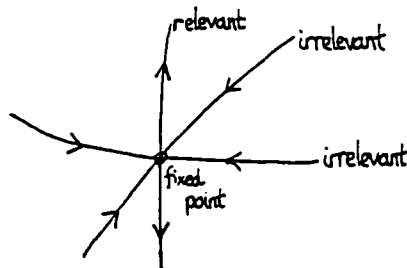
$$H' = R(H) \quad (\text{with } \zeta' = \zeta/2) \quad (1.10)$$

The transformation can be iterated, yielding a succession of equivalent Hamiltonians, $H^{(n+1)} = R(H^{(n)})$ where $H^{(0)} = H$. (To keep expectation values finite under repeated iterations, it may be necessary to add a rescaling of fields into the definition of R .) It is convenient to assume that an infinitesimal transformation T can be defined such that $R(H) = (e^T)H$. T will then generate a flow in the space of possible Hamiltonians, called the renormalization group flow. A line of equivalent Hamiltonians, generated from a given initial system, is called a renormalization group trajectory. Since each renormalization group transformation involves a rescaling of distances, moving further down the line corresponds to viewing the system at a larger scale.

Extra structure can be given to the space of possible Hamiltonians by drawing the surfaces S_ζ of constant correlation length ζ . A system at a second order transition will correspond to a point on S_∞ , the critical surface. From (1.10) it is clear that a trajectory starting on S_∞ will remain on that surface, while other trajectories cut through surfaces with successively lower ζ values.

An important concept is that of a fixed point. This is a Hamiltonian H such that $R(H) = H$, or equivalently $T(H) = 0$, and it must lie on S_0 or S_∞ . The main interest is in fixed points which lie on S_∞ , as these turn out to classify the possible types of critical behaviour. The reason for this is easily seen, given the assumption, well-supported in practice, that all trajectories ultimately converge to a fixed point (this rules out the existence of limiting cycles). Thus a suitable number of renormalization group transformations will bring any critical system into the vicinity of a fixed point. Conversely, a 'basin of attraction' on the critical surface can be associated to each fixed point, consisting of all systems whose renormalization group trajectories tend to that point. All systems in a given basin exhibit the same critical behaviour, and are said to lie in the same universality class. This 'topological' picture provides an appealing explanation of universality in general.

Near the fixed point, the renormalization group transformation may be linearized, and local axes defined by diagonalizing the transformation matrix. These axes define the scaling variables which, near the fixed point, simply change in scale under a group transformation. If the transformation involves a dilation s in the unit of length, then the scaling variable is multiplied by a factor s^y for some number y , called the anomalous dimension of that variable. An important distinction can be made according to the sign of the anomalous dimension: if positive, then renormalization group transformations will magnify the corresponding variable, and that variable is called relevant; if negative then small variations are made smaller and the variable is irrelevant. This is illustrated below.



As an aside, note that these ideas can explain the way in which details such as the direction of the lattice axes are lost near criticality at large distances – the variables encoding such effects turn out to be irrelevant.

There are generally finitely many relevant variables associated with a given fixed point – they correspond to unstable directions with respect to the renormalization group flow near that point, and must be fine-tuned to zero if the critical behaviour associated to that fixed point is to be observed. Such ideas will be important later.

For each scaling variable there is a conjugate local field with a well-defined scaling dimension (also called a scaling operator, borrowing language from quantum field theory). There is room for confusion in the terminology here, as the scaling variables are often called scaling fields in the statistical mechanics literature. Below, the word field will be reserved for objects corresponding to local fields in quantum field theory which are conjugate to the coupling constants. Anticipating the discussion of the continuum limit, it is convenient to replace the summations over lattice sites in (1.8) by integrals of local densities:

$$H^{\lambda_1 \lambda_2 \dots} = \int d^d \mathbf{x} (\lambda_1 O_1(\mathbf{x}) + \lambda_2 O_2(\mathbf{x}) + \dots) \quad (1.11)$$

where d is the dimensionality of the lattice. Changing the origin in parameter space if necessary so that the fixed point of interest is at $\lambda_1 = \lambda_2 = \dots = 0$, a dilation

$$\mathbf{x} \rightarrow \mathbf{x}' = \mathbf{x}/s$$

renormalizes both the scaling variable λ_α and its conjugate field $O_\alpha(\mathbf{x})$:

$$\lambda_\alpha \rightarrow \lambda'_\alpha = s^{y_\alpha} \lambda_\alpha$$

$$O_\alpha(\mathbf{x}) \rightarrow O'_\alpha(\mathbf{x}') = s^{x_\alpha} O_\alpha(\mathbf{x}).$$

Purely on dimensional grounds, x_α , the scaling dimension of the field O_α , is related to the already-defined y_α by $x_\alpha + y_\alpha = d$ (the Hamiltonian H defined by (1.11) must be dimensionless at the fixed point). Thus the relevant fields are those of scaling dimension less than d , the dimension of the lattice.

The scaling axes associated to a fixed point on the critical surface don't all lie in that surface – some will correspond to directions which take the system away from criticality. Since trajectories not starting on the critical surface all diverge away from it, any such axis is associated with a relevant scaling variable at the fixed point, the obvious example being temperature. (The external magnetic field in the Ising model, introduced in (1.2), is

another example and will be significant later.) The renormalization group trajectory for a system just off the critical surface will eventually be near a fixed point on S_0 , in a region where the correlation length is very small. Perturbation theory will be adequate in this region, and by running the renormalization group ‘backwards’, the critical exponents of the model may be deduced in terms of the anomalous dimensions of the scaling operators. There is no space to go into this here, but suffice it to say that very complete information on the critical behaviour of a system is provided once the relevant fixed point, scaling variables and anomalous dimensions are identified.

This section concludes with the idea of a continuum limit, already mentioned in passing following the discussion of the Ising model. Near the critical surface the correlation length is very large in lattice units, and furthermore it is this length rather than the lattice length which is governing the long-distance phenomena. Hence it makes sense to rescale so that distances are measured in the ‘physical’ units of the correlation length, so that the lattice spacing becomes a variable quantity, smaller the nearer the critical surface the system is. The limit of a series of models, all with the same ‘physical’ correlation length but getting nearer to the critical surface so that the lattice spacing is tending to zero, can now be taken. The hope is that this limit can be taken in such a way that correlation functions also have a finite limit, by suitably adjusting normalizations if necessary as the limit is taken. In field theory taking the lattice spacing to zero corresponds to removing the cutoff, and fiddling normalizations to ensure finite physical quantities to the renormalization of the bare quantities in the theory. The correlation functions obtained by such a limiting process will then be good approximations to the lattice correlators in a neighbourhood of the critical surface known as the scaling region. All of the universal physics is found here.

Keeping the physical correlation length finite as the lattice spacing tends to zero will result in a massive continuum theory. Alternatively the limit can be taken with a sequence of theories actually on the critical surface (so that the correlation length is infinite throughout), or in such a way that the physical correlation length diverges. (The latter case might also be thought of as studying the long-distance asymptotics of a massive continuum theory.) For such limits, renormalization must still happen to keep the correlation functions finite over physical distances, although of course the correlation length itself does become infinite. The exponential decay of some correlation functions is modified to a power-law, and the ‘physical’ distance scale of the correlation length disappears. Thus degrees of freedom in these theories can couple over long distances,

a fact which can be traced to the presence of massless particles in the spectrum of the theory – the mass gap is zero, the mass gap being the mass of the lightest particle in the spectrum. The simplest such theories correspond to taking the limit of theories on the critical surface at or towards a fixed point; these essentially have *only* massless degrees of freedom and in two dimensions are the conformal field theories to be discussed in the next section. However it should be realized that continuum field theories do exist corresponding to parts of the critical surface which are not fixed points, these possessing both massive and massless degrees of freedom. Such theories will be briefly touched on in a later section when perturbations of conformal field theories corresponding to directions lying in the critical surface are mentioned.

1.3 Conformal Field Theory

The first step towards understanding critical phenomena in general is to study, and perhaps classify, the possible fixed points of the renormalization group in their continuum limits. The Hamiltonians of such theories will be scale invariant and hence involve only massless particles (*any* other particle in the theory would introduce a length scale via the reciprocal of its mass). Correlation functions will then be long-range; two-point functions will decay by a simple power law determined from dimensional considerations. Polyakov^[25] noticed that if the rescaling is allowed to depend on some local factor and invariance under this increased symmetry group is assumed, rather more can be deduced. One reason why such local rescalings should be good symmetries of the fixed point Hamiltonian is that the renormalization group transformation is essentially local in character. Hence a fixed point for the ‘global’ blocking transformations will also be a fixed point for more general transformations where the size (though not the shape) of a block varies with position. In the continuum this becomes invariance under local rescalings.

The group of such local rescalings (along with translations and rotations) is called the conformal group, and consists of all transformations which multiply the metric by a scale factor. In dimensions $d \geq 3$, the group is finite dimensional, but not for $d = 2$. It is useful to use complex coordinates z, \bar{z} where $z = x^1 + ix^2$. The metric is $ds^2 = dzd\bar{z}$, which transforms to

$$dz'd\bar{z}' = \left(\frac{\partial z'}{\partial z} dz + \frac{\partial z'}{\partial \bar{z}} d\bar{z} \right) \left(\frac{\partial \bar{z}'}{\partial z} dz + \frac{\partial \bar{z}'}{\partial \bar{z}} d\bar{z} \right).$$

This is a multiple of the old metric if

$$\frac{\partial z'}{\partial \bar{z}} = \frac{\partial \bar{z}'}{\partial z} = 0.$$

Hence at least locally any analytic function $z' = f(z)$ will do, and the conformal group in two dimensions is infinite dimensional. The global conformal transformations, regular on the complex plane together with the point at infinity, form the finite dimensional subgroup of Mobius transformations. The consequences of this symmetry group were worked out by Belavin, Polyakov and Zamolodchikov.^[26] The important feature is the very strong control over the field content of the theory that the infinite symmetry provides, reducing many calculations to group theory. The viewpoint is non-perturbative and non-lagrangian, as much as possible being deduced on general grounds. Many detailed introductions to these ideas are available,^[27-31] and the brief review below is included mainly to establish notation.

The theory is completely specified once all correlation functions

$$\langle O_1(x_1)O_2(x_2)\dots \rangle \quad (1.12)$$

are known. The local fields $O_\alpha(x)$ for each x belong to an infinite dimensional vector space \mathcal{A} , assumed to be complete in the sense that any state can be generated by the linear action of these operators acting at, for example, the origin. This implies the operator product expansion:

$$O_\alpha(x)O_\beta(0) = \sum_\gamma C_{\alpha\beta}^\gamma(x)O_\gamma(0). \quad (1.13)$$

Equations such as (1.13), and any other equalities involving operators and states, are always given meaning as holding within any correlation function (1.12), the expansion implied being convergent for x in some domain depending on the location of the other fields in that correlator. The numbers $C_{\alpha\beta}^\gamma(x)$ are the structure constants of the operator product algebra.

The set of fields includes certain basic operators $\phi_i(x)$ (the primary fields) which transform covariantly under conformal transformations $z \rightarrow z' = f(z)$, $\bar{z} \rightarrow \bar{z}' = \overline{f(z)}$ as

$$\phi_i(z, \bar{z}) \rightarrow (f'(z))^{\Delta_i} (\overline{f'(z)})^{\bar{\Delta}_i} \phi_i(z', \bar{z}'). \quad (1.14)$$

(Complex coordinates will be used from this point on.) The pair of real numbers $(\Delta_i, \bar{\Delta}_i)$

are called the left and right dimensions of ϕ_i . The scaling dimension of ϕ_i is $\Delta_i + \bar{\Delta}_i$, the spin $\Delta_i - \bar{\Delta}_i$.

There must be at least one further field in the theory, namely the energy-momentum tensor $T_{\mu\nu}$. Scale invariance implies that the trace of this tensor vanishes, so in the complex coordinates there are just two independent components, T_{zz} and $T_{\bar{z}\bar{z}}$. Conservation of T , $\partial^\mu T_{\mu\nu} = 0$, then implies that T_{zz} depends only on z , $T_{\bar{z}\bar{z}}$ only on \bar{z} , and they will be written as $T(z)$ and $\bar{T}(\bar{z})$ respectively. $T_{\mu\nu}$ should generate the conformal transformations (1.14), and this requirement fixes the singular part of the operator product expansion of T and \bar{T} with the primary fields:

$$T(z)\phi_i(z_1) = \frac{\Delta_i}{(z-z_1)^2}\phi_i(z_1) + \frac{1}{(z-z_1)}\partial_1\phi_i(z_1) + \phi_i^{(-2)}(z_1) + (z-z_1)\phi_i^{(-3)}(z_1) + \dots \quad (1.15)$$

(A similar, ‘barred’, equation holds for \bar{T} .) The non-singular terms in the expansion are new fields which must also be in \mathcal{A} , by completeness. Operators L_{-n} , acting in \mathcal{A} , can be defined which generate these fields from the primary field ϕ_i :

$$\phi_i^{(-n)}(z_1) = L_{-n}(z_1)\phi_i(z_1).$$

In fact, within correlation functions

$$L_{-n}(z_1)\phi_i(z_1) = \frac{1}{2\pi i} \oint_{z_1} d\zeta (\zeta - z_1)^{n+1} T(\zeta)\phi_i(z_1), \quad (1.16)$$

the contour of integration surrounding only the point z_1 . From (1.15) it also follows that

$$\begin{aligned} L_n(z_1)\phi_i(z_1) &= 0 \quad (n \geq 1) \\ L_0(z_1)\phi_i(z_1) &= \Delta_i\phi_i(z_1) \\ L_{-1}(z_1)\phi_i(z_1) &= \partial_1\phi_i(z_1). \end{aligned}$$

Analogous operators \bar{L}_n can be defined from \bar{T} , corresponding to the transformations of the \bar{z} coordinate. Note, the L_0 and \bar{L}_0 eigenvalues are the left and right scaling dimensions.

Further operator product expansions with T and \bar{T} generate a whole family of further fields, known as the descendants of ϕ_i :

$$\phi_i^{(-n_1 \dots -n_N, -\bar{n}_1 \dots -\bar{n}_M)} = L_{-n_1} \dots L_{-n_N} \bar{L}_{-\bar{n}_1} \dots \bar{L}_{-\bar{n}_M} \phi_i .$$

(Descendant fields involving just L_{-n} will be called left descendants; those involving just \bar{L}_{-m} right descendants.) All have well-defined left and right dimensions:

$$\begin{aligned} L_0 \phi_i^{(-n_1 \dots -n_N, -\bar{n}_1 \dots -\bar{n}_M)} &= (\Delta_i + \Sigma n_i) \phi_i^{(-n_1 \dots -n_N, -\bar{n}_1 \dots -\bar{n}_M)} \\ \bar{L}_0 \phi_i^{(-n_1 \dots -n_N, -\bar{n}_1 \dots -\bar{n}_M)} &= (\bar{\Delta}_i + \Sigma \bar{n}_i) \phi_i^{(-n_1 \dots -n_N, -\bar{n}_1 \dots -\bar{n}_M)} , \end{aligned}$$

but no longer transform simply under more general conformal transformations. The set consisting of the primary field ϕ_i together with all of its descendants is called the conformal family of ϕ_i , and will be written $[\phi_i]$. All fields in the theory are either primary or descend from a primary field, so

$$\mathcal{A} = \bigoplus_i [\phi_i] .$$

Since T and \bar{T} , or equivalently $\{L_n\}$ and $\{\bar{L}_n\}$, generate the conformal transformations in the quantum theory, each conformal family forms a representation of the group of such transformations. In fact there is an anomaly, owing to the fact that T and \bar{T} are not themselves primary. However this is completely controlled once the commutation relations of the L and \bar{L} operators are known. These follow from the operator product expansions between the components of $T_{\mu\nu}$:

$$T(z)T(z_1) = \frac{c/2}{(z-z_1)^4} + \frac{2}{(z-z_1)^2}T(z_1) + \frac{1}{z-z_1}\partial_1 T(z_1) + \dots ,$$

a similar expression holding for $\bar{T}\bar{T}$, while $T\bar{T}$ is regular. Note the extra term proportional to c , compared to the operator product expansion (1.15) of $T(z)$ with a primary field. This, the most general possible additional singular term, is responsible for the anomaly. The real number c is called the central charge, and is a characteristic of the theory under consideration. The regularity of $T\bar{T}$ means that $[L, \bar{L}] = 0$, while manipulation of contour integrals shows that

$$[L_n, L_m] = (n-m)L_{n-m} + \frac{c}{12}n(n^2-1)\delta_{n,-m}$$

and similarly for \bar{L} . There are thus two mutually commuting copies of this, the Virasoro algebra, at work in the theory (one for T and one for \bar{T}), and the conformal family can

be considered as the direct product

$$[\phi_i] = \Phi_i \otimes \bar{\Phi}_i$$

of left and right representations, Φ_i being the space of left descendants of ϕ_i , $\bar{\Phi}_i$ the space of right descendants. The fact that the left and right algebras commute means that they can be treated to a large extent independently, and it is frequently possible to ignore the right algebra temporarily, so long as it is remembered to restore the \bar{z} -dependence at the end of a calculation. Hence the term ‘conformal family’ will often be used for the space Φ of left descendants alone; it should be clear from the context when this meaning is intended.

The identity operator I is the unique primary field of dimensions $(0, 0)$, and its conformal family will be written as

$$[I] = \Lambda \otimes \bar{\Lambda} .$$

Since $T = L_{-2}I$ and $\bar{T} = \bar{L}_{-2}I$, it follows that $T \in \Lambda$ and $\bar{T} \in \bar{\Lambda}$. It has already been remarked that $T_{\mu\nu}$ is a conserved current; in fact the other fields in Λ and $\bar{\Lambda}$ give rise to infinitely many further conserved currents, as will now be explained. Only the space Λ will be addressed, the discussion being identical for $\bar{\Lambda}$.

The first point to note is that translational invariance of the vacuum, $L_{-1}I = \bar{L}_{-1}I = 0$, together with the fact that $[L, \bar{L}] = 0$, means that $\bar{L}_{-1}\Lambda = 0$, or in other words that for any field $S \in \Lambda$, $\bar{\partial}S = 0$. (For this reason Λ is often called the space of holomorphic fields.) Now consider a general current, a one-form which in complex coordinates can be written

$$J(z, \bar{z}) = \alpha(z, \bar{z})dz + \beta(z, \bar{z})d\bar{z}.$$

Conservation of J , $dJ = 0$ (in components, $\partial^\mu J_\mu = 0$) becomes

$$\bar{\partial}\alpha = \partial\beta .$$

(Recall $d(\alpha dz) = (d\alpha)dz = (\partial\alpha dz + \bar{\partial}\alpha d\bar{z})dz = -(\bar{\partial}\alpha)dzd\bar{z}$.) Hence if $\bar{\partial}S = 0$, then the one-form $S(z)dz$ will by itself be conserved, and there is hence a conserved current for every field in Λ . Conserved currents should give conserved charges as their integrals over spacelike hypersurfaces. When developing an operator formulation of (Euclidean)

conformal field theories, it is most convenient to adopt a radial quantization scheme^[32] in which the infinite past corresponds to some finite position, for example the origin, and Euclidean time flows outwards from that point. In such a situation a spacelike hypersurface is just a contour enclosing the origin, and charges can be defined as

$$Q_f = \oint_0 dz f(z)S(z)$$

for any analytic f , conserved in that they are independent of the hypersurface, or contour, used to define them. For these purely holomorphic currents, this independence is just a consequence of Cauchy's theorem. The Virasoro generators (1.16) are the first set of such operators; there are many more, though all may be expressed as sums of products of the Virasoro generators. In the next section it will be shown that some of the 'zero-mode' ($f = 1$) charges survive for certain perturbations. These charges are

$$Q = \oint_0 dz S(z), \quad (1.17)$$

and if S has spin $s + 1$, the charge has spin s . (To call $S(z)dz$ a one-form is therefore slightly questionable, as the integral of a one-form ought to be a scalar, but the meaning intended should be clear.) Geometrically, that Q has spin s is easily seen, but it is helpful to see this from another point of view. The spin s of the operator Q is defined by

$$[M, Q] = sQ,$$

where M is the generator of Euclidean rotations, $M = L_0 - \bar{L}_0$. Since S in (1.17) is holomorphic, \bar{L}_0 plays no part and, recalling that $L_0(0) = 1/2\pi i \oint dw wT(w)$, the commutator is

$$\begin{aligned} \frac{1}{2\pi i} \left(\oint_0 dz \oint_{|w|>|z|} dw - \oint_0 dz \oint_{|w|<|z|} dw \right) wT(w)S(z) &= \frac{1}{2\pi i} \oint_0 dz \oint_z dw wT(w)S(z) \\ &= \oint_0 dz \frac{1}{2\pi i} \oint_z dw (w - z + z)T(w)S(z) \\ &= \oint_0 dz (L_0(z) - zL_{-1}(z))S(z) \\ &= \oint_0 dz (s + 1 - 1)S(z) = sQ, \end{aligned}$$

as required. (The relations $L_0(z)S(z) = (s + 1)S(z)$, $L_{-1}(z)S(z) = \partial S(z)$, true even for

non-primary S of dimensions $(s + 1, 0)$, were used.)

All the holomorphic fields so far considered owe their existence to the spin two field $T(z)$, and are descendants of the identity operator. The possibility of there being further holomorphic fields was initially investigated by Zamolodchikov,^[33] and will be very briefly described in the remainder of this section. When such fields are present, the idea of a descendant can be extended to encompass terms generated in operator product expansions with the extra holomorphic field, and the resulting conformal families are rather larger, containing a number of Virasoro families. With respect to the enlarged symmetry algebra of these models, there are correspondingly fewer primary fields. The simplest possibility is for there to be a field with dimensions $(1, 0)$, a holomorphic current. This extends the Virasoro symmetry to that of a Kac-Moody algebra, and the resulting theories have been much studied.^[34] Beyond this, and more relevant for subsequent sections, there are also models with holomorphic fields of spins higher than two, with symmetries described by the so-called W -algebras. These turn out to be associated with certain types of coset^[35] conformal theories, namely those of the form $g^{(1)} \times g^{(k)}/g^{(k+1)}$. Only the cases with g simply-laced will be needed below. If g has rank r , and (dual) Coxeter number h , then the central charge of such a theory is

$$c = r \left(1 - \frac{h(h+1)}{(k+h)(k+h+1)} \right).$$

Furthermore, for these models, there is a formula for the conformal dimensions of the primary fields with respect to the W -algebra.^[36] They are labelled by a pair of representations of g , with weights \mathbf{p} and \mathbf{q} , say, of levels less than or equal to k and $k+1$ respectively. The dimension of the corresponding field is then

$$\Delta_{\mathbf{p}\mathbf{q}} = \frac{((k+h+1)\mathbf{p} - (k+h)\mathbf{q}, (k+h+1)\mathbf{p} - (k+h)\mathbf{q} + 2\delta)}{(k+h)(k+h+1)}. \quad (1.18)$$

The scalar product is in the metric provided by the inverse Cartan matrix, and δ is the sum of the fundamental weights. For more details the original papers should be consulted; this formula is reproduced here mainly because it will be needed below.

Whatever the extended algebra happens to be, group theory alone allows correlators containing descendant fields to be evaluated in terms of those of primary fields alone. A theory is said to be minimal if it possesses only finitely many primary fields with respect to the possibly enlarged symmetry algebra. For such a model, exact expressions may be

obtained for the primary field correlators, and the theory can thus be completely solved. In particular, the operator product expansion coefficients appearing in (1.13) can be found, and ‘fusion rules’ obtained giving the conformal families which appear on the right-hand side of the expansion for any given pair of families on the left. The coset theories described above are all minimal in this sense. The simplest cases, with $g = a_1$, have no additional symmetries over Virasoro and only finitely many Virasoro-primary fields, and were studied in the initial paper of Belavin, Polyakov and Zamolodchikov.^[26] While attention below will first be concentrated on such models, it will become clear that larger algebras must also be considered in order to understand certain features that emerge from their study.

1.4 Perturbing a Conformal Field Theory

Equipped with a rather complete understanding of at least some of the fixed points of the renormalization group in two dimensions, it is natural to explore their immediate vicinity. For the study of critical phenomena this is important as an understanding of the positions of these fixed points, their basins of attraction and the renormalization group flows between them is required. In general these ‘non-conformal’ field theories are much harder to treat, as the integrable structure described above will be lost as soon as the fixed point is left. However Zamolodchikov^[1] pointed out that there are some directions away from a fixed point for which at least some of the integrals of motion survive, making the resulting theories much more tractable. The aim of this section is to describe his reasoning, together with a few of its implications.

A first point to note is that all the work below is done in the context of continuum field theory. Thus the continuum limits of lattice models are being described, and the results are only directly relevant to lattice models in the scaling region near to the critical surface.

Consider a particular fixed point, corresponding to a conformal field theory with Hamiltonian H_{cft} , say. The explicit form of this Hamiltonian will not be needed. A nearby point will have a Hamiltonian $H_{cft} + \lambda H_1$, where λ is small and λH_1 can be thought of as a perturbation of the original Hamiltonian. In particular the perturbation might be by one of the scaling fields, in which case

$$H_{pert} = H_{cft} + \lambda \int \phi(z, \bar{z}) d^2 z \quad (1.19)$$

where ϕ is a field with dimensions (h, h) . The coupling constant λ is one of the scaling

variables for the fixed point, and has dimensions $(1 - h, 1 - h)$. For the perturbation to influence the long-distance physics, it should be relevant and so $h < 1$. Note, this is consistent with the discussion in the section on the renormalization group, as the scaling dimension of ϕ is $2h$, and the dimensionality of space is 2, so the earlier criterion for relevance is just $2h < 2$. The ultraviolet limit of this new theory is the original conformal theory – short-distance physics is not affected by such a perturbation – and so the fields in the theory may be classified, via their short-distance behaviour, into the same conformal families as for the unperturbed model. In field theoretic language a relevant perturbation is super-renormalizable, requiring only a finite number of counterterms to remove divergences, and so it does not change the structure of the space of fields.

This observation is the basis of the counting argument used by Zamolodchikov to establish the persistence of some integrals of motion, for certain perturbations.

As described in the last section, the integrals of motion for the conformal theory are obtained as line integrals of the purely holomorphic or purely antiholomorphic fields. Assuming reflection symmetry, no new information comes from the antiholomorphic fields, so only holomorphic fields (independent of \bar{z}) will be discussed below. These fields are conserved currents, and the line integrals simply generate the corresponding conserved charges, acting as operators in the space of states. The algebra of these operators (the chiral algebra), by virtue of the conformal symmetry of the theory, always contains the Virasoro algebra, but it may well be larger. This fact will be important later, though for the time being it will be ignored.

Once the conformal symmetry is broken, the holomorphic fields will usually pick up some dependence on \bar{z} , and so the line integral (1.17) will depend on the contour chosen – the charge is no longer conserved. However there is no reason why a conserved current in the perturbed model, thought of as a one-form, should only contain the dz component. In other words, if the conserved one-form in the original theory was $S(z, \bar{z})dz$ with $\bar{\partial}S = 0$, this may survive the perturbation as $S(z, \bar{z})dz + A(z, \bar{z})d\bar{z}$, with $\bar{\partial}S = \partial A$. In such a case, the combined integral $\int Sdz + Ad\bar{z}$ is independent of the contour and one can say that the conserved charge remains in the perturbed theory.

Some more notations are needed for the details of Zamolodchikov's argument. Let Λ be the space spanned by the holomorphic fields in the conformal field theory, that is all the left descendants of the identity operator with respect to the chiral algebra. Then Λ can be decomposed by the spin s which, given that all fields in Λ are independent of \bar{z} , is

the same as splitting it into eigenspaces of L_0 :

$$\Lambda = \bigoplus_{s=0}^{\infty} \Lambda_s$$

where

$$L_0 \Lambda_s = s \Lambda_s \quad ; \quad \bar{L}_0 \Lambda_s = 0.$$

The charges obtained from elements of Λ will not be linearly independent, as some of the fields are total derivatives. To account for this, these derivatives are divided out yielding the factor space $\hat{\Lambda} = \Lambda / L_{-1} \Lambda$, also decomposable by spin:

$$\hat{\Lambda} = \bigoplus_{s=0}^{\infty} \hat{\Lambda}_s \quad ; \quad L_0 \hat{\Lambda}_s = s \hat{\Lambda}_s. \quad (1.20)$$

Now let S_s be some field in Λ_s . In the perturbed theory, $\bar{\partial} S_s \neq 0$. Instead,

$$\bar{\partial} S_s = \lambda R_{s-1}^{(1)} + \lambda^2 R_{s-1}^{(2)} + \dots \quad (1.21)$$

where $R_{s-1}^{(n)}$ are some other local fields in the theory, all belonging to the operator subalgebra generated by the perturbing field. If the right hand side of (1.21) is a total z -derivative, then the conserved current has survived the perturbation. It is possible in some cases to find the fields $R_{s-1}^{(n)}$ explicitly, but an indirect argument based on dimensions is quicker. The coupling constant λ has dimensions $(1-h, 1-h)$ while $\bar{\partial} S_s$ is $(s, 1)$ – all these dimensions being defined in terms of the short-distance scaling regime where the model looks like the original conformal theory. Hence $R_{s-1}^{(n)}$ has dimensions $(s-n(1-h), 1-n(1-h))$. In a unitary theory all dimensions are positive, so the first deduction is that the series (1.21) must terminate after a finite number of terms, $1-h$ being positive for a relevant perturbation. The classification of all possible scaling dimensions in the conformal theory allows rather more to be said. Unless

$$1 - n(1 - h) = \Delta \quad (1.22)$$

for some dimension Δ in the unperturbed theory, $R_{s-1}^{(n)}$ must vanish as there is no field of suitable dimension in the model. For $n = 1$, the perturbing field has the correct right-dimension and one of its descendants will then provide a candidate for $R_{s-1}^{(1)}$. If $n > 1$

then a solution Δ to (1.22) will be smaller than h , so the field ϕ_Δ will be more relevant than ϕ_h . Recalling that $R_{s-1}^{(n)}$ must belong to the subalgebra generated by ϕ_h , it is clear that if ϕ_h is the most relevant operator in some operator subalgebra then the only possible terms in (1.21) beyond the first order ($n = 1$) are descendants of the identity operator, for which $\Delta = 0$. In fact if there are other terms than these, counterterms have to be added to the Hamiltonian (1.19) proportional to the more relevant field ϕ_Δ , destroying the initial assumption of a single perturbing field. This unfortunate possibility will therefore be ignored, as for the time being will the chance of a solution to (1.22) for $n > 1$ and $\Delta = 0$. Hence the expansion (1.21) terminates after a single term:

$$\bar{\partial}S_s = \lambda R_{s-1}, \quad (1.23)$$

where R_{s-1} has dimensions $(h + s - 1, h)$. A left descendant of ϕ will certainly fit the bill on dimensional grounds. However care must be taken before jumping to conclusions, as there may be further candidates for R_{s-1} . When considering minimal theories there are frequently other primary fields with scaling dimensions differing by integers from those of the perturbing field, which could equally well contribute to R_{s-1} for large enough s . This fact seems to be linked to the presence of chiral algebras larger than Virasoro, and will be discussed in more detail in a later section. For now it is enough to know that a more careful study shows that if the field S_s is a Virasoro descendant of the identity (rather than a descendant only in some extended algebra) then R_s must indeed be a left descendant of ϕ . This situation will be assumed to start with; for the next two sections, only the Virasoro algebra will be involved. The space of left (Virasoro) descendants of ϕ , Φ , may be decomposed in the same way as Λ :

$$\Phi = \bigoplus_{s=0}^{\infty} \Phi_s ; \quad L_0 \Phi_s = (h + s) \Phi_s, \quad \bar{L}_0 \Phi_s = h \Phi_s. \quad (1.24)$$

Matching dimensions shows that $R_{s-1} \in \Phi_{s-1}$. Hence $\bar{\partial}$ can be thought of as a linear operator

$$\bar{\partial} : \Lambda_s \rightarrow \Phi_{s-1}$$

or, after suitable restriction and projection,

$$\bar{\partial} : \hat{\Lambda}_s \rightarrow \hat{\Phi}_{s-1}, \quad (1.25)$$

where the factor space $\hat{\Phi} = \Phi/L_{-1}\Phi$ has been introduced. For a conserved current, R_{s-1}

must be a z -derivative and so must lie in $L_{-1}\Phi$ (recall that $L_{-1} = \partial$) and be zero after projection into $\hat{\Phi}$. In other words, for S_s to be part of a nontrivial conserved current in the perturbed theory it must lie in the kernel of the restricted projected mapping defined by (1.25), and conversely whenever this mapping does have a nonzero kernel the existence of a conserved current can be inferred with no further effort. The corresponding conserved charge will then have spin $s - 1$.

Since $\bar{\partial}$ is a linear mapping, the kernel will certainly be nonzero if the dimension of the space on the left hand side of (1.25) is greater than that of the space on the right (this is Zamolodchikov's counting argument). For the minimal conformal theories, these dimensions may be obtained from a simple character formula. The next section describes some work that was done to investigate the implications of this.

1.5 Implementing the Counting Argument

The field content of a conformal theory with central charge less than one is completely accounted for by finitely many representations of the left and right Virasoro algebras. Hence for these theories it is safe to apply Zamolodchikov's argument with the assumption that the chiral algebra consists of the Virasoro algebra alone – all the states of a given scaling dimension can be counted just by using the Virasoro characters. There may in fact be a larger algebra present in some Virasoro-minimal models, in which case some further conserved currents might exist. A signal of a larger algebra is a non-diagonal partition function, and it is important to realize that to specify a theory more is needed than just the central charge – the way in which left and right Virasoro representations are glued together to make up the field content must also be known. These issues can be ignored to start with. Furthermore, the counting argument only needs information on the spaces of left descendants of primary fields, and so only the left Virasoro algebra needs consideration. Proving the existence of conserved currents then reduces to a 'mathematical' question of comparing the degeneracies in various pieces of representations of this single algebra.

Unitary theories with $c < 1$ are labelled by an integer m , $m = 3, 4, \dots$, the m^{th} theory having central charge

$$c = 1 - \frac{6}{m(m+1)}.$$

For each value of m , the possible unitary representations are indexed by a pair of integers

a and b , $1 \leq a, b \leq m$, their highest weights having L_0 eigenvalues

$$h_{ab} = \frac{((m+1)a - mb)^2 - 1}{4m(m+1)}. \quad (1.26)$$

(Note that ab and $m - a, m + 1 - b$ in fact label the same representation.) This formula is just the $g = a_1$ case of (1.18), with $k = m - 2$.

The Virasoro character, encoding the number of descendant states at each level (*ie* spin) in the representation with highest weight h_{ab} , is defined as

$$\chi_{ab}(q) = \sum_{s=0}^{\infty} q^s \dim(\Phi_s^{ab})$$

where Φ^{ab} is the conformal family with highest weight h_{ab} , and Φ_s^{ab} is the spin s subspace, as in equation (1.24). The character χ_h is usually defined multiplied by an extra factor $q^{h-c/24}$ which gives it nice properties under modular transformations (and can be physically motivated by considering the conformal theory on a torus). Purely as a 'mathematical' device to count dimensions, though, the definition without this factor is more convenient. For the unitary representations, the characters are given by

$$\chi_{ab}(q) = q^{-h_{ab}} \prod_{l=1}^{\infty} (1 - q^l)^{-1} \sum_{k=-\infty}^{\infty} (q^{h_{2mk+a,b}} - q^{h_{2mk+a,-b}}). \quad (1.27)$$

The real interest is in the factor space $\Phi/L_{-1}\Phi$. The states 'removed' from Φ_s by this factoring are precisely the elements of $L_{-1}\Phi_{s-1}$, so the appropriate generating function for these dimensionalities is in fact

$$\hat{\chi}_h(q) = \sum_{s=0}^{\infty} q^s \dim(\hat{\Phi}_s) = (1 - q)\chi_h(q) \quad (1.28)$$

The chiral algebra is (for now) just Virasoro, so $\Lambda = \Phi^{11}$, the conformal family of the identity operator I . In this case alone, there is a slight modification to (1.28) as $L_{-1}I = 0$ and $\dim(\Phi_1^{11}) = 0$ even before going to the factor space. This is easily taken into account:

$$\hat{\chi}_0(q) = (1 - q)\chi_0(q) + q. \quad (1.29)$$

Armed with (1.28) and (1.29), (and a computer algebra program) it is now straightforward to search for conserved currents in various perturbations of minimal models. As

explained in the last section, the perturbing field ϕ_{ab} should be relevant ($h_{ab} < 1$), and furthermore it should be the most relevant field, at least in some subalgebra of the operator product algebra. This focuses attention on perturbations by the operators ϕ_{22} (the most relevant of all), ϕ_{13} , ϕ_{12} and ϕ_{21} .

Using REDUCE, the polynomials

$$\hat{\chi}_{ab}(q) - q^{-1}\hat{\chi}_0(q)$$

were evaluated up to order 35, for $m = 3 \dots 12$. Appendix 1 gives the relevant REDUCE programs. A term q^s appearing with a negative coefficient shows that the counting argument has ‘worked’, signalling the presence of a conserved quantity of spin s . The pattern found was that in all but two ‘exceptional’ cases any negative coefficients died out long before spins as high as 35 were encountered, so it is reasonably safe that nothing was missed by the limitation on the order. The fact that the counting argument fails to show conserved currents of high spin does not of course rule them out, the comparison of dimensions in (1.25) giving a sufficient but not necessary condition for $\bar{\delta}$ to have a nontrivial kernel.

For what it was worth, all possible perturbing fields, relevant and irrelevant, were considered. Table 1 records the outcome, showing only cases where signs of a conserved current of spin greater than one were discovered and ordering these cases by increasing dimension of the perturbing field. Note, for *any* perturbing field the resulting theory is translation invariant and so there will always be a conserved, spin one, charge corresponding to momentum – the hint of integrability lies in any further conserved charges beyond this.

1.6 General Discussion of the Results

To start with the relevant perturbations ($h_{ab} < 1$) will be addressed. The first point to note is that of all the possible relevant perturbations only those by ϕ_{13} , ϕ_{12} and ϕ_{21} show any sign of preserving some higher spin integrals of motion. Before proceeding further, a check should be made to ensure that even these are not destroyed by solutions to (1.22) with $n > 1$ and $\Delta = 0$. The condition for there to be a solution here is just that $1 - h$ should be an inverse integer; for the m^{th} minimal theory (1.26) gives that

$$1 - h_{13} = \frac{2}{m+1} \quad , \quad 1 - h_{12} = \frac{3(m+2)}{4(m+1)} \quad , \quad 1 - h_{21} = \frac{3(m-1)}{4m} .$$

Hence there is never any danger for ϕ_{12} , and for ϕ_{21} there is only potential for trouble when $m = 3$, for which case $\phi_{21} = \phi_{13}$. For ϕ_{13} , the condition (1.22) is met whenever m is odd, in such cases there being the possibility of a term of order $\lambda^{(m+1)/2}$ in (1.21). However as Zamolodchikov pointed out,^[1] this does not spoil the conclusions of the counting argument which (see the table) predicts conserved charges of spin 1, 3, 5 and 7 for the ϕ_{13} perturbation, at least for $m \geq 5$. (The one remaining case to worry about, $m = 3$, will receive a mention below.) The possible extra term, $\lambda^{(m+1)/2} R_{s-1}^{((m+1)/2)}$, must belong to Λ_{s-1} , $s-1$ being the spin of the potential conserved charge. The character formula (1.29) can be used to show that for $s-1 = 1, 3, 5, 7$, $\dim(\hat{\Lambda}_{s-1}) = 0$. Thus the extra term is a total z derivative and the conserved charge survives, although with an extra piece of order $\lambda^{(m+1)/2}$ over what might have been expected.

Finally to the case of the ϕ_{13} perturbation of the $m = 3$, $c = \frac{1}{2}$ model, for which the counting argument predicts a wealth of conserved charges (see table 1). This is a thermal perturbation of the Ising model described in the introductory section, or more precisely (given that the discussion has all along been in the context of continuum field theory) to taking the continuum limit of the theory (1.3) with zero external magnetic field but initially non-critical temperature. This is known to be a theory of a free massive Majorana fermion, and conserved charges of *all* odd spins can be explicitly constructed starting from fermion bilinears.^[1]

Beyond $m = 4$ the pattern of conserved charges predicted by the characters settles down, with spins 1, 5, 7, 11 for ϕ_{12} and ϕ_{21} , and 1, 3, 5, 7 for ϕ_{13} . This is not unexpected.^[1] The structure of a conformal family Φ is influenced by the presence of null states – descendant states which are ‘unexpectedly’ zero owing to a linear dependence between the descendant states at that level. For the unitary representations Φ^{ab} there are in fact two independent null states (*ie* neither occurs as a descendant of the other), found at levels ab and $(m-a)(m+1-b)$ (note that this reflects the degeneracy in labelling mentioned after (1.26)). These null states control the characters, $\dim(\Phi_s^{ab})$ being smaller than expected for all s larger than or equal to the level of the null state. Indeed, in (1.27) the product part gives the correct counting of states if *all* descendant states at each level are independent; the other factor corrects this for the influence of the null states. It is not too hard to check directly that the first two correction terms in (1.27) are q^{ab} and $q^{(m-a)(m+1-b)}$, consistent with the levels of the two independent null states. This is important as it means that χ_{ab}^m , the character χ_{ab} for the m^{th} theory, is independent of m up to order $(m-a)(m+1-b)$. For m larger than 4, all the predicted conserved

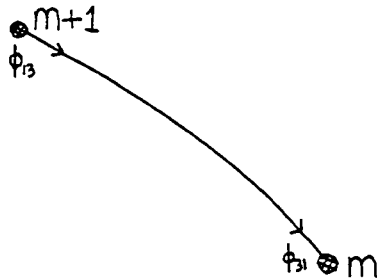
charges for the ϕ_{13} , ϕ_{12} and ϕ_{21} perturbations lie below this level and hence do not owe their existence to the particular value of m . (Note, this also explains why the patterns of spins for ϕ_{ab} and ϕ_{ba} perturbations often coincide, as the first correction term in the character formula is q^{ab} in both cases.)

The reader might now question the need for the REDUCE computations at all, apart perhaps from a single ‘universal’ calculation of the m -independent characters obtained by disregarding all but the first correction term in (1.27). To answer this a couple of points can be made. First, the extra degeneracy caused by the second null state increases the chance that the comparison of dimensions in (1.25) will be favourable, so it is possible that there are some extra successes of the counting argument lurking at or above the level of this state; indeed, this is what happens for $m = 3$ and $m = 4$ although not, as it turns out, for any higher values of m (at least up to $m = 12$, and the chances of anything happening get progressively smaller as m increases). Second, all possible perturbations were examined, and so the main, if somewhat negative, result of the computer investigation is that already mentioned at the beginning of this section – there are no signs of integrability in any relevant perturbations apart from those by ϕ_{13} , ϕ_{12} and ϕ_{21} .

The implications, if any, of the results in table 1 for irrelevant perturbations are unclear. The validity of the counting argument depends on the perturbation leaving the structure of the space of states unchanged, and this is certainly not true of an irrelevant perturbation which radically changes the short-distance properties of the theory (in contrast to a relevant perturbation which is felt in the behaviour of long-distance degrees of freedom). Perhaps the only ‘physical’ remark that can be made is that there may in fact be some sense in the idea that the ϕ_{31} perturbation has conserved charges of spins 1, 3, 5 and 7, and it is worth pausing briefly to explain why.

In his initial study of perturbations of conformal field theories,^[37] Zamolodchikov was able to show that, at least for large m , the ϕ_{13} perturbation of the m^{th} minimal theory with $\lambda > 0$ generates a renormalization group trajectory which terminates at the $(m - 1)^{\text{th}}$ theory. Thus the perturbed theory has ultraviolet and infrared asymptotics governed by two neighbouring minimal conformal field theories, while at intermediate scales there are also massive excitations in the model. The renormalization group flow stays on the critical surface joining two fixed points, and the continuum theory is an example of the non-conformal field theories with zero mass gap mentioned at the end of the discussion of the renormalization group. This picture is expected to hold true all the way down to $m = 4$. Zamolodchikov was also able to show that along this trajectory the operator ϕ_{13}

in the initial (short-distance) minimal model flows to the operator ϕ_{31} in the $(m - 1)^{th}$ minimal model lying at the far end of the trajectory. Thus in this case sense can possibly be made of the ϕ_{31} perturbation, though not from within a perturbative treatment based on the unperturbed model. Rather, the perturbed theory has a field structure different from the unperturbed model, being that of the minimal theory one place higher. An attempt to illustrate this idea is given below.



Hence the ϕ_{31} perturbation of the m^{th} model is expected to have the same set of conserved charges as the ϕ_{13} perturbation of the $(m+1)^{th}$ model, as the two perturbed theories are in fact identical. Thus conserved charges of spins 1, 3, 5 and 7 might indeed be found. However, there seems to be no direct link between this fact and the success of the counting argument. These successes are better explained, at least for $m \geq 5$, by the remark above that the pattern of spins for ϕ_{ab} and ϕ_{ba} perturbations often coincide, merely because their respective characters are equal up to a suitably high order – a ‘mathematical’ fact with no obvious physical import. For the record, the successes of the ϕ_{31} perturbation of the $m = 4$ model occurred at spins 1, 3, 5, 7^2 , 9, 11^2 , 13^2 , 15^2 , 17^3 , 19^4 , 21^2 , 23^4 , 25^4 , 27^2 , 29^2 and 31^2 (superscripts indicate spins for which the difference of dimensions was greater than one). The characters were evaluated up to order 45 here, without finding any more cases.

Little can be said about the ϕ_{15} and ϕ_{51} perturbations. Once there has been a success for $s = 5$ in the $m = 6$ theory, this must persist for the same reasons of character structure already described.

Finally returning to the relevant perturbations, it is worth stressing that a ‘failure’ of the counting argument at a certain spin does not forbid the existence of a conserved charge of that spin, and for high spins the characters behave in such a way that the counting is bound to be too crude to see any charges. Zamolodchikov⁽¹⁾ has conjectured the general pattern that the ϕ_{13} perturbation preserves conserved charges of all odd spins, while conserved charges with all spins having no common divisor with 6 survive the ϕ_{12} and ϕ_{21} perturbations. For small m this breaks down somewhat, as can be seen from

table 1. Some light is shed on the early discrepancies when the coset constructions^[35] of these theories are considered, together with the hints of extended algebras at work in them. This will be the subject of the next two sections.

1.7 The Rôle of Lie Algebras

As background to the considerations of this section, it is worth going back to Zamolodchikov's original motivations.^[2] While the Ising model with zero external field (1.1) has long been solved at arbitrary temperature, the exact evaluation of quantities in the large-lattice limit once an external magnetic field is introduced is a famous unsolved problem. The introduction of a magnetic field, even at $T = T_c$, shifts the Ising model away from the critical surface, so it has a finite correlation length in lattice units for any nonzero value of h in (1.2). A step towards solving the lattice problem would be to understand its continuum limit, in other words the massive field theory that results as a suitable limit of Ising models with smaller and smaller external magnetic fields, viewed at successively larger scales in lattice units. Such an understanding would give information on the long-distance properties of the lattice model when h is small. This is precisely the situation in which the techniques of perturbed conformal field theory described above should be useful. The $m = 3$, $c = \frac{1}{2}$ minimal model is the continuum limit of the Ising model at $T = T_c$, $h = 0$ and perturbing by ϕ_{13} and ϕ_{12} allows the neighbourhood of this fixed point to be explored. As touched on earlier, the ϕ_{13} perturbation corresponds to a shift in the temperature, the field ϕ_{13} being the continuum limit of the interaction term ϵ_i defined in (1.9) (for this reason ϕ_{13} is usually called the energy operator when $m = 3$, and written ϵ). The field ϕ_{12} corresponds to $\psi^{(2)}$ in (1.9), *ie* to the order parameter σ (indeed, $\phi_{12}(z, \bar{z})$ is usually written as $\sigma(z, \bar{z})$ here). Hence taking $\phi = \phi_{12}$ in (1.19) (with H_{cft} the $m = 3$ conformal field theory) should give the continuum limit of (1.2) at $T = T_c$. Note, from the point of view of the continuum field theory h in (1.2) is the 'bare' value of the magnetic field while λ in (1.19) corresponds to the renormalized or 'physical' quantity.

Continuum limits in which h and $T - T_c$ simultaneously tend to zero could also be taken; these correspond to perturbing the conformal theory with σ and ϵ simultaneously, so that (1.19) would have two perturbing terms on the right hand side. However signs of a nice integrable structure have only been seen in perturbations by a single scaling field, and the more general problem will not be discussed below.

A glance at table 1 shows that the magnetic perturbation of the Ising model might

indeed be integrable, the counting argument showing that there are conserved charges of spins 1, 7, 11, 13, 17 and 19. This is slightly fewer than would be expected from the general pattern for ϕ_{12} perturbations – the spin 5 charge is missing, an example of the ‘exceptional’ nature of the first few theories. Nevertheless Zamolodchikov conjectured that here also there is an infinite sequence of conserved charges only the first few members of which are spotted by the counting argument. Rather than having all spins that have no common divisor with 6, the simplest rule that fits the data of table 1 is that the spins should have no common divisor with 30.

Zamolodchikov went on to use this information to make a conjecture for the scattering theory of the Minkowski version of the massive perturbed theory. More information on these ideas will be given in subsequent chapters, but the relevant facts for now are that the theory comprised eight massive particles, their masses being related to the Cartan matrix of the rank eight Lie algebra E_8 . Add to this the facts that the proposed set of conserved spins makes up precisely the exponents* of E_8 repeated modulo 30 (the Coxeter number of E_8) and that the $c = \frac{1}{2}$ conformal field theory can be obtained from the coset $e_8^{(1)} \times e_8^{(1)} / e_8^{(2)}$, and there are strong hints of a deep connection between this perturbed theory and E_8 , though at the time there was no explanation for this.

Zamolodchikov also stated that similar hints of Lie algebra structure emerged from study of the ϕ_{12} perturbations of the $m = 4$ and $m = 6$ conformal field theories, involving the algebras E_7 and E_6 respectively. Table 4 (taken from [38]) lists a selection of coset constructions for $c < 1$ (for current purposes it seems to be cosets of the form $g^{(1)} \times g^{(k)} / g^{(k+1)}$ that are important, so only these are shown). Consider first the $m = 4$ theory. This does indeed have an e_7 coset construction, and table 1 shows that the ϕ_{12} perturbation has conserved charges of spins 1, 5, 7, 9, 11 and 13, consistent with the E_7 exponents shown in table 3.

There are a number of problems when going beyond this case. The $m = 6$ theory does have an e_6 coset construction, but the conserved charges found for the ϕ_{12} perturbation do not include spins 4 and 8, while these are exponents of E_6 . Similarly, one might expect to find evidence of A_2 in the ϕ_{12} -perturbed $m = 5$ model, given the $a_2^{(1)} \times a_2^{(1)} / a_2^{(2)}$ coset for the unperturbed theory shown in table 4. The A_2 exponents are 1, 2, 4, 5, 7, ... while the only spins seen in table 1 for this particular perturbed model are 1, 5, 7, 11. Thus spins 2, 4, ... are missing. One explanation might be that they were simply missed by the

* The exponents of the simple Lie algebras are listed in table 3. They are one less than the orders of the independent Casimir operators.

counting argument, but it is possible to show, using the explicit formula for the $\bar{\partial}$ operator to be given below, that there is for example no spin 3 descendant of the identity (as would give a conserved charge of spin 2) that remains conserved after the ϕ_{12} perturbation of the $m = 5$ model.

These two puzzles have related resolutions, and the A_2 case will be discussed first. One aspect of a more general understanding of the Lie algebra connection would be to understand why the particular perturbation ϕ_{12} should be important. As mentioned in the review of conformal field theory, a coset of the form $g^{(1)} \times g^{(k)} / g^{(k+1)}$ is thought to be associated with a particular extension of the Virasoro algebra, the W_g algebra, the primary fields with respect to this extended algebra being indexed by a pair of representations (p, q) of the Lie algebra, their conformal weights being given by (1.18). It is natural to ask how the perturbing field looks in terms of this alternative classification of fields provided by the extended algebra. The finding is that for $m = 3, 4$ and 6 , the pair of representations $(0, \text{adj})$ (of E_8, E_7 and E_6 respectively) corresponds to the primary field of conformal weight h_{12} , ie to ϕ_{12} . (Here 0 refers to the trivial representation, and adj to the adjoint.) Furthermore (1.18) used for $g = a_1$ (the ‘pure Virasoro’ case) with the same pair of representations gives the field ϕ_{13} , and the conjectured conserved spins for the ϕ_{13} perturbation of a minimal theory are the odd integers. The exponent of A_1 (1) repeated modulo the Coxeter number (2) gives precisely the odd integers. Now to return to A_2 . The formula (1.18) used with the pair of A_2 representations $(0, \text{adj})$ gives a conformal weight $h = \frac{2}{5}$, which is *not* the conformal weight of ϕ_{12} . Rather it is equal to h_{21} , and so a possible resolution of the A_2 puzzle is that the ‘correct’ perturbation to consider is not by ϕ_{12} at all, but by ϕ_{21} . This is the case, although there is one further subtlety. Table 1 shows that the ϕ_{21} perturbation also misses the spin 2 and spin 4 conserved charges. However earlier work by Zamolodchikov^[39] (before the study of the Ising model had given hints of Lie algebra structure) had been on exactly this perturbation of the $m = 5$ model. He discovered that in addition to the conserved charges sitting in the conformal family of the identity, there were charges which survived the ϕ_{21} perturbation in the extended algebra of the model, the W_{a_2} (or W_3) algebra generated by the spin 3 field ϕ_{15} . Explicitly exhibited were conserved charges of spins 2 and 4, exactly the spins missing from table 1.

Thus a tentative (though very natural-looking) hypothesis can be made that a Lie algebra structure – in particular, conserved charges at spins given by the relevant set of exponents – will emerge in the perturbation of any $g^1 \times g^{(k)} / g^{(k+1)}$ coset by the primary

field labelled by the pair of G representations $(0, \text{adj})$. Further support for this will come from the $m = 6$ theory, but rather than look at this directly the discussion will now be widened slightly to describe some work that was done to look at possible extended algebras in general.

1.8 The Rôle of Extended Algebras

Whenever there are holomorphic fields in a conformal field theory in addition to those provided by the Virasoro algebra acting on the identity, there are further candidates for conserved quantities when that theory is perturbed. There is also a need to be careful when drawing conclusions from comparisons of dimensions, as discussed in the paragraph following (1.23), arising from the presence of Virasoro primary fields with dimensions differing by integers. The reason for this is that the field content of the theory can now be arranged into representations of the higher algebra generated by the extra holomorphic fields. Within any given representation of this extended algebra there will usually be a number of Virasoro representations, one of which will be the primary field with respect to the full algebra, the others being descendants of this field. The scaling dimension of a descendant field, even with respect to an enlarged algebra, always differs by an integer from its primary, so these other Virasoro-primary fields will always have dimensions an integer away from that of the 'full' primary field, highest-weight for the full extended algebra.

An extended algebra can be used to generate a modular invariant partition function, simply by taking the diagonal combination of characters of the extended algebra. When expanded out into Virasoro characters, this will of course be non-diagonal. Conversely, given a non-diagonal combination of Virasoro characters one can look to 'explain' this by finding an extended algebra. This can be illustrated within the minimal series, for which there exists the famous 'ADE' classification of all possible modular invariant partition functions.^[40] In terms of Virasoro characters χ_h , write the partition function as

$$Z(q, \bar{q}) = \sum_{h, \bar{h}} N_{h\bar{h}} \chi_h(q) \chi_{\bar{h}}(\bar{q})$$

Taking $N_{h\bar{h}} = \delta_{h, \bar{h}}$ always gives a modular invariant Z , but for $m \geq 5$ there's always at least one further possibility. The diagonal sum corresponds to the A series of Lie algebras, the extra option present for all $m \geq 5$ is associated with the D series, and there are three

further ('exceptional') pairs of solutions, for E_6, E_7 and E_8 . Thus for $m = 5$, the grid of dimensions of Virasoro primary fields (calculated using (1.26)) is:

3	$\frac{13}{8}$	$\frac{2}{3}$	$\frac{1}{8}$	0
$\frac{7}{5}$	$\frac{21}{40}$	$\frac{1}{15}$	$\frac{1}{40}$	$\frac{2}{5}$
$\frac{2}{5}$	$\frac{1}{40}$	$\frac{1}{15}$	$\frac{21}{40}$	$\frac{7}{5}$
0	$\frac{1}{8}$	$\frac{2}{3}$	$\frac{13}{8}$	3

and in addition to the diagonal sum, Z can also be

$$Z = |\chi_0 + \chi_3|^2 + |\chi_{\frac{2}{5}} + \chi_{\frac{7}{5}}|^2 + 2|\chi_{\frac{2}{3}}|^2 + 2|\chi_{\frac{1}{15}}|^2. \quad (1.30)$$

Note that this is a different physical theory to the one with Virasoro-diagonal partition function. In particular, some scaling dimensions of that theory are missing completely here (for example, there is no $\chi_{\frac{1}{10}}$) the corresponding Virasoro primaries appearing neither as primary nor secondary fields with respect to the larger algebra. The extended algebra in this case is the above-mentioned W_3 algebra, one of the first higher-spin algebras to be studied.^[33] It is generated by the spin 3 field ϕ_{15} , and this field appears in the partition function in the same term as the identity, as would be expected if (1.30) were indeed the diagonal combination of extended characters. The BPZ fusion rules^[26] for minimal theories give that $\phi_{15} \times \phi_{ab} = \phi_{a,6-b}$, so it is easy to check that this interpretation holds good for the other terms, the Virasoro primary field corresponding to the first character (that of lowest dimension) in each term being the full primary, and the rest descendants with respect to W_3 . Note that the dimensions appearing in a given term do differ by integers, as has to be not only because of the extended algebra but also to ensure invariance under the T modular transformation, $q \rightarrow e^{2\pi i} q$.

The picture obtained here persists for higher m , although only in the cases $m = 5$ and $m = 6$ are the algebras involved at all studied. For the m^{th} theory, (1.26) shows that

$$h_{1m} = \frac{1}{4}(m-1)(m-2).$$

Thus for $m = 1$ or 2 modulo 4, $h_{1m} \in \mathbb{Z}$, and in general $h_{1m} \in \frac{1}{2}\mathbb{Z}$. Now one further fact about the ADE partition functions must be quoted: the partition functions associated with D_{even}, E_6 and E_8 can all be written as a ('diagonal') sum of the squared moduli of a linear combination of Virasoro characters, while the others (apart of course from the A

series) can not. The above example fits this pattern, (1.30) being one of the two partition functions connected with D_4 (the other is the alternative $m = 6$ partition function). In general, the algebra D_n labels partition functions for minimal theories with $m = 2n - 2$ and $m = 2n - 3$. Thus the D_{even} theories, with ‘diagonal’ partition functions, are precisely those for which h_{1m} is an integer. The speculation that the D_{even} partition functions are explained by some algebra generated by ϕ_{1m} is further supported by the facts that ϕ_{1m} and the identity form a closed operator algebra, and that the D_{even} partition functions start with a term $|\chi_0 + \chi_{1m}|^2$. (One might speculate further that the non-diagonal nature of the D_{odd} partition functions is connected with the algebra responsible in these cases being again generated by ϕ_{1m} , which now has half integer spin, so that the diagonal sum would fail to respect T invariance.)

There is certainly evidence for some larger algebra based on the field ϕ_{1m} , holomorphic for $m = 1$ or 2 modulo 4 , and so it seemed worthwhile to investigate the general question as to whether these fields lead to additional conserved charges on perturbation.

Since a given field may belong to different left and right Virasoro representations in the theories with alternative partition functions, more care than has been used up to now will be taken in specifying both left and right transformation properties of any fields considered. The general idea is to look at fields in $\Phi^{1m} \times \bar{\Phi}^{11}$, and in particular left Virasoro descendants of the ‘Virasoro \times Virasoro-bar’ primary field. Note that such a primary field, with dimensions $(h_{1m}, 0)$, is present in the theory with D -type partition function, though not in the A -type. For convenience, set $h_{1m} = n$, an integer for the theories under consideration. A level- k descendant will have dimensions $(n + k, 0)$, so it is certainly holomorphic. The space of left descendants will be written simply as Φ^{1m} , the transformation properties of such fields with respect to the right hand (‘barred’) Virasoro algebra being simply that of the identity operator. This space may be decomposed by the level, exactly as in (1.24). In this case though the level is not equal to the spin, as even the level zero field has spin n . Thus if S_s has spin s , it lies in Φ_{s-n}^{1m} . Aping the earlier discussion, the question now is whether this field remains part of some conserved current after perturbation, and to answer it $\bar{\partial}S_s$ should be calculated in the perturbed theory. As before,

$$\bar{\partial}S_s = \lambda R_{s-1}. \quad (1.31)$$

(The possibility of higher order terms will be ignored.) The earlier discussion assumed $R_{s-1} \in \Phi^{ab}$, the conformal family of the perturbing field ϕ_{ab} . Here this turns out not

to be the case, so a more careful derivation is required. On the basis of a ‘perturbative’ evaluation of correlators in the perturbed theory in terms of those in the conformal theory, Zamolodchikov^[1] was able to show that the first order contribution to $\bar{\partial}S_s$ (applicable in both (1.23) and (1.31)) is given by

$$\bar{\partial}S_s(z, \bar{z}) = \lambda \oint_z \phi_{ab}(\zeta, \bar{z}) S_s(z) \frac{d\zeta}{2\pi i}. \quad (1.32)$$

The right hand side of this equation is understood to be evaluated using the operator product expansion in the original conformal theory. The small contour about z closes owing to the relative locality of the fields $S_s(z)$ and $\phi_{ab}(z, \bar{z})$ in the (modular invariant) conformal theory.

Equation (1.32) can be used to obtain a further ‘selection rule’ on the possibilities for R_{s-1} , in addition to the comparison of dimensions already used. The BPZ fusion rules give the conformal families to which fields appearing in the operator product expansion of S_s and ϕ_{ab} must belong, and only such fields will contribute to right hand side of (1.32). The simplest case justifies the assumptions made in an earlier section: if S_s is in the conformal family of the identity then the fusion rule $\phi_{11} \times \phi_{ab} = \phi_{ab}$ is enough to prove that R_{s-1} must belong to Φ^{ab} , as claimed. (Being more careful about left and right algebras, $R_{s-1} \in \Phi^{ab} \times \bar{\Phi}^{ab}$, the right hand algebra going through equally trivially.) Slightly more complicated is the case under current consideration, namely $S_s \in \Phi^{1m}$ (or, more pedantically, $S_s \in \Phi^{1m} \times \bar{\Phi}^{11}$). The relevant fusion rule here is $\phi_{1m} \times \phi_{ab} = \phi_{a,m+1-b}$ and hence

$$R_{s-1} \in \Phi^{a,m+1-b} \times \bar{\Phi}^{ab}. \quad (1.33)$$

Now this rule can be ‘intersected’ with the comparison of dimensions argument. As before, the left hand side of (1.31) has dimensions $(s, 1)$, λ has dimensions $(1 - h_{ab}, 1 - h_{ab})$ and so R_{s-1} must have dimensions $(s - 1 + h_{ab}, h_{ab})$. The available dimensions for left descendants in $\Phi^{a,m+1-b} \times \bar{\Phi}^{ab}$ are $(h_{a,m+1-b} + k, h_{ab})$, where $k \in \mathbb{Z}$ is the level of the descendant. Comparing dimensions, the requirement is $k = s - 1 + h_{ab} - h_{a,m+1-b}$. Note that it is not a priori obvious that k so defined will be an integer; however this is ensured by the fact that the pair of conformal families on the right hand side of (1.33) appears in the D_{even} -type partition functions under consideration, and modular invariance under T requires that left and right conformal dimensions must differ by an integer; hence, $h_{ab} - h_{a,m+1-b}$ is indeed an integer. (Alternatively, it is easy to check that $h_{ab} - h_{a,m+1-b}$ is an integer if

(and only if) m is equal to 1 or 2 modulo 4, as is being assumed.) Recalling the remark that spin and level differ by $n = h_{1m}$ in Φ^{1m} , it is clear that $\bar{\partial}$ defines a mapping

$$\bar{\partial} : \Phi_{s-n}^{1m} \rightarrow \Phi_{s-1+h_{ab}-h_{a,m+1-b}}^{a,m+1-b}.$$

Total z derivatives may be discarded on left and right by restriction and projection, and the counting argument then gives a non-zero kernel for $\bar{\partial}$ and a conserved charge of spin s whenever

$$\dim(\hat{\Phi}_{s+h_{ab}-h_{a,m+1-b}}^{a,m+1-b}) - \dim(\hat{\Phi}_{s+1-n}^{1m}) \quad (1.34)$$

is negative. (Note, in (1.34) s has been substituted for $s - 1$ so as to be equal to the spin of the conserved charge rather than the spin of the current S .)

Thus the relevant character calculation is to look for negative coefficients in

$$q^{h_{a,m+1-b}-h_{ab}} \hat{\chi}_{a,m+1-b} - q^{n-1} \hat{\chi}_{1m}.$$

The details of the REDUCE calculation are given in appendix 1; again, all possible perturbing fields were examined. The successful results for $m = 5, 6, 9, 10, 13$ and 14 are recorded in table 2. Somewhat disappointingly, only two cases were found, one for $m = 5$ and one for $m = 6$ (the irrelevant perturbation for $m = 5$ will be ignored). In retrospect this is not too surprising, and one certainly shouldn't expect any more successes of the counting argument for higher values of m . The reason is the discrepancy of the levels involved in the comparison (1.34), which gets worse as m is increased, in contrast to the earlier situation (see equation (1.25)) where the levels involved always differed only by one. The extreme growth in the number of states at higher levels means that this fact quickly swamps any other effects that may occur. As before, this failure does not rule out the existence of further conserved currents, here associated with the ϕ_{1m} field, but more powerful methods will have to be developed to answer this question.

Returning to the successes of table 2, the first case is just the A_2 related perturbation of the $m = 5$ theory already described, and the charges at spins 2, 4 and 8 fill out the first few terms previously missing from the A_2 exponents. The second, at $m = 6$, is the $(0, \text{adj})$ perturbation of the $e_6^{(1)} \times e_6^{(1)} / e_6^{(2)}$ coset, and the observed spins of 4 and 8 are indeed those required to complete the set of E_6 exponents.

1.9 Discussion and Conclusions

The most specific claim that can be made on the basis of the above results is that a perturbation of the $g^{(1)} \times g^{(1)}/g^{(2)}$ coset conformal field theory by the field labelled by the pair of G representations $(0, \text{adj})$ yields, at least for simply-laced G , an integrable field theory with conserved currents at spins given by the exponents of G , repeated modulo the Coxeter number.

However all the evidence that has been gathered is essentially circumstantial, and gives no real understanding of why the claim should be true. One direction to look in this context is that of affine and non-affine Toda field theory, and this will be mentioned in a later chapter. Alternatively, there might be hope to find more insight purely within the ideas of conformal field theory. Here, the extended algebras should play a more central part. It has already been mentioned that for any Lie algebra G , the coset models $g^{(1)} \times g^{(k)}/g^{(k+1)}$ form a sequence (a 'discrete series') connected with the extended algebra W_g . The $k \rightarrow \infty$ limit of such a sequence is just the $g^{(1)}$ WZW model, within which the W algebra appears as the algebra generated by the Casimirs in the basic currents. For k sufficiently large, the coset model will still possess extra holomorphic primary fields of the same spins, generating the W algebra.^[36, 41] The orders of the Casimirs, giving the spins of the W -currents (the basic currents being of course spin one), are just one greater than the exponents so any charges obtained from these currents would have spins at the exponents of G . Thus it is tempting to conjecture that the currents which survive perturbation are those generating the W algebra, although I know of no proof of this. One further point needs to be made in this connection: for k small the W -algebra structure is certainly 'hidden' - for example, in the $m = 3$ theory there are no integer spin primary fields, while one of spin eight might be expected on the basis of the E_8 coset. However for current needs the traditional definition of a W -algebra in terms of primary fields seems unduly restrictive, and it is quite possible that vestiges of the W_{e_8} algebra might be found *within* the conformal family of the identity for $m = 3$. Indeed this seems plausible given that the exponents of E_8 were 'derived' from a suitable comparison of $m = 3$ Virasoro characters. More ambitiously, one might hope that a productive way to study these extended algebras in conformal theories in general might be to take an indirect route and look at the suitable perturbation first, a process that seems to freeze out symmetries of the conformal theory not directly related to the particular Lie algebra under discussion.

One might ask about cosets with values of k greater than one. Looking at table 4,

there is only one case with $c < 1$, namely the $m = 11$ $e_8^{(1)} \times e_8^{(2)}/e_8^{(3)}$ theory. The pair of E_8 representations $(0, \text{adj})$ labels the $h = \frac{1}{11}$ primary field ϕ_{45} and so a conjecture can be made that perturbation by this field would give conserved charges at the E_8 exponents. This would be especially interesting as it would be the first perturbing field outside the set ϕ_{12}, ϕ_{21} and ϕ_{13} seen to preserve some of the integrability of the minimal models. However little conclusive can be said on this point. Certainly the counting argument within the conformal family of the identity doesn't help, as otherwise the ϕ_{45} perturbation would appear in table 1 for $m = 11$. There is however a potential extra holomorphic field in the conformal grid, ϕ_{17} of conformal weight eight. Evidence from the coset construction, including the fact that this coset corresponds to an E -type modular invariant partition functions (in fact, one of the two associated with $E_6^{[36]}$), can be used to support the idea that this field is part of an extended algebra, even though it is not one of the ϕ_{1m} fields connected with the D partition functions discussed in the last section. If this was preserved after perturbation, it would indeed give a charge of suitable spin for an E_8 exponent. Repeating the operator product expansion and dimension comparison arguments demonstrates that $\bar{\partial}\phi_{17}$ must be a descendant of the perturbing field at level 7, but there are far too many states here to know by counting alone that this field is a total z -derivative.

Finally, to the possible physical implications of these results for the perturbed theories. The key question here is the ultimate destination of the renormalization group trajectory. If it remains on the critical surface and hits another fixed point there, the long-distance behaviour will again be a conformal field theory (with smaller central charge^[37]). Otherwise it will develop a finite correlation length and questions can be asked about the resulting massive field theory, as Zamolodchikov did in the case of the magnetic perturbation of the Ising model. The difficulty here is that the original theory provides only short-distance information after perturbation, while objects such as S-matrices that might be of interest in the massive theory are only seen in the long-distance asymptotics. Zamolodchikov was able to show that an important aid to gluing together short and long distance behaviour is provided by the conserved charges, which will of course be respected by the S-matrix of the massive theory, even though they were derived purely from short-distance conformal field theory considerations. (One way of seeing the truth of this is to note that the expansion (1.21) terminated at finite order and hence could be evaluated exactly.)

This motivates a general study of S-matrices which conserve higher spin charges, and

this will be the main subject of the rest of this thesis. Such S-matrices, as has been known for some time, should be exactly soluble. The next chapter is a review of the general technology involved in their study.

Chapter 2

Exact S-Matrices

2.1 Introduction

The theories seen up to this point have all been formulated in Euclidean space and studied via their correlation functions. For massless theories in two dimensions this is the only satisfactory approach known, but once a theory has been perturbed in such a way that a non-zero mass gap develops it becomes legitimate to ask questions of the Wick-rotated theory living in Minkowski space, and to study the S-matrix of the model. As the S-matrix deals with long-distance asymptotics of the model, this approach reveals interesting features not previously visible. For most of the rest of this thesis the emphasis will be on massive quantum field theories in Minkowski space.

The general S-matrix is a very complicated object, even in 1+1 dimensions. A two-particle scattering process at sufficiently high energy will produce a plethora of outgoing particles, and the analytic structure of the S-matrix will be exceedingly complicated, a situation which only gets worse as more incoming particles are allowed. It is a remarkable fact that for some 1+1 dimensional theories, an exact expression for the multiparticle S-matrix can be postulated. These are the theories with so-called exact, or factorized, S-matrices (the reason for the latter terminology will be seen below). The key property shared by all such theories appears to be their integrability, in the sense that they all possess, in addition to the momentum P_μ of spin one, infinitely many conserved charges of higher spin. This was exactly the feature observed in the perturbed conformal theories of the previous chapter.

The emphasis of the following sections will be on the rôle of the conserved charges in ensuring the factorizability of the S-matrix, and on the various consistency requirements that should be imposed.

2.2 Conserved Charges in 1+1 Dimensions

A theory with N types of particle will be assumed, labelled A_1, \dots, A_N . For later convenience, define a charge conjugation operation on the labels so that the antiparticle of A_i is $A_{\bar{i}}$ (and if A_i is neutral, $\bar{i} = i$). Any internal quantum numbers are incorporated into the particle label, so all that remains to characterize an asymptotic one particle state is to specify its two-momentum p_a^μ , satisfying

$$(p_a^\mu)^2 = (p_a^0)^2 - (p_a^1)^2 = m_a^2, \quad (2.1)$$

where m_a is the mass of particle type A_a . Multiparticle asymptotic states will be written as

$$|A_{i_1}(p_1), A_{i_2}(p_2), \dots\rangle_{in,out}, \quad (2.2)$$

and may be taken to be simultaneous eigenstates of all the (commuting) conserved charges. A slight smearing of each momentum results in a collection of wave packets; given that the theory is massive all interactions are short range, and so long as the particles are well separated the multiparticle state behaves as a superposition of one-particle states, each moving freely.

The form of Lorentz transformations in 1+1 dimensions permits a very simple characterization of higher spin conserved quantities. Writing the momentum of a particle in terms of its rapidity θ ,

$$p_a^\mu = m_a(\cosh \theta_a, \sinh \theta_a).$$

Lorentz covariance implies that a charge P_s of spin s acts on a one particle eigenstate as

$$P_s |A_i(\theta)\rangle = \gamma_s^i e^{s\theta} |A_i(\theta)\rangle,$$

where γ_s^i is a scalar depending only on the spin s and the particle type i . Since we can always deal with localized, separated wave packets and the charges are all integrals of local conserved currents (this is certainly true of the charges defined in the last chapter), P_s acts additively on multiparticle states:

$$P_s |A_{i_1}(\theta_1), A_{i_2}(\theta_2), \dots\rangle = (\gamma_s^{i_1} e^{s\theta_1} + \gamma_s^{i_2} e^{s\theta_2} + \dots) |A_{i_1}(\theta_1), A_{i_2}(\theta_2), \dots\rangle. \quad (2.3)$$

The simplest example, found in all translationally invariant theories, is of course the

momentum operator P^μ . The light-cone components are

$$P_1 = P^0 + P^1, \quad P_{-1} = P^0 - P^1,$$

and

$$P_1 |A_a(\theta)\rangle = m_a e^\theta |A_a(\theta)\rangle$$

$$P_{-1} |A_a(\theta)\rangle = m_a e^{-\theta} |A_a(\theta)\rangle.$$

Hence

$$\gamma_1^a = \gamma_{-1}^a = m_a. \quad (2.4)$$

(Note that in 1+1 dimensions the Lorentz group acts independently on left and right light-cone coordinates enabling conserved quantities at each spin to be split into positive and negative parts, paralleling the left and right algebras in the conformal theory. As before, assuming reflection symmetry the right half can be ignored.)

Equation (2.3) shows that the action of P_s on asymptotic states is completely specified by the numbers γ_s^a . If they are all zero then, assuming asymptotic completeness, $P_s \equiv 0$ and there is no nontrivial conserved charge at that spin. Such a situation can often arise as there are very strong restrictions on the $\{\gamma_s^a\}$, coming from the bootstrap requirement that they be consistent with the singularity structure of the S-matrix. However even conserved charges at a subset of the possible spins are sufficient to deduce factorizability of the S-matrix, and this will be described in the next section.

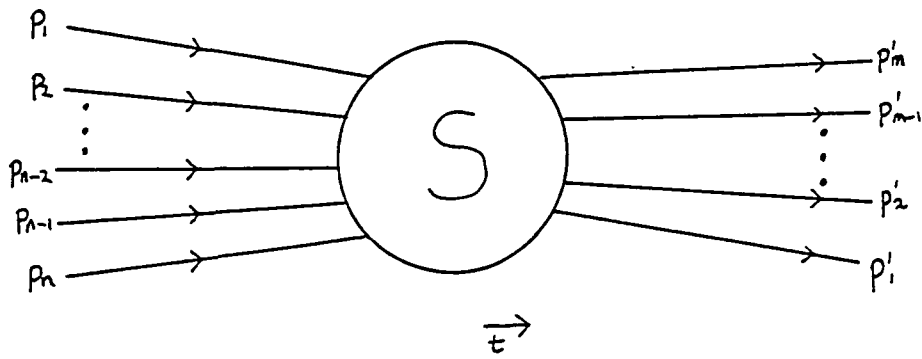
2.3 Factorization^[42, 43]

A general process might involve the n -particle state $|A_{i_1}(\theta_1), A_{i_2}(\theta_2), \dots, A_{i_n}(\theta_n)\rangle$ scattering into the m -particle state $|A_{j_1}(\theta'_1), A_{j_2}(\theta'_2), \dots, A_{j_m}(\theta'_m)\rangle$, as shown in figure 1.

Conservation of momentum requires that

$$\sum_{k=1}^n p_k = \sum_{l=1}^m p'_l.$$

This is usual; the special feature of the models under discussion is the presence of higher spin charges, also conserved. Imposing that each nontrivial P_s has the same value on


 Figure 1 : n -particle scattering.

initial and final states leads to an infinite set of further equations to be satisfied:

$$\sum_{k=1}^n \gamma_s^{i_k} e^{s\theta_k} = \sum_{l=1}^m \gamma_s^{j_l} e^{s\theta'_l}. \quad (2.5)$$

For general initial momenta these can be simultaneously satisfied only if $m = n$ and, after suitable reordering, $\theta_k = \theta'_k$ and $\gamma_s^{i_k} = \gamma_s^{j_k}$. (The discussion of the bootstrap will show that there are some isolated values of momenta for which there are other solutions, but analyticity of the S-matrix can be invoked to see that the corresponding S-matrix elements must vanish even at these points.) Thus particle production is forbidden and the set of final momenta must be the same as the set of initial momenta. The particle types may alter, but only if the values of γ_s^i are preserved for all $s \neq 0$ — in other words, ‘internal’ quantum numbers may be changed, so long as they correspond to scalar quantities. These selection rules imply that an *in* state can be expanded as a finite superposition of *out* states:

$$|A_{i_1}(\theta_1), A_{i_2}(\theta_2), \dots, A_{i_n}(\theta_n)\rangle_{in} = S_{i_1 i_2 \dots i_n}^{j_1 j_2 \dots j_n}(\theta_1, \theta_2, \dots, \theta_n) |A_{j_1}(\theta_1), A_{j_2}(\theta_2), \dots, A_{j_n}(\theta_n)\rangle_{out}, \quad (2.6)$$

with the condition that $\gamma_s^{i_k} = \gamma_s^{j_k}$ for all nonzero s .

Note that in more than one space dimension, the deduction would have been that the S-matrix must be trivial, if it satisfies the usual analyticity requirements; this is the Coleman-Mandula theorem. To see why, it is best to consider a $2 \rightarrow 2$ process, the space part of which is shown in figure 2.

The S-matrix (or, to be more precise, the T matrix defined by $S = 1+iT$ containing the nontrivial scattering amplitudes) is expected to be analytic in the angle β made by

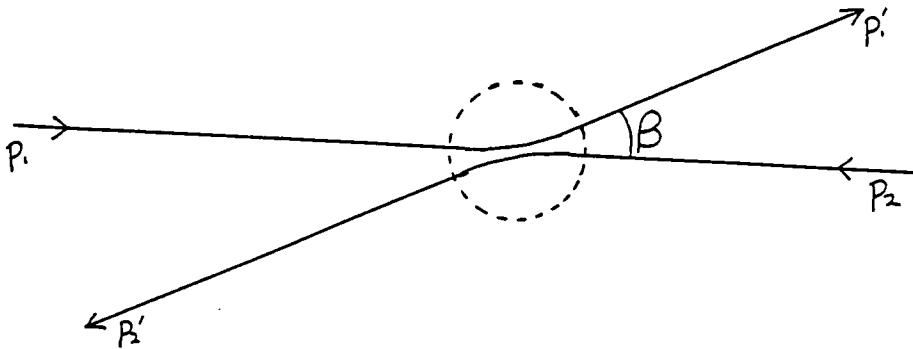


Figure 2.

outgoing particles relative to the incoming track. The selection rule on the momenta requires that the scattering amplitude should vanish for β not equal to 0 or π , and hence for all β , by analyticity. This leaves only the trivial part of the S-matrix. The situation is different in one spatial dimension since then 0 and π are the *only* possible values for β .

It might appear that even in one space dimension such an S-matrix is effectively trivial, especially if there are no degeneracies in the particle spectrum allowing mixing in scattering, as it is then nothing but a collection of phases. However these phases may depend on the relative momenta of the incoming particles. Such a momentum-dependent phase shift will produce a finite displacement of a wave packet, so a scattering process, while preserving particle types within multiplets sharing the same values of γ_s and leaving momenta unchanged, may induce time delays as compared to the free motion of the particles involved – a situation very similar to that in classical soliton scattering.

As the most intuitive way to think about scattering is to work consistently with wave packets, it is worth pausing briefly to see this finite displacement explicitly. Consider a Gaussian wave packet with (un-normalized) wave function

$$\psi(x) = \int_{-\infty}^{\infty} dp e^{-a^2(p-p_0)^2} e^{ip(x-x_0)}.$$

The momentum is approximately p_0 , the position approximately x_0 and the width a . Now multiply this by a momentum-dependent phase factor, $e^{-i\phi(p)}$. The new wave function is

$$\tilde{\psi}(x) = \int_{-\infty}^{\infty} dp e^{-a^2(p-p_0)^2} e^{ip(x-x_0)} e^{-i\phi(p)}.$$

If a is small the momentum of the packet is sharply peaked about p_0 and $\phi(p)$ can be

expanded in powers of $(p - p_0)$. Hence

$$\begin{aligned}\tilde{\psi}(x) &\approx \int_{-\infty}^{\infty} dp e^{-a^2(p-p_0)^2} e^{ip(x-x_0)} e^{-i\phi(p_0)} e^{-i\phi'(p_0)(p-p_0)} \\ &= \int_{-\infty}^{\infty} dp e^{-a^2(p-p_0)^2} e^{ip(x-x_0-\phi'(p_0))} e^{-i(\phi(p_0)-p_0\phi'(p_0))}.\end{aligned}$$

So $\tilde{\psi}$ is approximately Gaussian, but now centred at $x_0 + \phi'(p_0)$. (Expanding ϕ to one higher order, it is easy to see that the new width² is $a^2 + \frac{\phi''^2}{4a^2}$.)

Now consider the time-dependent wave function,

$$\psi(x, t) = \int_{-\infty}^{\infty} dp e^{-a^2(p-p_0)^2} e^{ip(x-x_0)} e^{-i\sqrt{m^2+p^2}t}.$$

Time-dependence enters as a phase factor in the form already treated, taking $\phi(p) = t\sqrt{m^2+p^2}$. The result above then gives that at time t the packet is centred at $x_0 + p_0t/\sqrt{m^2+p_0^2}$, as expected, and an additional phase shift $e^{-i\alpha(p)}$ just shifts this by a further amount $\alpha'(p_0)$.

To deal with a scattering process, the wave function for a multiparticle state must be used. This does not cause problems for asymptotic states when all particles are well separated, and a product of one-particle wave functions can be used to a good approximation. For simplicity, consider the scattering of a pair of non-degenerate particles (so the outgoing state consists of the same two particles). Initially one is near x_0 and one near y_0 with mean momenta p_0 and q_0 respectively, (both packets with width $a \ll |x - y|$) and the wave function is

$$\psi_{in}(x, y) = \int_{-\infty}^{\infty} dp \int_{-\infty}^{\infty} dq e^{-a^2(p-p_0)^2} e^{ip(x-x_0)} e^{-a^2(q-q_0)^2} e^{iq(y-y_0)}.$$

A momentum dependent phase factor will have the form $e^{-i\phi(p,q)}$ and the above discussion generalizes easily to see that this shifts the first particle from x_0 to $x_0 + \partial_1\phi(p_0, q_0)$, and the second from y_0 to $y_0 + \partial_2\phi(p_0, q_0)$. To discuss scattering, time-dependence should also

be incorporated and the *out* wave function, correct when t is large, is

$$\psi_{out}(x, y) = \int_{-\infty}^{\infty} dp \int_{-\infty}^{\infty} dq e^{-a^2(p-p_0)^2} e^{ip(x-x_0)} e^{-a^2(q-q_0)^2} e^{iq(y-y_0)} e^{-i\phi(p, q, t)}$$

where

$$\phi(p, q, t) = t\sqrt{m_1^2 + p^2} + t\sqrt{m_2^2 + q^2} + \alpha(p, q),$$

the final term coming from the two-particle S-matrix:

$$S_{12}^{12}(p, q) = e^{-i\alpha(p, q)}.$$

Subsequent discussion will show that it is most convenient to work in terms of the rapidities θ_1 and θ_2 and that the S-matrix depends only on their difference $\theta \equiv \theta_1 - \theta_2$. (This is due to Lorentz invariance, but note that the rest of the expression for ϕ *does* depend on the Lorentz frame; this is no surprise as to specify the wave function a frame must be chosen.) The rapidities are related to the spatial momenta by $p_0 = m_1 \sinh \theta_1$, $q_0 = m_2 \sinh \theta_2$, and so, using all the above results (and taking $x_0 < y_0$, $p_0 > q_0$), for t large enough the interaction has occurred, particle 1 is at

$$x_0 + \tanh \theta_1 \left(t + \frac{i}{m_1 \sinh \theta_1} \frac{S'(\theta)}{S(\theta)} \right)$$

and particle 2 at

$$y_0 + \tanh \theta_2 \left(t - \frac{i}{m_2 \sinh \theta_2} \frac{S'(\theta)}{S(\theta)} \right).$$

Now move to the centre of mass frame. Then $m_1 \sinh \theta_1 = -m_2 \sinh \theta_2 = p$, and the particles are at

$$x_0 + \tanh \theta_1 t' \quad \text{and} \quad y_0 + \tanh \theta_2 t', \quad (2.7)$$

where

$$t' = t + \frac{iS'(\theta)}{pS(\theta)}. \quad (2.8)$$

This is exactly as claimed: if there were no interaction the particle positions would be given by (2.7) with $t' = t$, and so the effect of the S-matrix has been to cause a time delay given by (2.8). The result is also interesting for the form of the dependence on the S-matrix – the logarithmic derivative of S that appears in (2.8) will occur in a very different context when the bootstrap is discussed.

Returning now to the discussion of general scattering processes, the above information can also be put to use to see the effect of the higher spin conserved charges on wave packets.^[44]

For simplicity, consider the purely spatial component of the spin s charge, and denote this by $P^{(s)}$. Ignoring any constant factor, this multiplies a state with momentum p by p^s , and so acting on a wave packet with $e^{-icP^{(s)}}$ inserts a momentum dependent phase factor e^{-icp^s} . In other words, $\alpha(p) = cp^s$, and a wave packet of momentum p_0 is shifted by an amount $\alpha'(p_0) = csp_0^{(s-1)}$. For $s = 1$ this is just the fact that the momentum operator generates spatial translations, packets of all momenta being shifted by an equal amount. The important point to note is that any conserved charge of higher spin generates a translation by an amount which depends on the mean momentum p_0 of the wave packet being acted on. Acting on a multiparticle state it will move the particles relative to each other.

Now turn to the scattering of three particles, each represented by a wave packet localized in position and momentum. Depending on the relative initial positions of the particles, the interaction may happen in three different ways: the collision may be roughly simultaneous, or it may occur as a sequence of well separated two-body collisions. The possibilities are illustrated in figure 3.

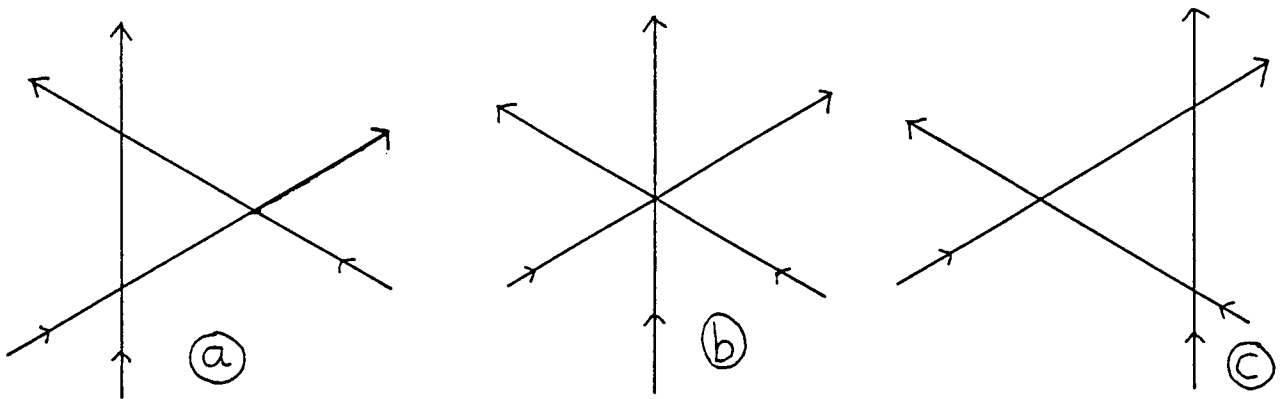


Figure 3.

The amplitudes for processes (a) and (c) are simply products of two-particle amplitudes, but (b) is not fixed a priori. However when a higher spin charge is present in the theory, it can be used to translate the initial particles relative to each other, and hence to shift between the three diagrams. Conservation of the charge means that the amplitude is unchanged by this, and so for the theories under study the three particle scattering

amplitudes (and, by a trivial extension of the above argument, all multiparticle amplitudes) are completely determined once the two-particle S-matrix is known. Furthermore there is a restriction on the two-particle S-matrix, coming from the requirement that the amplitudes for diagrams (b) and (c) be the same. It is:

$$S_{i_1 i_2}^{k_1 k_2}(\theta_{12}) S_{k_1 i_3}^{j_1 k_3}(\theta_{13}) S_{k_2 k_3}^{j_2 j_3}(\theta_{23}) = S_{k_1 k_2}^{j_1 j_2}(\theta_{12}) S_{i_1 k_3}^{k_1 j_3}(\theta_{13}) S_{i_2 i_3}^{k_2 k_3}(\theta_{23}).$$

(Lorentz invariance dictates that the momentum dependence is only through the rapidity differences $\theta_{ij} = \theta_i - \theta_j$.) This is the Yang-Baxter equation,^[45] also called the factorization equation, ensuring as it does that the three-particle S-matrix can be ‘factorized’ into a product of two-particle S-matrices. It is straightforward to see that no further consistency conditions arise from the factorization of amplitudes involving larger numbers of particles.

In many models, combining the factorization equations with the imposition of a suitable symmetry structure on the multiplets allows a ‘minimal’ hypothesis for the S-matrix to be inferred. An example is the sine-Gordon model: the soliton and antisoliton are assumed to lie in one multiplet (being distinguished only by a scalar, the $s = 0$ soliton number), transforming as a vector under $O(2)$ rotations, and from this Zamolodchikov’s soliton scattering amplitudes can be deduced.^[42]

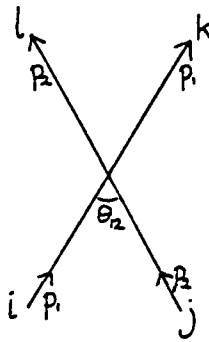
However if the particle spectrum contains no multiplets, the two particle S-matrices are diagonal and the Yang-Baxter equation is trivially satisfied. For this reason such theories were often thought uninteresting,^[42] but they will be the main topic of discussion below. As later stressed by Zamolodchikov,^[1] there are other constraints which can be imposed in situations where no information is provided by the Yang-Baxter equation. However before moving on to these, some more details of the analytic structure of the S-matrix are required.

2.4 General Properties of the Two-Particle S-Matrix

The conclusion of the last section was that the problem of finding the complete S-matrix is solved once the two particle matrix elements are known. This section will describe some of the constraints on these coming from general field-theoretic principles, in particular analyticity, unitarity and crossing symmetry.

The two-particle S-matrix, defined by

$$|A_i(\theta_1)A_j(\theta_2)\rangle_{in} = S_{ij}^{kl}(\theta_{12}) |A_k(\theta_1)A_l(\theta_2)\rangle_{out}, \quad (2.9)$$

Figure 4 : $S_{ij}^{kl}(\theta_{12})$.

is depicted in figure 4, with time running up the page.

Parity invariance implies that $S_{ij}^{kl} = S_{ji}^{lk}$; invariance under CT that $S_{ij}^{kl} = S_{\bar{k}\bar{l}}^{\bar{j}\bar{i}}$.

Analyticity is usually expressed in terms of the Mandelstam variables s, t and u . An important simplifying feature of theories in 1+1 dimensions is that only one independent variable enters into the discussion, which can be taken to be s , the momentum in the forward channel:

$$s = (p_1 + p_2)^2 = m_i^2 + m_j^2 + 2m_i m_j \cosh \theta_{12}. \quad (2.10)$$

For a physical process θ_{12} is real (since both p_1 and p_2 are real), and hence s must also be real and satisfy $s \geq (m_i + m_j)^2$. The postulate of analyticity states that the matrix $S_{ij}^{kl}(s)$ can be continued up from this segment of the real axis to an analytic (matrix-valued) function defined on the complex s plane, single-valued after suitable cuts have been made. For the theories under discussion only two cuts are needed, both running along the real axis. The complex s plane is shown in figure 5, and the following paragraphs describe and attempt to justify some of its features. This cut plane is called the physical sheet; other, 'unphysical', sheets may be reached by continuing S through the cuts.

The edges of the branch cuts are labelled A, B, C and D . Given that the physical amplitude was continued *up* into the complex plane, it is clear that the physical amplitudes are found on the upper edge of the right hand cut, *ie* along C . The crosses for real s between $(m_i - m_j)^2$ and $(m_i + m_j)^2$ correspond to possible bound-state poles occurring below threshold; these are the only other singularities expected on the physical sheet.

The general requirement of unitarity, required to hold for all physical values of s , is $S(s)S^\dagger(s) = 1$. The usual situation is that as s is increased beyond thresholds allowing additional decay products, new terms enter into the unitarity equation giving rise to

5

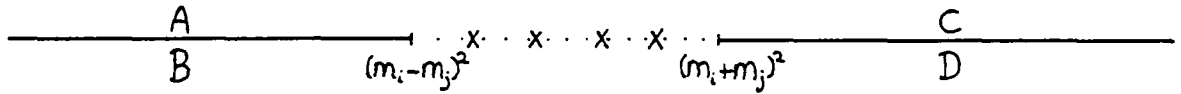


Figure 5 : The complex s plane.

further branch points along the real axis. However for the integrable theories under discussion, it has already been shown that the amplitudes for $2 \rightarrow 3$ and higher processes vanish. Hence no further branch cuts are expected, and for all real $s \geq (m_i + m_j)^2$ the unitarity equation involves only the $2 \rightarrow 2$ S-matrix elements:

$$S_{ij}^{kl}(s) \overline{S_{kl}^{nm}(s)} = \delta_i^n \delta_j^m. \tag{2.11}$$

Since s in this equation is real, $\overline{S(s)}$ can be replaced by $\overline{S(\bar{s})}$. It follows that $\overline{S(s)}$ is also a boundary value of an analytic function, $S^-(s)$ say, given the theorem that if $f(z)$ is analytic then so is $g(z) \equiv \overline{f(\bar{z})}$. It is natural to continue this function down from the real axis, so that there are now two analytic functions in play: $S(s)$, defined in some domain bordering on C (the upper edge of the right-hand cut), and $S^-(s)$, defined in a domain which borders on D , the lower edge of the same cut. However it can be shown that these two functions are in fact the same, sharing a common analytic continuation into the below-threshold region $(m_i - m_j)^2 < s < (m_i + m_j)^2$. This property is called Hermitian analyticity; a proof can be found in [46], page 226. The threshold $s = (m_i + m_j)^2$ must then be a square-root branch point. To see why, let $S(s_\gamma)$ denote the analytic continuation of the matrix S up from the point s on the real axis, anticlockwise around the branch point and back to the point s from below. Hermitian analyticity amounts to the statement that

$$S(s_\gamma) = S^\dagger(s) = S^{-1}(s),$$

the latter equality coming from (2.11). Inverting all the matrices (and noting that if M continues to M' , certainly M^{-1} continues to $(M')^{-1}$) shows that $S^{-1}(s_\gamma) = S(s)$, and

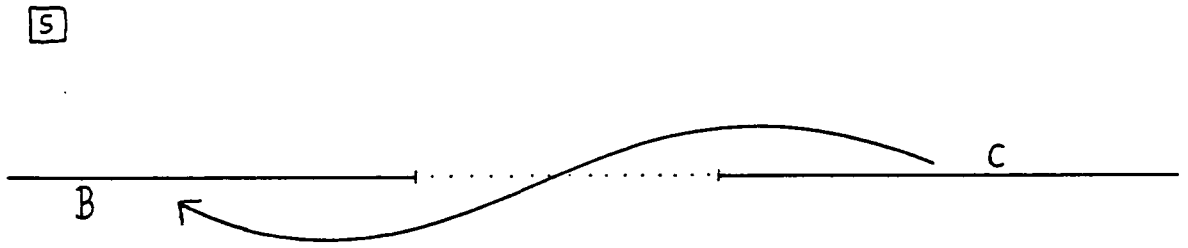


Figure 6 : Crossing.

hence that $S((s_\gamma)_\gamma) = S(s)$. In other words circling the branch point twice returns the variable to the original sheet, and the branch point is indeed of square root type.

The fact that S and S^- are the same function allows the unitarity equation to be rewritten. Taking s to be real, larger than $(m_i + m_j)^2$ and above the branch cut, (2.11) becomes

$$S_{ij}^{kl}(s)S_{kl}^{nm}(\bar{s}) = \delta_i^n \delta_j^m, \quad (2.12)$$

where \bar{s} is again real, but now just below the cut. This form is more appropriate for analytic continuation.

The right hand half of figure 5 has now been justified; to see the need for the second branch cut, crossing must be discussed. Figure 4 may be viewed from the side, becoming the diagram of a scattering process $A_i A_{\bar{l}} \rightarrow A_k A_{\bar{j}}$. The forward channel variable is now t ,

$$t = (p_1 - p_2)^2 = 2m_i^2 + 2m_j^2 - s. \quad (2.13)$$

(Note, $u \equiv 0$, consistent with $s + t + u = 2m_i^2 + 2m_j^2$.) Crossing symmetry states that the amplitude for this process may be obtained from the previous amplitude by analytic continuation to the region of the s plane where t becomes physical. So t must be real and larger than $(m_i + m_j)^2$, physical amplitudes corresponding to approaching this line segment from above in the t plane. Converting this into a statement about s , the amplitudes for the cross-channel process are found on the lower edge of a cut in the s plane running along the real axis from $(m_i - m_j)^2$ to $-\infty$, that is along B in figure 5. Hence for s on C ,

$$S_{i\bar{l}}^{k\bar{j}}(s) = S_{ij}^{kl}(2m_i^2 + 2m_j^2 - s), \quad (2.14)$$

the path of analytic continuation being shown in figure 6.

The second branch point must also be of square root type. Note though that this does not imply that the Riemann surface of the function S is just a double cover of the physical sheet, since the unphysical sheet reached by going once round the left hand branch point is not necessarily the same as that coming from a single circuit on the right. The general S , even in these integrable theories, lives on an infinite cover of the physical sheet.

This apparently very complicated situation is dramatically simplified if, following Zamolodchikov, the rapidity variable θ ($\equiv \theta_{12}$) is used instead of s . The transformation

$$\theta = \cosh^{-1} \frac{s - m_i^2 - m_j^2}{2m_i m_j},$$

the inverse of (2.10), maps the s plane into the strip $0 \leq \text{Im}\theta \leq \pi$, known as the physical strip. Furthermore this transformation opens up the two cuts, so that $S(\theta)$ is analytic at the images 0 and $i\pi$ of the two branch points, given that it had a square root singularity in s at these points. Since these are the only thresholds, S will be a meromorphic function of θ . The other sheets of the cover of the s plane simply map to a succession of strips $n\pi \leq \text{Im}\theta \leq (n+1)\pi$. The reality of $S(s)$ for real s between the branch points means that $S(\theta)$ must be real for purely imaginary θ . The θ plane is shown in figure 7, together with the images of the lines A, B, C and D . Possible bound state poles lie in the physical strip between 0 and $i\pi$; there may be (and in general are) many further poles off the physical strip.

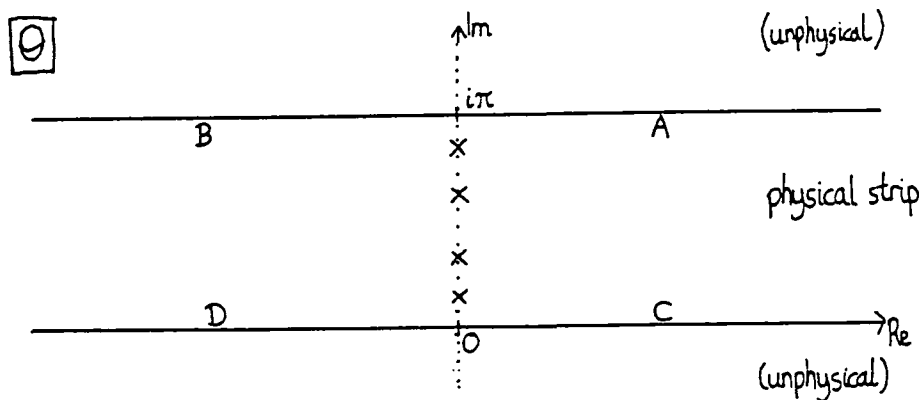


Figure 7 : The complex θ plane.

The unitarity and crossing equations (2.12) and (2.14) were previously defined only for s lying on the line C corresponding to physical momenta. When converted into equations in the θ variable (this is straightforwardly done, given the positions of the images of

A, B, C and D shown in figure 7), both equations are of a form that can be analytically continued (in particular, the unitarity equation no longer involves a complex conjugation) and hence should hold for all complex θ . They are:

$$\text{Unitarity : } S_{ij}^{nm}(\theta)S_{nm}^{kl}(-\theta) = \delta_i^k \delta_j^l, \quad (2.15)$$

$$\text{Crossing : } S_{i\bar{l}}^{k\bar{j}}(\theta) = S_{ij}^{kl}(i\pi - \theta).$$

2.5 Purely Elastic S-Matrices and the Bootstrap

The discussion up to now has been very general, applying to any theory possessing a factorizable S-matrix. However it turns out that the issues to be described below are considerably more complicated in theories possessing multiplets, within which particles mix during scattering. The Toda theories which will be the main concern of the remainder of this thesis do not appear to possess these multiplets (in other words, each asymptotic particle type a is uniquely distinguished by the numbers γ_s^a , $s \neq 0$). Hence from this point onwards a simplification will be made, and only theories possessing no multiplets will be considered. As remarked earlier, for such theories the S-matrix is diagonal, and for this reason the scattering is often said to be 'purely elastic'. The Yang-Baxter equation is no help here, and the purpose of this section is to discuss an alternative set of constraints which can be employed.

The notation can now be somewhat simplified: given that the only scattering processes are $A_a A_b \rightarrow A_a A_b$ there is no need for the upper pair of indices in (2.9) and the relevant S-matrix element will be written $S_{ab}(\theta)$. Factorization of multiparticle amplitudes implies that the problem of finding the complete S-matrix of the theory has been solved once this function is known for each pair of particle types in the theory. The unitarity and crossing equations now become:

$$\text{Unitarity : } S_{ab}(\theta)S_{ab}(-\theta) = 1, \quad (2.16)$$

$$\text{Crossing : } S_{a\bar{b}}(\theta) = S_{ab}(i\pi - \theta).$$

In contrast to the general situation, the lack of a matrix structure in (2.16) as compared to (2.15) means that here the full s Riemann surface is just a double cover of the physical

sheet: this follows from the implication of (2.16) that $S_{ab}(\theta)$ is $2\pi i$ -periodic. Periodicity in $i\theta$ means that all S-matrix elements can be made from products of hyperbolic functions; a basic $2\pi i$ -periodic building block satisfying the unitarity equation can be defined as:

$$(x) = \frac{\sinh\left(\frac{\theta}{2} + \frac{i\pi x}{2h}\right)}{\sinh\left(\frac{\theta}{2} - \frac{i\pi x}{2h}\right)}. \quad (2.17)$$

(The constant h is inserted into the definition for later convenience.) The crossed version of (x) is $-(h-x)$, and some other useful properties of this function are:

$$(0) = 1 \quad (h) = -1 \quad (x)^{-1} = (-x) \quad (x) = (x \pm 2h). \quad (2.18)$$

Now to the bootstrap itself.^[47, 1] As already stated, the S-matrix may have poles in the physical strip between 0 and $i\pi$. Simple poles correspond to possible bound states, while any higher order poles are explained in terms of anomalous thresholds in a way to be explained later. The bootstrap hypothesis is that any bound state is itself one of the possible asymptotic particles appearing in (2.2), of type \bar{c} , say (the antiparticle label is used for convenience only). In a perturbative treatment the pole can then be traced to the Feynman diagram shown in figure 8, and for the bound state to form there must be a non-zero three point coupling C^{abc} .

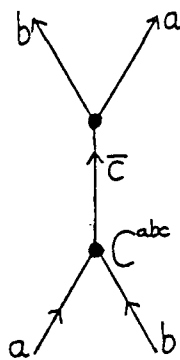


Figure 8.

The intermediate particle \bar{c} is in the forward channel and so has momentum² equal to s . The pole in the amplitude occurs when \bar{c} is on shell, at $s = m_{\bar{c}}^2$. This corresponds to a

rapidity difference $\theta_{ab} \equiv iU_{ab}^c$. From (2.10), U_{ab}^c must then satisfy

$$m_c^2 = m_a^2 + m_b^2 + 2m_a m_b \cos U_{ab}^c. \quad (2.19)$$

Note that if the fusing $ab \rightarrow \bar{c}$ is allowed (so $C^{abc} \neq 0$) then so are the fusings $bc \rightarrow \bar{a}$ and $ca \rightarrow \bar{b}$, and

$$U_{ab}^c + U_{bc}^a + U_{ca}^b = 2\pi. \quad (2.20)$$

The real numbers U will be called fusing angles, and as a consequence of (2.20) can be drawn as in figure 9.

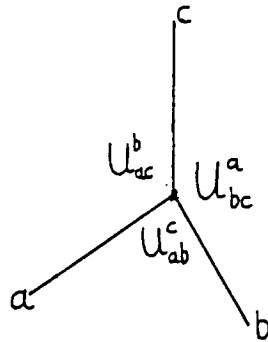


Figure 9.

Note also that (2.19) implies that the 'dual' diagram to figure 9 is a triangle with sides given by the masses of the participating particles, shown in figure 10.

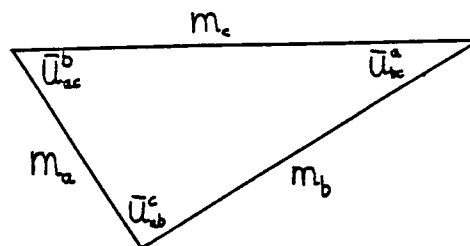


Figure 10.

The internal angles marked in the triangle are defined by

$$\bar{U}_{ab}^c = \pi - U_{ab}^c. \quad (2.21)$$

(Since $m_c = m_{\bar{c}}$, it is acceptable to be fairly cavalier about the distinction between particle and antiparticle in this particular context.) Viewing figure 5 from the side shows that $S_{a\bar{b}}$ is expected to have a pole (with opposite residue) at \bar{U}_{ab}^c , given that S_{ab} has a pole at U_{ab}^c , exactly in agreement with the crossing relation (2.16).

The reality of all fusing angles U , equivalent to the closing of the triangle drawn in figure 10 whenever C^{abc} is nonvanishing, is necessary to ensure stability of the particles in the theory. Otherwise, a fusing $ab \rightarrow \bar{c}$ would occur above threshold, in a kinematically accessible region, and there would be nothing to prevent the decay of particle c into an \bar{a}, \bar{b} pair, in violation of the assumption that c was a possible asymptotic state.

Note that if such a fusing were permitted, then near the resonance pole a long-lived intermediate particle would be formed, and the two-particle state with appropriate rapidity difference should be dominated for a time by the corresponding one-particle state. (It is helpful to think in terms of wave packets at this stage.) The idea behind the bootstrap equations is that this picture can be analytically continued to the below-threshold rapidity differences corresponding to the bound state poles actually observed in the integrable theories.

In other words, near $\theta_{ab} = iU_{ab}^c$, the two particle state $|A_a(\theta_a)A_b(\theta_b)\rangle$ should be dominated by the one particle state $|A_{\bar{c}}(\theta_c)\rangle$, with $\theta_{\bar{c}} = \theta_a + i\bar{U}_{ac}^b$. (The value of $\theta_{\bar{c}}$ is fixed by momentum conservation.) This has consequences both for the S-matrix elements and the conserved charges.

First, the S-matrix. The idea of the two-particle state being dominated for a time by a one-particle state allows diagram (b) of figure 3 to be 'expanded', as shown in figure 11.

Using the conserved charges to move from this picture to that represented by figure 3(a) and equating the corresponding two expressions yields

$$S_{d\bar{c}}(\theta) = S_{da}(\theta - i\bar{U}_{ac}^b)S_{db}(\theta + i\bar{U}_{bc}^a). \quad (2.22)$$

(In fact (2.22) corresponds to equating two expressions for the residue of a pole in the three-particle S-matrix, as a common pole factor of $S_{ab}(\theta_{ab})$ has been cancelled from both sides.) Equation (2.22) is represented pictorially in figure 12.

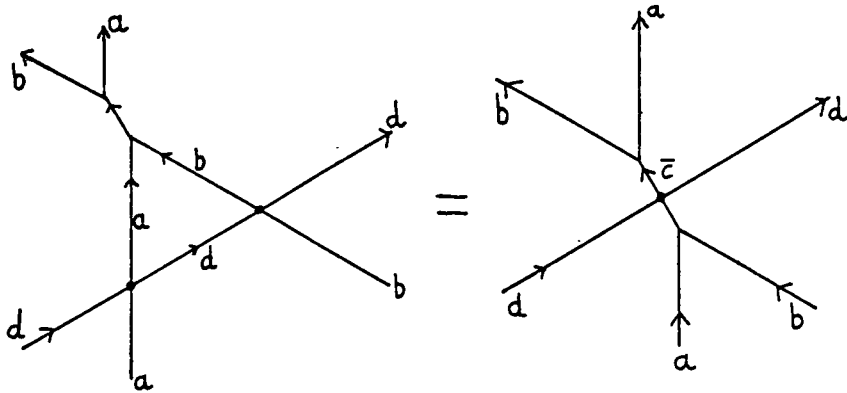


Figure 11.

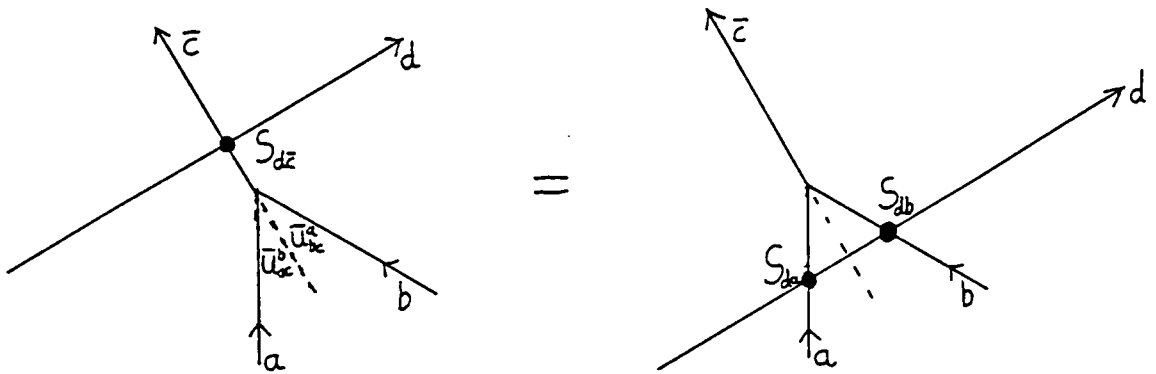


Figure 12.

Furthermore, any conserved charge can be evaluated either before or after the fusing of the two particles in figure 12, and at resonance the result should be the same. An analyticity assumption for the conserved quantities allows (2.3) to be continued to the relevant region of θ , giving the bootstrap condition for the conserved charges:

$$\gamma_s^{\bar{c}} = \gamma_s^a e^{-is\bar{U}_{ac}^b} + \gamma_s^b e^{is\bar{U}_{bc}^a}. \quad (2.23)$$

Taking (2.23) for all possible fusings yields an overdetermined set of linear equations between the constants γ_s^a at given s . These may well have no solution, in which case $P_s \equiv 0$. For $s = 1$, (2.23) is automatically satisfied as it is just the condition of momentum conservation already used in the derivation of (2.19). The surprise is that there are sets of masses (*ie* values for γ_1^a) such that nontrivial solutions to (2.23) exist for larger values of s , these values being the spins at which conserved charges might consistently exist in the theory. Note also that (2.23) shows that there *are* solutions to (2.5) other than the 'trivial' case for which $m = n$, but since these solutions only exist for isolated values of

momenta, and unphysical ones to boot, this does not affect the conclusion that inelastic scattering is forbidden by the conserved quantities.

Similarly (2.22) yields an overdetermined set of functional equations for the two-particle S-matrix elements. It reduces the problem of finding the full S-matrix one stage further, as now only members of a suitable subset of 'fundamental' S-matrix elements need to be found, the others following via (2.22). Often S_{11} , the S-matrix element for the scattering of two lightest particles, is enough. Checks on any ansatz for S_{11} come from the many equations left in the set (2.22) even after some have been used to deduce the rest of the S-matrix.

Based as they are on a single physical idea, it would be surprising indeed if (2.22) and (2.23) were unrelated. In fact a formal connection between the two sets of equations can be established, and the remainder of this section will be devoted to showing how this works.^[6]

First, define a new matrix T :

$$T_{ab}(\theta) \equiv \frac{d}{d\theta} \ln S_{ab}(\theta).$$

Taking the logarithmic derivative of (2.22),

$$T_{d\bar{c}}(\theta) = T_{da}(\theta - i\bar{U}_{ac}^b) + T_{db}(\theta + i\bar{U}_{bc}^a). \quad (2.24)$$

Now T is $2\pi i$ periodic, so at least formally it can be expanded as a fourier series in $i\theta$:

$$T_{ab}(\theta) = \sum_{-\infty}^{\infty} t_s^{ab} e^{s\theta}.$$

As a consequence of (2.24), the coefficients t_s^{ab} must satisfy

$$t_s^{d\bar{c}} = t_s^{da} e^{-is\bar{U}_{ac}^b} + t_s^{db} e^{is\bar{U}_{bc}^a}, \quad (2.25)$$

an equation which has the same form as (2.23). Hence for any particle type d in the theory, the set of numbers $(t^d)_s^a$, found as fourier components of the logarithmic derivative of the S-matrix, solve the bootstrap equations for the conserved quantities and hence provide candidates for the numbers γ_s^a .

The appearance of the S-matrix in this context is reminiscent of the situation in lattice models where conserved quantities appear as the logarithmic derivative of the transfer matrix. This similarity is all the more marked if the correspondence between factorized S-matrices and lattice models^[43] is recalled, in which the transfer matrix is produced by scattering one particular particle across all the others. Of course, these are all models with non-trivial Yang-Baxter structure, and the conserved quantities are thought of in a rather different sense. Despite these provisos, it would be interesting to pursue this connection, and perhaps find some alternative physical insights into the bootstrap equations from the lattice analogy.

Leaving such speculations to one side, there are still a number of immediate implications. These come from the unitarity and crossing relations (2.16). Unitarity gives

$$T_{ab}(\theta) = T_{ab}(-\theta) \ ; \ t_s^{ab} = t_{-s}^{ab},$$

while crossing symmetry becomes

$$T_{a\bar{b}}(\theta) = -T_{ab}(i\pi - \theta) \ ; \ t_s^{ab} = (-)^{s+1} t_{-s}^{a\bar{b}}.$$

Taken together these two equations hint that $\gamma_s^{\bar{a}} = (-)^{s+1} \gamma_s^a$. However this does not provide a proof, as in particular the overall normalization of γ_s^a may well differ from that of $(t^d)_s^a$. Fortunately a direct proof from (2.23) is easily found:

First, note that if C^{abc} is non-zero, then so also is $C^{\bar{a}\bar{b}\bar{c}}$. Taking (2.23) for the fusings $ab \rightarrow \bar{c}$ and $\bar{a}\bar{c} \rightarrow b$ gives

$$\begin{aligned} \gamma_s^{\bar{c}} &= \gamma_s^a e^{-is\bar{U}_{ac}^b} + \gamma_s^b e^{is\bar{U}_{bc}^a}, \\ \gamma_s^b &= \gamma_s^{\bar{c}} e^{-is\bar{U}_{bc}^a} + \gamma_s^{\bar{a}} e^{is\bar{U}_{ab}^c}. \end{aligned}$$

Substituting for γ_s^b from the second equation into the first, subtracting $\gamma_s^{\bar{c}}$ from both sides and using the consequence of (2.20) that $\bar{U}_{ab}^c + \bar{U}_{bc}^a + \bar{U}_{ca}^b = \pi$ then gives the desired result:

$$\gamma_s^{\bar{a}} = (-)^{s+1} \gamma_s^a. \tag{2.26}$$

Note in particular that for a theory with only self-conjugate particles, all even spin conserved charges should vanish. This matches well with the results in specific models to be described below.

Finally, it should be noticed that while a solution of (2.22) implies a solution of (2.23), the reverse does not hold. This is because in taking the logarithmic derivative of S the normalization has been lost, and so a solution of (2.24) will not necessarily integrate up to solve the full bootstrap relation (2.22). This is unfortunate because, at least for the Toda theories to be treated below, the form of the conserved charges is better understood than that of the S-matrix. In some senses (2.23) is a classical equation, while (2.22) involves some of the essentially quantum mechanical aspects of the problem. More will be said on this question later, when some of the problems encountered when trying to construct consistent S-matrices for specific models are described.

Chapter 3

Classical Affine Toda Field Theory

3.1 Introduction

The previous two chapters were concerned with non-perturbative approaches to field theories. Both dealt with attempts to use very general properties to deduce constraints on possible models. In each case, there remains the problem of identifying any solution to the constraints with a particular field theory, and the question as to whether the general properties assumed actually hold. For these reasons it is of interest to find explicit examples. The affine Toda theories to be described below are particularly well suited to studying the bootstrap equations, as they seem to be free from any multiplet structure. Furthermore, the coupling constant allows the development of a perturbative treatment for comparison with any non-perturbative hypothesis for an exact S-matrix. In addition to providing a check for the non-perturbative results, such studies may eventually yield new insights into the workings of perturbation theory, applicable in situations where integrability does not hold.

One further remark before entering into details. In conformal field theory, the standard illustrative example is a theory of free massless bosons, perhaps compactified on a torus. It is tempting to claim a similar rôle in the context of exact S-matrices for the Toda theories — in particular, their lack of Yang-Baxter structure mirrors the trivial monodromy properties of the free boson theory, and in both cases standard field-theoretic techniques based on an explicit lagrangian seem to be reliable. This point is of some importance, as a further motivation for the study of the Toda theories was the thought that they might provide explicit realizations for some of the perturbed conformal theories discussed in chapter one. As will become clear below, it seems that they are indeed examples of theories possessing exact S-matrices with the correct spin-spectrum of conserved charges. However the fact that the relevant conformal theories belong to the minimal sequences — in particular, they do not have a straightforward lagrangian formulation — is perhaps a first sign that there may be some difficulties with the hoped-for identification.

This chapter deals with certain classical features of the theory, while the next chapter

goes on to use these results in a discussion of the quantum theory.

3.2 The Classical Lagrangian

Classically, affine Toda field theory^[48-51] is a massive integrable 1+1 dimensional theory of r (say) scalar fields ϕ^a , with lagrangian

$$\mathcal{L} = \frac{1}{2} \partial_\mu \phi^a \partial^\mu \phi^a - \frac{m^2}{\beta^2} \sum_{i=0}^r n_i e^{\beta \alpha_i \cdot \phi}. \quad (3.1)$$

The set of r -dimensional vectors $\{\alpha_i\}$ is described by one of the affine Dynkin diagrams, and integers n_i can always be found such that $\sum n_i \alpha_i = 0$. The possible diagrams can be found in [52] and are listed in tables 5 and 6, together with the set $\{n_i\}$ for each case.

A feature of these diagrams is that in each case the removal of a suitably chosen spot results in a non-affine Dynkin diagram. It is convenient to label the vectors so that α_0 corresponds to the removed spot, candidates for which can then be found using the facts that $n_0 = 1$ and that the residual diagram is connected. The remaining vectors $\{\alpha_1, \dots, \alpha_r\}$ are the simple roots for one of the simple Lie algebras. For the untwisted affine diagrams, α_0 is the lowest root of the algebra, and so given that $n_0 = 1$ the numbers n_1, \dots, n_r also appear as the coefficients of the highest root $\psi = \sum_{i=1}^r n_i \alpha_i$.

The lagrangian can now be split into two pieces,

$$\begin{aligned} \mathcal{L} &= \frac{1}{2} \partial_\mu \phi^a \partial^\mu \phi^a - \frac{m^2}{\beta^2} \sum_{i=1}^r n_i e^{\beta \alpha_i \cdot \phi} - \frac{m^2}{\beta^2} n_0 e^{\beta \alpha_0 \cdot \phi} \\ &\equiv \mathcal{L}_0 + \mathcal{L}_1 \end{aligned} \quad (3.2)$$

where \mathcal{L}_1 is the final term containing α_0 and \mathcal{L}_0 the rest. This split is interesting because the piece \mathcal{L}_0 is the lagrangian for a non-affine Toda theory, which has a form of conformal invariance. To see this, consider a conformal transformation which acts on the light cone coordinates $x^\pm = x \pm t$ as

$$x^\pm \rightarrow x'^\pm = f^\pm(x^\pm).$$

If this is accompanied by a shift in the fields

$$\phi \rightarrow \phi'(x') = \phi(x) - \frac{\delta}{\beta} \ln(\partial_+ f^+ \partial_- f^-),$$

where δ is the sum of the fundamental weights, then up to total derivatives \mathcal{L}_0 is multiplied by $\partial_+ f^+ \partial_- f^-$. This is exactly the local scale factor, so the integrated lagrangian is indeed

invariant. The key property of δ which ensures that the potential term scales correctly is

$$\delta \cdot \alpha_i = 1 \quad i = 1, \dots, r. \quad (3.3)$$

Alternatively, note that the potential term in \mathcal{L}_0 is always positive, but that the linear independence of $\alpha_1, \dots, \alpha_r$ means that a direction in field space may be found along which $\alpha_i \cdot \phi \rightarrow -\infty$ for $i = 1, \dots, r$. Along this direction the potential tends towards its lower bound of zero, becoming flatter and flatter as it does so. In an intuitive sense, the classical ground state is at infinite distance from the origin in field space, and about that point the potential is flat in all directions — a sign of conformal invariance. However the lack of a true classical ground state makes quantization of this model in a perturbative framework difficult. It turns out that the quantum theory *is* conformal, with a central charge given by^[53, 54]

$$c = r + 48\pi|\delta|^2 \left(\frac{1}{\beta} + \frac{\beta}{4\pi} \right)^2. \quad (3.4)$$

(Even classically, the Poisson bracket algebra of conformal transformations has a central charge — this arises from the total derivative terms in the transformation of \mathcal{L} .) A link can be made between each non-affine Toda theory and the series of minimal conformal theories based on the corresponding Lie algebra. To obtain the correct central charge, the coupling constant β must be tuned correctly, and in fact one must indulge in some kind of analytic continuation in β before (3.4) will yield a value small enough. Hence, \mathcal{L}_0 does not provide a straightforward lagrangian framework for the minimal models, and the subtleties encountered will not be entered into here. The reason for mentioning this splitting of the affine lagrangian at all is that it provided one of the original motivations for looking at the affine Toda theories in the context of perturbed conformal field theory.^[5]

To see why this should be so, consider the reverse procedure, of *starting* with the non-affine lagrangian \mathcal{L}_0 and then adding an extra ('perturbing') piece \mathcal{L}_1 . (Any small coefficient multiplying the perturbation can be absorbed into a shift of origin in field space.) Classically both non-affine and affine theories are integrable, and furthermore the affine theories are known to possess conserved charges with spins given by the exponents of the relevant Lie algebra. Conformal invariance is lost in the perturbation, the affine theory having a well defined ground state about which there are only massive excitations. This can also be seen in the fact that \mathcal{L}_1 does not scale in the same way as the other

terms in the potential under the combined conformal transformation and field shift defined above, since instead of (3.3) α_0 satisfies

$$\delta \cdot \alpha_0 = - \sum_{i=1}^r n_i = 1 - h,$$

where h is the Coxeter number of the algebra.* Thus, this picture certainly provides a classical model for the idea of an integrable perturbation of a conformal theory. The unanswered question is whether this remains valid in the quantum domain. A promising sign is that in the non-affine theories thought to be related to the minimal coset models, the perturbing term \mathcal{L}_1 represents the primary field associated with the $(0, \text{adj})$ pair of representations, already mentioned above as important. Furthermore the spectrum of conserved spins possessed by the classical affine theory is given by the exponents of the relevant Lie algebra,^[48, 50] and if preserved on quantization is exactly that hypothesised for such perturbations at the end of chapter one. However the necessity to choose β to be imaginary is a hint of potential trouble ahead.

If one is merely interested in a lagrangian model for theories possessing purely elastic S-matrices with which to check the assumptions made in the last chapter, then such questions should not be a worry. Putting aside the issue as to whether they correspond to precisely the perturbed theories considered in chapter one, there remains the question of the quantum integrability and S-matrix of the affine Toda theories defined by (3.1) (with β real). A perturbative treatment of these theories appears to be perfectly valid, and when it is combined with some non-perturbative hypotheses culled from the last chapter a number of interesting features emerge. The remainder of this chapter and all of the next will be devoted to this task, with other questions only being returned to in the final chapter.

3.3 Classical Data for the Simply-Laced Theories

The coupling constant β will henceforth be taken to be a small, *real*, parameter, so the usual perturbative techniques of quantum field theory should apply. Before going into this, some classical information must be extracted from (3.1).

* Note that this does *not* of itself imply any asymmetry between α_0 and the other vectors α_i once the full lagrangian (3.1) is considered, as the field shift was defined with \mathcal{L}_0 specifically in mind.

The first step is to expand the potential term perturbatively in β (the coupling constant) about its minimum at $\phi^a = 0$, $a = 1, \dots, r$:

$$\begin{aligned}
 V(\phi) = & \frac{m^2}{\beta^2} \sum_{i=0}^r n_i + \frac{m^2}{2} \sum_{i=0}^r n_i \alpha_i^a \alpha_i^b \phi^a \phi^b \\
 & + \frac{m^2 \beta}{3!} \sum_{i=0}^r n_i \alpha_i^a \alpha_i^b \alpha_i^c \phi^a \phi^b \phi^c + \dots
 \end{aligned} \tag{3.5}$$

This results in a (mass)² matrix

$$(M^2)^{ab} = m^2 \sum_{i=0}^r n_i \alpha_i^a \alpha_i^b, \tag{3.6}$$

a set of three-point couplings

$$C^{abc} = \beta m^2 \sum_{i=0}^r n_i \alpha_i^a \alpha_i^b \alpha_i^c, \tag{3.7}$$

and infinitely many higher couplings, of successively higher orders in β .

Low order perturbation theory will be simplest if a basis of fields is taken for which the bare propagator is diagonal. This diagonalizes (M^2) , the classical masses emerging as the eigenvalues of (M^2) . To compute the three point couplings (3.7) in this basis of mass eigenstates is a lengthy task, but answers in closed form can be obtained for all the affine Toda field theories.

A simplification comes from the fact that detailed calculations need only be carried out for the simply laced theories (associated to the untwisted a, d, e affine diagrams for which all roots have equal length), results for the other theories following from a folding procedure^[55] to be described in a later section. The remainder of this section will concentrate on the simply laced theories, the results for which reveal a number of particularly simple ‘universal’ features. No real understanding exists for these features — they were only observed after a case-by-case examination of the individual theories. However they seem to be vital for quantum integrability, and before giving details of each theory in turn, these general results will be described.

The first surprise is that the classical masses computed as the r eigenvalues of the (mass)² matrix (3.6) form an eigenvector of the Cartan matrix of the associated Lie

algebra. (Note that for the simply-laced theories, each affine diagram is an extension of one and only one non-affine diagram, so there is no ambiguity here.) More precisely, they form the eigenvector of lowest eigenvalue, $2 - 2 \cos \frac{\pi}{h}$, the Perron-Frobenius eigenvector of the adjacency matrix of the non-affine diagram. (As usual, h is the Coxeter number of the algebra.) Thus if (with a suitable ordering)

$$\mathbf{m} = (m_1, m_2, \dots, m_r)$$

then

$$C\mathbf{m} = \lambda_{min}\mathbf{m} = (2 - 2 \cos \frac{\pi}{h})\mathbf{m}, \quad (3.8)$$

C being the Cartan matrix

$$C_{ij} = \frac{2\alpha_i \cdot \alpha_j}{\alpha_j^2} \quad i, j = 1, \dots, r.$$

The Perron-Frobenius theorem guarantees that all the components of this vector can be taken positive, consistent with their identification with the particle masses.

This result is particularly curious since it shows that the affine diagram involved in the definition of (M^2) somehow 'knows' about its non-affine subdiagram. This feature allows the masses to be associated unambiguously to spots on the appropriate non-affine diagram. Table 7 shows how this works, the labels being in increasing order of mass with the convention of chapter 2 applying, that \bar{a} labels the antiparticle of a . The masses themselves can be extracted from table 8, which gives *all* the eigenvectors of the Cartan matrices, by setting $s = 1$. (The other eigenvectors will be needed later, for a generalization of (3.8).) Note though that the eigenvector result only gives information on the ratios of the classical masses, but not on their overall normalization which *is* fixed in terms of m^2 in the classical affine Toda theory. Since m^2 is arbitrary and plays no part in subsequent calculations (and is in any case renormalized in the quantum theory), the eigenvectors in table 8 have been given a simple form by assuming m^2 to have been set to a suitable value in each case. For reference, the 'raw' values for the squared masses, obtained from the characteristic equation for (M^2) , are listed below.

$$\begin{aligned}
 \mathbf{A}_n \text{ series} \quad m_a^2 &= 4m^2 \sin^2 \frac{a\pi}{n+1} \\
 \mathbf{D}_n \text{ series} \quad m_s^2 &= m_{s'}^2 = 2m^2 \\
 & m_a^2 = 8m^2 \sin^2 \frac{a\pi}{2(n-1)} \\
 \mathbf{E}_6 \quad m_1^2 &\equiv m_1^2 = (3 - \sqrt{3})m^2 \\
 & m_2^2 = 2(3 - \sqrt{3})m^2 \\
 & m_3^2 \equiv m_3^2 = (3 + \sqrt{3})m^2 \\
 & m_4^2 = 2(3 + \sqrt{3})m^2 \\
 \mathbf{E}_7 \quad m_1^2 &= 8m^2 \sin^2 \frac{\pi}{9} \\
 & m_2^2 = 8\sqrt{3}m^2 \sin \frac{\pi}{18} \sin \frac{2\pi}{9} \\
 & m_3^2 = 8m^2 \sin^2 \frac{2\pi}{9} \\
 & m_4^2 = 8\sqrt{3}m^2 \sin \frac{5\pi}{18} \sin \frac{\pi}{9} \\
 & m_5^2 = 6m^2 \\
 & m_6^2 = 8m^2 \sin^2 \frac{4\pi}{9} \\
 & m_7^2 = 8\sqrt{3}m^2 \sin \frac{7\pi}{18} \sin \frac{4\pi}{9} \\
 \mathbf{E}_8 \quad m_1^2 &= 4\sqrt{3}m^2 \sin \pi/30 \sin \pi/5 \\
 & m_2^2 = 16\sqrt{3}m^2 \sin \pi/30 \sin \pi/5 \cos^2 \pi/5 \\
 & m_3^2 = 16\sqrt{3}m^2 \sin \pi/30 \sin \pi/5 \cos^2 \pi/30 \\
 & m_4^2 = 64\sqrt{3}m^2 \sin \pi/30 \sin \pi/5 \cos^2 \pi/5 \cos^2 7\pi/30 \\
 & m_5^2 = 4\sqrt{3}m^2 \sin 11\pi/30 \sin \pi/5 \\
 & m_6^2 = 4\sqrt{3}m^2 \sin 7\pi/30 \sin 2\pi/5 \\
 & m_7^2 = 4\sqrt{3}m^2 \sin 13\pi/30 \sin 2\pi/5 \\
 & m_8^2 = 256\sqrt{3}m^2 \sin \pi/30 \sin \pi/5 \cos^2 2\pi/15 \cos^4 \pi/5.
 \end{aligned}$$

One final observation is that the mass ratios above coincide with those found by Ogievetsky and Wiegmann^[56] for some rather different S-matrices, namely those possessing a Lie group symmetry. In contrast to the affine Toda models, these have a multiplet structure, and a non-trivial Yang-Baxter equation to be satisfied. Each multiplet is taken to belong to a (fundamental) representation of the Lie group, and scattering amplitudes are required to be invariant under simultaneous group transformations of all

particles involved. This fixes the mass ratios to be equal to those found for the Toda theories. Furthermore, since each fundamental representation is associated with a single spot on the Dynkin diagram (the highest weight λ^a of a fundamental representation satisfies $\lambda^a \cdot \alpha_b = \delta_b^a$, $b = 1, \dots, r$), each multiplet of the Lie group invariant S-matrices can also be assigned unambiguously to a spot on a non-affine diagram; this assignment agrees with that given above for the Toda particles.* Note that the appearance of non-affine diagrams is much less surprising here than it was in the affine Toda theory, given that the explicit symmetry of the theory is described by the non-affine algebra. The coincidence of the two sets of masses may well lead to deeper insights into the bootstrap, if properly understood.

The three point couplings C^{abc} also exhibit 'unreasonably' simple features when given in a basis of mass eigenstates. Many vanish; for those that don't, the masses involved form a triangle and the magnitude of the coupling is given by^[11, 8]

$$|C^{abc}| = \frac{4\beta}{\sqrt{h}} \Delta^{abc} = \frac{2\beta}{\sqrt{h}} m_a m_b \sin U_{ab}^{\bar{c}}, \quad (3.9)$$

where Δ^{abc} is the area of the triangle in question and $U_{bc}^{\bar{c}}$ the fusing angle defined in (2.20). The triangle is exactly that drawn in figure 10; the fact that objects of interest in the bootstrap equations of the last chapter are also emerging from the Toda theory is a promising sign. Even better, the fusing angles obtained from the non-vanishing Toda couplings have a particularly nice form: they, and hence all the angles in the triangle $m_a m_b m_c$, are all multiples of π/h :

$$U_{ab}^{\bar{c}} = \frac{n\pi}{h}, \quad n \in \mathbb{Z}. \quad (3.10)$$

This empirical rule in fact characterizes the non-vanishing couplings, at least when there are no mass degeneracies (when there are, the Clebsch-Gordon rule below must also be used). Note though that the signs of the couplings have not yet been given. These are important but to date no general rule has been found for their determination, so reference must be made to the individual tables for these.

An alternative and perhaps deeper selection rule can be given for the allowed couplings. Recall from above the association of particles with fundamental representations. In the

* Actually, this description is something of an oversimplification. Particles in fact transform under (isomorphic) left and right representations of the group, and furthermore some of these representations are reducible. However each reducible representation may be associated with a unique fundamental representation, so the correspondence with Toda particles can still be made.

context of group-invariant S-matrices it is expected that a three-point coupling will only be found between multiplets when a singlet can be found in the tensor product of their three representations. The same rule holds for the Toda couplings^[14, 9]; in symbols

$$C^{abc} \neq 0 \Rightarrow (a) \otimes (b) \supset (\bar{c}) \quad (3.11)$$

where $(a), (b)$ and (c) are the three fundamental representations associated with particles a, b and c . (Note that $(\bar{c}) = \overline{(c)}$; the antiparticle is always associated with the conjugate representation.) The implication does not hold in the reverse direction except for the A_n and D_4 theories, and the ‘holes’ in the Clebsch-Gordon series that this entails are not well understood, except to say that in every case, allowing the coupling would violate (3.10). The first example appears in the D_5 theory: in the Clebsch-Gordon series $(2) \otimes (2) \supset (2)$, but according to the rules to be given below, the $2 \ 2 \rightarrow 2$ fusing does not occur. The fusing angle such a coupling would imply is $2\pi/3$, which is not an integer multiple of π/h since for D_5 , $h = 8$. Such holes do not seem to have been emphasised in the work of Ogievetsky and Wiegmann, possibly because the bootstrap is so much harder to carry through when multiplets are present. They are perhaps a sign that group theory alone is not enough to unravel the bootstrap, and at the very least some form of truncation rule must be defined when fusing particles or multiplets. This would be reminiscent of, although it cannot be the same as, the situation found in the Wess-Zumino-Witten models.^[34]

In the absence of general proofs for any of the above, a case-by-case treatment is the best that can be achieved, and this will now be given. Before detailing the individual cases, there is one more general comment to be made. A number of theories turn out to have degeneracies in their mass spectrum, so the basis for fields is not completely fixed by the requirement that the $(\text{mass})^2$ matrix be diagonal — there remains the freedom to rotate the basis within the mass eigenspaces. However this symmetry does not persist when higher terms in (3.5) are examined, and in particular the three-point couplings *do* depend on the particular basis chosen in each eigenspace. To resolve the ambiguity in the couplings that this implies, the higher spin conserved charges must be considered. Diagonalizing the $(\text{mass})^2$ matrix amounts to ensuring that the spin 1 conserved charge — the momentum — is diagonal, but for the discussion of purely elastic scattering in the last chapter to apply, a basis of eigenstates of *all* the higher spin charges is needed. The assumption made in that discussion, that all particles may be distinguished by these charges, is precisely the requirement that any ambiguities of basis are resolved once all

charges are diagonalized. However there is little detailed information on the form of these charges, so in practice one must work 'backwards' via the bootstrap consistency conditions (2.24). This set of equations is dependent on the non-vanishing three couplings and hence feels the effect of the basis taken for the mass-degenerate fields. The choices made below were motivated by the requirement that (2.24) should have nontrivial solutions for as many values of the spin s as possible, and will only be fully justified in a later section. There it will be shown that these choices allow conserved charges corresponding to all spins found in the classical theory (*ie* the exponents of the algebra) and that these charges *do* distinguish all the particles.

In fact, a complex basis will occasionally be necessary, leading to non self-conjugate particles (recall the remark at the end of the last chapter that only on such particles can a (diagonal) even spin charge be non-zero). In these cases, it is natural to define the (mass)² matrix to connect particle with antiparticle (in other words, to consider one of its indices to be outgoing rather than ingoing). However three point couplings will always refer to all particles as ingoing, a point to be borne in mind when considering possible fusings.

$$\mathbf{a}_n^{(1)} \equiv \bar{D}(A_n)$$

Easiest to describe is the $n = 1$ case, for which (3.1) is just the sinh-Gordon lagrangian. There is a single massive particle and zero three point coupling. For this reason the theory is rather special, and the techniques of later sections cannot be applied directly — certainly higher order couplings do not vanish, so a trivial S-matrix is not expected, but equally perturbation theory does not predict any bound state poles. This case will therefore receive a separate mention when the quantum theory is discussed, and for now it will not be considered further.

In all other cases, a basis must be chosen so that the (mass)² matrix (3.6) is diagonal. For $\mathbf{a}_n^{(1)}$, this is relatively easy because of a special relationship with the roots of unity. Let $\omega = e^{2i\pi/n+1}$ so that $\omega^{n+1} = 1$, and consider the spray of vectors γ_i with complex components given by

$$\gamma_i^a = \omega^{ia} \quad i = 0, 1, \dots, n \quad a = 1, \dots, n. \quad (3.12)$$

Then their inner products, using the fundamental property of ω , $\sum_0^n \omega^k = 0$, are

$$\gamma_i^* \cdot \gamma_j = (n + 1)\delta_{ij} - 1,$$

and hence setting

$$\alpha_i = \frac{1}{\sqrt{n+1}}(\gamma_{i+1} - \gamma_i)^* \quad (3.13)$$

gives a complex representation of the simple roots of A_n , together with the extra root α_0 . It is easy to check that $\sum_{i=0}^n \alpha_i = 0$ and

$$\alpha_i^* \cdot \alpha_j = \begin{cases} 0 & i \neq j, j \pm 1 \\ -1 & i = j \pm 1 \\ 2 & i = j \end{cases}$$

as desired. Note too, that a choice of complex basis for the scalar fields in which

$$(\phi^a)^* = \phi^{n+1-a}$$

has the nice property

$$(\alpha_i^* \cdot \phi)^* = \alpha_i^* \cdot \phi \quad (3.14)$$

as a consequence of the definitions (3.12) and (3.13). Property (3.14) implies that the potential term in the Lagrangian is real when Lagrangian is taken to be

$$\mathcal{L} = \frac{1}{2} \partial \phi^* \partial \phi - \frac{m^2}{\beta^2} \sum_{i=0}^n e^{\beta \alpha_i^* \cdot \phi}.$$

In this basis, the (mass)² matrix (3.6) is

$$\begin{aligned} (M^2)^{ab} &= \frac{m^2}{n+1} \sum_{i=0}^n (\gamma_{i+1}^* - \gamma_i^*)^a (\gamma_{i+1} - \gamma_i)^b \\ &= \begin{cases} 0 & a \neq b \\ 4m^2 \sin^2 \frac{a\pi}{n+1} & a = b \end{cases} \end{aligned}$$

and is diagonal, the masses being

$$m_a = 2m \sin \frac{a\pi}{n+1} \quad a = 1, \dots, n. \quad (3.15)$$

Thus, each particle (except for one when n is odd), occurs with its mass degenerate conjugate partner. When n is odd, the heaviest particle occurs as a singlet. This degeneracy

is a reflection of the obvious \mathbb{Z}_2 symmetry of the A_n Dynkin diagram. The choice of a complex basis, with degenerate particles occurring in conjugate pairs, leaves open the possibility of these particles being eigenstates of an even spin charge in the quantum theory (making the charge diagonal in this basis). This is desirable, given the fact that some of the exponents of A_n are even.

The three-point couplings of the mass eigenstates are also easily computable from

$$\sum_{i=0}^n \alpha_i^{*a} \alpha_i^{*b} \alpha_i^{*c} = \begin{cases} 0 & a + b + c \neq 0 \pmod{n+1} \\ \frac{1}{\sqrt{n+1}} (\omega^a - 1)(\omega^b - 1)(\omega^c - 1) & a + b + c = 0 \pmod{n+1}. \end{cases} \quad (3.16)$$

Noting from (3.15) that

$$m^2(\omega^a - 1)(\omega^b - 1) = -\omega^{\frac{a+b}{2}} m_a m_b,$$

it is clear that provided $c = k(n+1) - (a+b)$ (for $k = 1$ or 2) the product combination in (3.16) may be re-expressed as

$$m^2(\omega^a - 1)(\omega^b - 1)(\omega^c - 1) = m_a m_b 2i \sin \frac{(a+b)\pi}{n+1}. \quad (3.17)$$

The fusing angles, found from (2.20), are

$$U_{ab}^c = \begin{cases} \frac{a+b}{n+1}\pi & a + b + c = n + 1 \\ (2 - \frac{a+b}{n+1})\pi & a + b + c = 2(n + 1). \end{cases} \quad (3.18)$$

Thus the magnitude of the coupling constant is given by

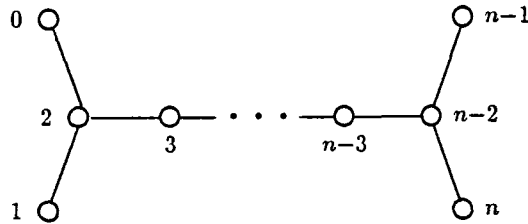
$$|C^{abc}| = \frac{2\beta}{\sqrt{n+1}} m_a m_b \sin U_{ab}^c, \quad (3.19)$$

verifying (3.9) in this case, since the Coxeter number of A_n is $n+1$. Finally, (3.11) is easily verified given that the fundamental representations appearing in the decomposition of the relevant A_n tensor products are

$$(a) \otimes (b) = \begin{cases} (a+b) + \dots, & a+b < n, \\ (a+b-n) + \dots, & a+b \geq n. \end{cases}$$

$$d_n^{(1)} \equiv \bar{D}(D_n)$$

In this case there is rather less mass degeneracy and initially a real basis will be taken. Labelling the affine diagram as follows



the roots are expressible in terms of n orthonormal vectors e_i :

$$\begin{aligned} \alpha_0 &= -(e_1 + e_2) & \alpha_n &= e_{n-1} + e_n \\ \alpha_i &= e_i - e_{i+1} & i &= 1, 2, \dots, n-1. \end{aligned} \quad (3.20)$$

These orthonormal vectors must now be re-expressed in a basis for which the (mass)² matrix is diagonal. One way is to take

$$\begin{aligned} e_1 &= (0, 0, \dots, 1, 0) \\ e_n &= (0, 0, \dots, 0, 1) \\ e_{k+1} &= (l_k^1, l_k^2, \dots, l_k^{n-2}, 0, 0) \quad k = 1, 2, \dots, n-2 \end{aligned} \quad (3.21)$$

where

$$l_k^a = \sqrt{\frac{2}{n-1}} \sin \frac{ak\pi}{n-1}.$$

It is then easy to check that the mass matrix is diagonal with (mass)² eigenvalues

$$\begin{aligned} (a) \quad m_{n-1}^2 &= m_n^2 = 2m^2 \\ (b) \quad m_k^2 &= 8m^2 \sin^2 \frac{k\pi}{2(n-1)} \quad k = 1, 2, \dots, n-2. \end{aligned} \quad (3.22)$$

Note with reference to the assignment of masses to the Dynkin diagram, table 7, that the masses of the particles increase along the long arm of the diagram towards the fork in the same sense as the dimensions of the fundamental representations. Occasionally (for $n \equiv 1 \pmod{3}$) the mass of the degenerate pair (3.22)(a) coincides with one of the masses on the arm of the diagram, but in general the dimension of the corresponding spinor

representations does not coincide with any of the others. The algebra D_4 is the exception. It is a particularly symmetrical case with three light particles of mass $\sqrt{2}m$ and a heavy particle of mass $\sqrt{6}m$. In this case the light particles are associated with the vector, spinor and conjugate spinor representations, which *do* have the same dimensionality — a reflection of the triality symmetry of D_4 .

The discrepancy of dimensions mentioned above suggests that the extra degeneracy for $n \equiv 1 \pmod{3}$ is purely accidental, and that the only real freedom left in the choice of basis is a rotation in the space spanned by ϕ^{n-1} and ϕ^n . This turns out to suffice in the case of D_4 also. A distinction can be made between n even and n odd. For n even it is natural to take the degenerate particles to be self-conjugate and set

$$\phi^s = \frac{1}{\sqrt{2}}(\phi^{n-1} + \phi^n) \quad \phi^{s'} = \frac{1}{\sqrt{2}}(\phi^{n-1} - \phi^n). \quad (3.23)$$

In contrast for n odd, D_n has an even exponent (cf table 3), and furthermore the spinor representations are conjugate to each other. These two facts suggest that the corresponding particles should be taken with respect to a complex basis, and motivate the choice

$$\phi^s = \frac{1}{\sqrt{2}}(\phi^{n-1} + i\phi^n) \quad \phi^{\bar{s}} = \frac{1}{\sqrt{2}}(\phi^{n-1} - i\phi^n). \quad (3.24)$$

These choices will only be properly justified later, when conserved charges are discussed and they will be seen to be diagonal in the above bases.

It is now straightforward to read off the three point couplings. Clearly, the coupling between three particles chosen from s or s' is zero whatever the choice of basis in the degenerate subspace, but one effect of the choices (3.24) and (3.23) is to render zero half of the couplings between a pair such as s and s or s' and one of the others. Thus for even n :

$$C^{ssa} = C^{s's'a} = \begin{cases} 0 & a \text{ odd} \\ \frac{2\beta}{\sqrt{2(n-1)}} m_s m_s \sin U_{ss}^a & a \text{ even} \end{cases}$$

$$C^{ss'a} = \begin{cases} \frac{2\beta}{\sqrt{2(n-1)}} m_s m_{s'} \sin U_{ss'}^a & a \text{ odd} \\ 0 & a \text{ even} \end{cases} \quad (3.25)$$

On the other hand, for n odd:

$$\begin{aligned}
 C^{ssa} = C^{s\bar{s}a} &= \begin{cases} \frac{2\beta}{\sqrt{2(n-1)}} m_s m_{\bar{s}} \sin U_{s\bar{s}}^a & a \text{ odd} \\ 0 & a \text{ even} \end{cases} \\
 C^{s\bar{s}a} &= \begin{cases} 0 & a \text{ odd} \\ \frac{2\beta}{\sqrt{2(n-1)}} m_s m_{\bar{s}} \sin U_{s\bar{s}}^a & a \text{ even} \end{cases} \quad (3.26)
 \end{aligned}$$

In each case, the fusion angles are, in multiples of $\pi/2(n-1)$,

$$U_{s\bar{s}}^a = 2(n-1-a) = U_{s\bar{s}'}^a \quad U_{s\bar{s}}^s = n-1+a = U_{s'\bar{s}}^s = U_{s\bar{s}'}^s. \quad (3.27)$$

For the other particles, the couplings are given by

$$C^{abc} = \begin{cases} -\frac{2\beta}{\sqrt{2(n-1)}} m_a m_b \sin U_{ab}^c & a+b+c = 2(n-1) \\ \frac{2\beta}{\sqrt{2(n-1)}} m_a m_b \sin U_{ab}^c & a \pm b \pm c = 0 \\ 0 & \text{otherwise} \end{cases} \quad (3.28)$$

where the fusion angles are, again in multiples of $\pi/2(n-1)$,

$$U_{ab}^c = a+b \quad U_{ac}^b = a+c \quad U_{bc}^a = b+c \quad \text{if } a+b+c = 2(n-1)$$

and

$$\left. \begin{aligned} U_{ab}^c &= 2(n-1) + a - b \\ U_{bc}^a &= 2(n-1) + c - b \\ U_{ac}^b &= a + c \end{aligned} \right\} \text{if } a - b + c = 0. \quad (3.29)$$

Again, the area formula (3.9) can be verified in equations (3.25), (3.26) and (3.28). The Clebsch-Gordon decompositions for D_n are considerably more involved than for A_n , but again (3.11) is found to hold good. The list below is extracted from appendix C3 of [56]. ((+) and (-) denote the representations (s) and (s') or (s) and (\bar{s}) for n even or odd respectively, (0) denotes the scalar representation, and all other non-fundamental representations are omitted.)

$$\begin{aligned}
 (a) \otimes (b) &= \sum_{p=0}^b (a + b - 2p), \quad a \geq b, \\
 (\pm) \otimes (\pm) &= \begin{cases} (0) + (2) + \dots + (n-2), & k \text{ even,} \\ (1) + (3) + \dots + (n-2), & k \text{ odd,} \end{cases} \\
 (\pm) \otimes (\mp) &= \begin{cases} (1) + (3) + \dots + (n-3), & k \text{ even,} \\ (0) + (2) + \dots + (n-3), & k \text{ odd.} \end{cases}
 \end{aligned}$$

$e_6^{(1)}, e_7^{(1)}$ and $e_8^{(1)}$

The particle masses for these theories have been given above, and their assignments to the relevant Dynkin diagrams are shown in table 7. One feature to note is that the algebra E_6 has an even exponent and so, just as for the $a_n^{(1)}$ and $d_{odd}^{(1)}$ theories, the appropriate choice of basis for the mass degenerate fields of the $e_6^{(1)}$ theory is complex, the scalar fields satisfying the conjugation relations

$$(\phi^1)^* = \phi^{\bar{1}} \quad (\phi^2)^* = \phi^2 \quad (\phi^3)^* = \phi^{\bar{3}} \quad (\phi^4)^* = \phi^4.$$

Note that the conjugation properties again reflect the symmetry of the non-affine diagram.

Calculational details for these theories will be omitted; the results for the three point couplings are summarized in the upper right halves of tables 9, 10 and 11. The conventions adopted in the tables are as follows. The rows and columns are labelled by the particle labels, running from the top left in ascending mass order. The first row in each box lists the possible fusions for the row-column pair corresponding to the box, so for example the top left box of table 9 shows that in the E_6 theory the fusions $1\ 1 \rightarrow \bar{1}$ and $1\ 1 \rightarrow \bar{3}$ may occur, the couplings C^{111} and $C^{11\bar{3}}$ being nonzero (note that couplings consider all particles to be incoming so a charge conjugation is necessary for the outgoing particle of a fusing). The superscript refers to the phase of the coupling (+1 if the superscript is absent) and in all cases, the magnitude of the coupling is given by the area formula (3.9).

The second row lists the fusion angles in multiples of π/h , the Coxeter number h being 12, 18 and 30 for E_6 , E_7 and E_8 respectively. Thus, referring again to table 9, the second row of the top left box shows that $U_{11}^{\bar{1}} = 2\pi/3$ and $U_{11}^{\bar{3}} = \pi/6$ in the E_6 theory.

The two rules (3.9) and (3.10) are almost implicit in the construction of these tables, but they were of course verified by explicit calculations. It is also possible to verify (3.11) for these theories: the relevant data on the Clebsch-Gordon series is contained in the lower left halves of the tables, which list the fundamental representations appearing in the decomposition of each tensor product.

3.4 Folding and the Non Simply-Laced Cases

It would in principle be possible to proceed for these theories in the same manner as above, explicitly diagonalizing the relevant mass matrix in each case and computing the three-point couplings. However, all the necessary information has already been gathered. This follows from the fact that the Dynkin diagrams of these theories may each be obtained by ‘folding’ one and only one of the simply-laced diagrams.^[55] The idea is as follows: a symmetry of the Dynkin diagram, permuting the points as $\alpha \rightarrow p(\alpha)$, corresponds to a mapping of the field space to itself, $\phi \rightarrow p(\phi)$, which is a symmetry of the classical field equations derived from the Lagrangian with the potential (3.1). This means that if the fields initially take values in the subspace invariant under p , they will remain there, at least classically. Since the subspace is of smaller dimension than the original field space, the evolution of fields within it can be described in terms of an equation with fewer variables than the original equation. The latter is obtained by projecting the variables α_i in (3.1) onto the invariant subspace. This process of obtaining new equations and their solutions from old, by exploiting diagram symmetries, is known as reduction. The so-called direct reductions are those such that $\alpha \cdot p(\alpha) = 0$ for each root α (ie the symmetry does not relate points linked by a line on the Dynkin diagram), and these yield the equations for all the non simply-laced and twisted affine theories. ‘Folding’ will be taken to mean a direct reduction of this type, and only these will be considered below, as non-direct reductions in fact lead to nothing new, as explained by Olive and Turok.

For the direct reductions, the projection of the roots of the simply-laced theories onto the invariant subspace under the relevant automorphism yields the roots of the ‘reduced’ theory together with the correct multiplicities n_i . If the fields are themselves invariant under the automorphism p , the projection has no effect—the value of $\alpha \cdot \phi$ is unchanged*—and so the masses and three-point couplings arising from (3.5) for the new theory may be obtained from those of the parent simply by substituting the invariant part of the mass

* But note, when a complex basis is used, for example in the a_n theories, it is $\alpha^* \cdot \phi$ that is unchanged.

eigenstates into the results already derived. This is the strategy that will be adopted below. One immediate observation is that since the automorphism commutes with the $(\text{mass})^2$ matrix, the set of masses in the reduced theory is always a subset of those in the parent. In fact, rather more can be said, based on the distinction between twisted and untwisted diagrams. Before going into details, this will be described.

A symmetry of an extended Dynkin diagram which is also a symmetry of the unextended subdiagram will yield one of the untwisted non simply-laced diagrams shown in table 5, corresponding to the extension of a non-affine diagram by the highest root. In fact the symmetry group of the extended diagram is always at least that of the unextended diagram, as shown by Olive and Turok, and so there may be further possibilities for reductions. These result in affine Toda theories based on the twisted affine Dynkin diagrams, shown in table 6. The various possible 'parent-child' relationships are summarized below. (Details of the specific foldings will be given later.)

Untwisted	Twisted
$d_{n+1}^{(1)} \rightarrow b_n^{(1)} \equiv \bar{D}(B_n)$	$d_{2n}^{(1)} \rightarrow a_{2n-1}^{(2)} \equiv \bar{D}^T(B_n)$
$a_{2n-1}^{(1)} \rightarrow c_n^{(1)} \equiv \bar{D}(C_n)$	$d_{n+2}^{(1)} \rightarrow d_{n+1}^{(2)} \equiv \bar{D}^T(C_n)$
$d_4^{(1)} \rightarrow g_2^{(1)} \equiv \bar{D}(G_2)$	$e_7^{(1)} \rightarrow e_6^{(2)} \equiv \bar{D}^T(F_4)$
$e_6^{(1)} \rightarrow f_4^{(1)} \equiv \bar{D}(F_4)$	$e_6^{(1)} \rightarrow d_4^{(3)} \equiv \bar{D}^T(G_2)$
	$d_{2n+2}^{(1)} \rightarrow a_{2n}^{(2)} \equiv GD(H_n)$
	$d_4^{(1)} \rightarrow a_2^{(2)} \equiv GD(BD)$

The foldings leading to untwisted theories turn out merely to remove degeneracies from the mass spectrum, and the resulting non degenerate particles are always linear combinations of the degenerate particles in the parent theory. The 'rediagonalization' of the original $(\text{mass})^2$ matrix that this necessitates means that some work is required to extract the new couplings as linear combinations of the old. Note also that this change will tend to spoil some of the special properties of the original basis. More will be said on this point later, but the net effect is that some conserved charges are 'lost', the set of equations (2.24) implied by the new three point couplings having rather fewer solutions than was the case in the parent theory. The charges lost are exactly so as to reduce the set of conserved spins to the exponents of the non simply-laced algebra. As in the simply-laced cases, the masses for these untwisted theories may assigned to the relevant

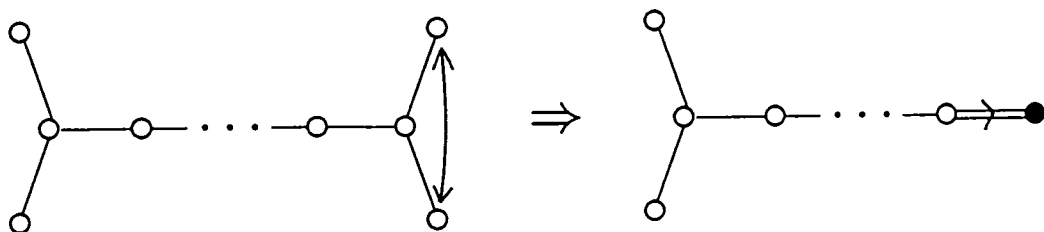
non-affine diagram via an eigenvector of the Cartan matrix (see equation (3.8)). This is shown in the continuation of table 7, the labelling being chosen to match that in the parent theory.

In contrast, foldings leading to twisted diagrams remove some particles from the spectrum altogether, and leave the others unchanged. The couplings of these particles are thus the same as those in the unfolded theory, and always form a subalgebra of the algebra of three-point couplings. In fact all possible subalgebras can be found in this way. Note that the first four of the twisted diagrams listed above may again be associated with non-affine algebras: the alternative labelling for these models indicates that their (extended) Cartan matrices are just the transposes of the usual extended Cartan matrix appropriate to the non simply-laced algebra. It is a curious and unexplained fact that the coincidence of simply-laced mass spectra with those derived by Ogievetsky and Weigmann, commented on above, extends to these four twisted theories rather than to the untwisted ones when S-matrices possessing a non simply-laced Lie algebra symmetry are examined.

There turn out to be problems in the quantum treatment of all these non simply-laced theories, and so their treatment will be fairly brief. The following subsections derive the results for masses and couplings, starting with the untwisted cases.

$$b_n^{(1)} \equiv \bar{D}(B_n)$$

This is obtained from $d_{n+1}^{(1)}$ using the automorphism which interchanges the prongs of the fork on the D_{n+1} diagram:



From (3.20) it is clear that to interchange the roots corresponding to the prongs, only the sign of e_{n+1} needs to be changed leaving the rest of the basis the same. Whatever the orientation chosen in the subspace of the two mass degenerate particles corresponding to the fork, the subspace spanned by e_2, \dots, e_n , or equivalently, the non-degenerate fields $\phi^1, \dots, \phi^{n-1}$, see (3.21), is preserved. Thus, the masses and mutual couplings of these particles are exactly the same in the $b_n^{(1)}$ theory as they are in the $d_{n+1}^{(1)}$ theory and are given

by equations (3.22) (b) and (3.28) with n replaced by $n + 1$. The invariant combination in the degenerate subspace is simply e_1 , so the $b_n^{(1)}$ theory has just one further particle, of mass $\sqrt{2}m$. This is associated with the short root of the non-affine diagram (see table 7). Using (3.24) and (3.23), in either the odd or even cases the invariant combination is a mixture of ϕ^s and $\phi^{s'}$:

$$\phi^n = \frac{1}{\sqrt{2}}(\phi^s + \phi^{s'})$$

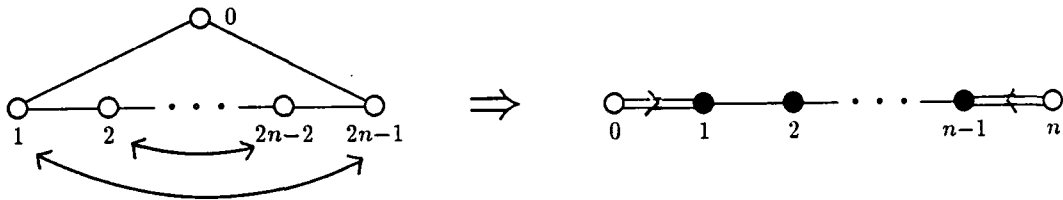
Unlike the degenerate particles in the $d^{(1)}$ theories, this couples to all of the others:

$$\begin{aligned} C^{nnn} &= 0 = C^{nab} \\ C^{nna} &= \frac{2\beta}{\sqrt{2n}} m_n m_n \sin U_{nn}^a. \end{aligned} \tag{3.30}$$

Note that these couplings all obey the area formula (3.9), the Coxeter number of B_n being $2n$.

$$c_n^{(1)} \equiv \bar{D}(C_n)$$

This may be obtained by exploiting a \mathbb{Z}_2 symmetry of the non-affine diagram A_{2n-1} , which is also a symmetry of $a_{2n-1}^{(1)}$:



The automorphism of the roots is

$$\alpha_i \rightarrow \alpha_{2n-i} \quad i = 1, 2, \dots, 2n - 1 \quad \alpha_0 \text{ and } \alpha_n \text{ fixed.} \tag{3.31}$$

The two roots α_0 and α_n form the long roots of $c_n^{(1)}$. Recalling the basis (3.13),

$$\alpha_i = \frac{1}{\sqrt{2n}}(\gamma_{i+1} - \gamma_i)^* \quad \gamma_i^a = \omega^{ia} \quad \omega^{2n} = 1,$$

it is clear that the transformation

$$\gamma_i^* \rightarrow -\gamma_{2n+1-i}^*$$

will have the desired effect on the roots. It is implemented by the matrix $A_b^a = -\delta_{2n-b}^a \omega^{-a}$:

$$\gamma_i^{*a} \rightarrow A_b^a \gamma_i^{*b} = -\omega^{-a} \gamma_i^{*2n-a} = -\omega^{-a} \omega^{-(2n-a)i} = -\gamma_{2n+1-i}^{*a} \quad (3.32)$$

Clearly, $A^2 = 1$. The effect on the particles of the $a_{2n-1}^{(1)}$ theory is, up to a phase, just to swap particle with antiparticle. The particles of the $c_n^{(1)}$ theory are to be found in the subspace invariant under the transformation (3.32). As A preserves each eigenspace of the mass² matrix and each eigenspace has a one-dimensional A -invariant subspace, the particle spectrum of the $c_n^{(1)}$ theory is just that of the $a_{2n-1}^{(1)}$ theory, with the degeneracy removed. Explicitly, the real A -invariant combinations of the fields of the $a_{2n-1}^{(1)}$ theory are:

$$\frac{-i\omega^{a/2}}{\sqrt{2}}(\phi + A\phi)^a = \frac{-i\omega^{a/2}}{\sqrt{2}}(\phi^a - \omega^{-a}\phi^{2n-a}) \quad a = 1, 2, \dots, n-1, \quad \text{and } \phi^n$$

with associated particle masses:

$$m_a = 2m \sin \frac{a\pi}{2n},$$

which may be attached to the non-affine diagram as shown in table 7. The three-point couplings being trilinear in the fields may now be found as combinations of the couplings in the $a_{2n-1}^{(1)}$ theory. After some algebra the $c_n^{(1)}$ couplings among the first $n-1$ particles are found to be

$$C^{abc} = \frac{1}{\sqrt{2}} \frac{2\beta}{\sqrt{2n}} m_a m_b \sin U_{ab}^c \quad \text{if } a \pm b \pm c = 0 \pmod{2n} \quad a, b, c = 1, \dots, n-1 \quad (3.33)$$

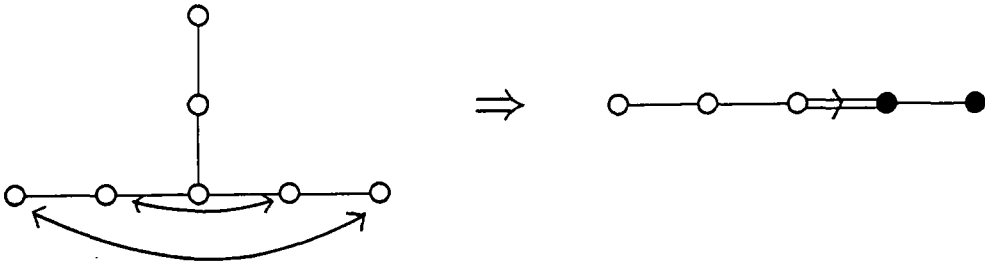
while those involving the extra particle n , invariant under the automorphism, are

$$\begin{aligned} C^{abn} &= \frac{-2\beta}{\sqrt{2n}} m_a m_b \sin U_{ab}^n \quad \text{if } a + b + n = 0 \pmod{2n} \\ C^{ann} &= 0 = C^{nna}. \end{aligned} \quad (3.34)$$

The Coxeter number of C_n is $2n$, so (3.34) obeys the area rule (3.9), while there is an extra factor of $1/\sqrt{2}$ in (3.33).

$$f_4^{(1)} \equiv \bar{D}(F_4)$$

The \mathbb{Z}_2 symmetry of the E_6 Dynkin diagram,



yields the $f_4^{(1)}$ theory. The degeneracy in the e_6 masses is removed leaving four self-conjugate particles. Their couplings are (in multiples of $\pi/12$):

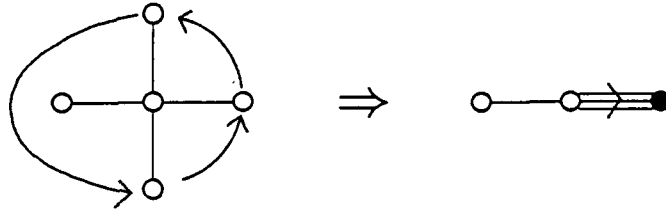
1			2		3				4		
1*	2	3*	1	3	1*	2	3*	4	3	1	
8	6	2	9	5	11	9	7	3	10		
			2	4	1			2	4 ⁻	2	
			8	2	10			11	7		
						1*	3*	4 ⁻	1	3 ⁻	
						10	8	6	11	9	
									2 ⁻	4	
									10	8	
											4

In this table the couplings follow the rule (3.9) with $h = 12$ (the Coxeter number of F_4), apart from an overall sign and a factor of $1/\sqrt{2}$ in the cases marked with a *.

$$g_2^{(1)} \equiv \bar{D}(G_2)$$

Finally in the untwisted sector, the D_4 Dynkin diagram possesses a three-fold symmetry in addition to the symmetry used earlier. This reflects the three-fold degeneracy of light particles in this theory. The invariant subspace under this symmetry yields the $g_2^{(1)}$

theory:



The result is a theory containing one light and one heavy particle of masses $\sqrt{2}m$ and $\sqrt{6}m$, respectively. The invariant combination of the degenerate d_4 particles is simply

$$\phi^1 = \frac{1}{\sqrt{3}}(\phi^s + \phi^{s'} + \phi^1),$$

while ϕ^2 remains unchanged. The corresponding non-zero couplings are

$$C^{222} = \frac{2\beta}{\sqrt{6}}m_2^2 \sin U_{22}^2 \quad C^{112} = \frac{-2\beta}{\sqrt{6}}m_1^2 \sin U_{11}^2 \quad C^{111} = \frac{-2}{\sqrt{3}} \frac{2\beta}{\sqrt{6}}m_1^2 \sin U_{11}^1,$$

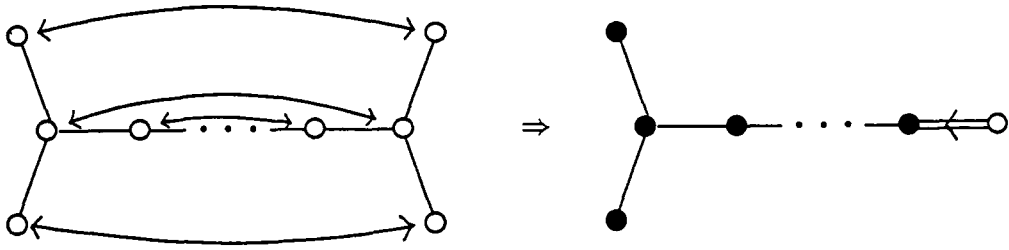
where $U_{22}^2 = U_{11}^1 = 2\pi/3$ and $U_{11}^2 = \pi/3$. The first two couplings obey (3.9); for the last there is an additional factor of $2/\sqrt{3}$.

Note the general rule for all untwisted theories that the area formula (3.9) only fails for couplings between three particles all of which are associated with short roots on the non-affine diagram. The correction factor required is $1/\sqrt{2}$ when the length of the short roots is 1, and $2/\sqrt{3}$ when the length is $\sqrt{2/3}$, corresponding to second and third order diagram automorphisms respectively. It is hard to see why such a universal rule should apply — the signs of the simply-laced couplings being combined to make up the non-simply laced answers must conspire in exactly the right way in each case.

Next, the twisted diagrams. For these the area formula always holds, as the couplings are always a subset of those in the relevant simply-laced theory, with the value of h always being the Coxeter number of the non-affine algebra for the *parent*, untwisted, theory.

$$a_{2n-1}^{(2)} \equiv \bar{D}^T(B_n)$$

This theory is obtained from the $a_{2n}^{(1)}$ theory by folding the diagram using an automorphism which interchanges the two forks:



The automorphism of the roots is

$$\alpha_i \rightarrow \alpha_{2n-i}$$

with α_n remaining fixed; this becomes the long root of $a_{2n-1}^{(2)}$. The automorphism is implemented by mapping the basis vectors of (3.20) as follows,

$$e_i \rightarrow -e_{2n+1-i}$$

which in turn, given the particular basis (3.21), corresponds to

$$l_{k-1}^a \rightarrow -l_{2n-k}^a$$

Noting that $l_{2n-k}^a = (-)^{a+1} l_{k-1}^a$, and that l_{k-1}^a is the a^{th} component of e_k , the mapping on the fields is just

$$\phi^i \rightarrow (-)^i \phi^i \quad i = 1, 2, \dots, 2n - 2.$$

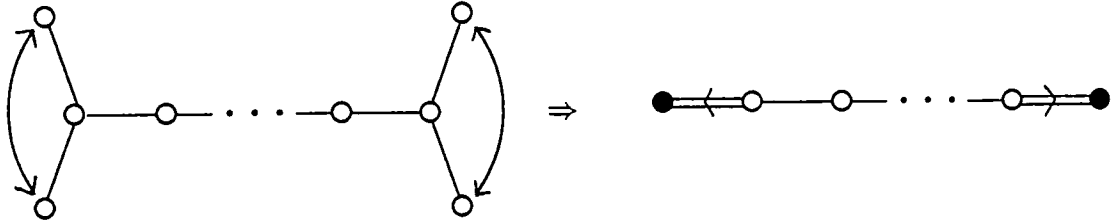
Hence, particles corresponding to the fields ϕ^i for i even survive the folding, and their three-point couplings are unchanged since they already lie in the invariant subspaces. In addition, the vector $\frac{1}{\sqrt{2}}(0, 0, \dots, 1, -1)$ in the subspace of mass $\sqrt{2}m$ also remains. This is precisely the particle s' used in the $d_{2n}^{(1)}$ theory ($2n$ is even, so the real basis is natural). In other words, the spectrum is

$$m_k^2 = 8m^2 \sin^2 \frac{k\pi}{2n-1} \quad k = 1, 2, \dots, n-1 \quad \text{and} \quad m_n^2 = 2m^2$$

with couplings extracted from (3.25) and (3.28), with n replaced by $2n$.

$$d_{n+1}^{(2)} \equiv \bar{D}^T(C_n)$$

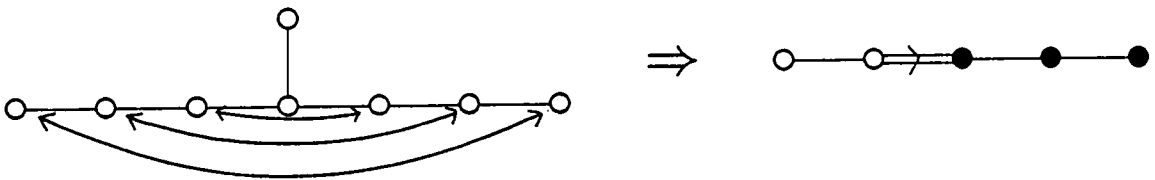
This, the simplest case, comes from the symmetry of the extended diagram $d_{n+2}^{(1)}$ which flips the two forks, leaving everything else alone:



In order to interchange α_0 with α_1 and α_{n+1} with α_{n+2} , the sign of both e_1 and e_{n+2} must be reversed. As in the case of $b_n^{(1)}$, the nondegenerate particles ϕ^1, \dots, ϕ^n are unaffected by this and so survive unchanged in the truncated theory. However, there are now no invariant vectors in the subspace spanned by e_1 and e_{n+2} , so the degenerate pair of particles s and s' are lost. Hence, the masses are given by (3.22) (b) and the couplings by (3.28) with n replaced by $n + 2$.

$$e_8^{(2)} \equiv \bar{D}^T(F_4)$$

The \mathbb{Z}_2 symmetry of the $e_7^{(1)}$ diagram yields $e_8^{(2)}$:



whose masses are a subset of those for e_7 , *i.e.*

$$m_2^2 = 8\sqrt{3}m^2 \sin \frac{\pi}{18} \sin \frac{2\pi}{9}$$

$$m_4^2 = 8\sqrt{3}m^2 \sin \frac{5\pi}{18} \sin \frac{\pi}{9}$$

$$m_5^2 = 6m^2$$

$$m_7^2 = 8\sqrt{3}m^2 \sin \frac{7\pi}{18} \sin \frac{4\pi}{9}$$

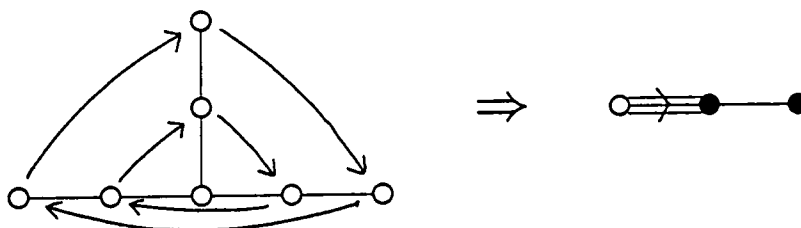
and whose couplings are given in the table:

2	4	5	7	
2 ⁻ 4 5 ⁻ 12 8 2	2 5 14 8	2 ⁻ 4 7 ⁻ 17 13 3	5 ⁻ 7 16 10	2
	4 5 7 ⁻ 12 10 4	2 4 7 ⁻ 15 13 7	4 5 ⁻ 16 14	4
		5 12	2 ⁻ 4 ⁻ 7 ⁻ 17 15 11	5
			2 5 ⁻ 7 16 14 12	7

This is a subset of table 10.

$$d_4^{(3)} \equiv \bar{D}^T(G_2)$$

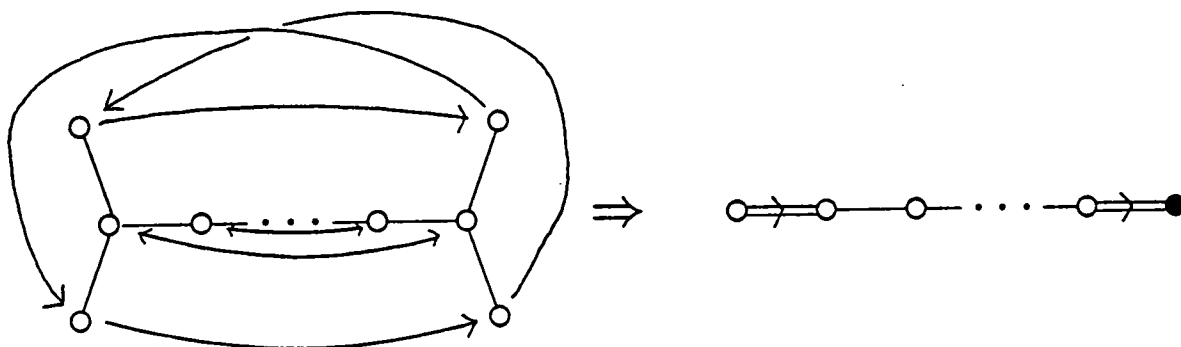
The $e_6^{(1)}$ diagram has a threefold symmetry:



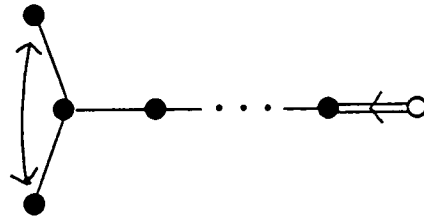
The resulting theory contains just the two heavy particles 2, 4 of the $e_6^{(1)}$ theory, with the couplings given in table 9.

$$a_{2n}^{(2)} \equiv GD(H_n)$$

This case comes from the $d_{2n+2}^{(1)}$ theory via the folding:



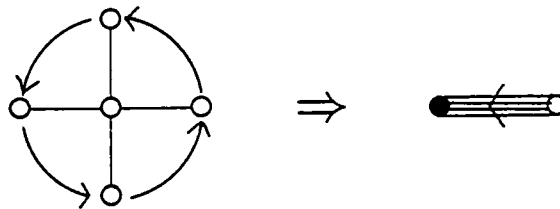
Alternatively, for $n > 1$ this can be viewed differently, exploiting the residual symmetry of the $a_{2n+1}^{(2)}$ diagram:



This way of looking at the folding makes it easy to see that the effect is simply to remove the particle with mass $\sqrt{2}m$ from the $a_{2n+1}^{(2)}$ theory, leaving all else unchanged.

$$a_2^{(2)} \equiv GD(BD)$$

The picture here is:



giving $a_2^{(2)}$, the Bullough-Dodd theory, which contains just one particle with a three point coupling equal to C^{222} in the $d_4^{(1)}$ theory.

Chapter 4

The Quantum Theory

4.1 Conserved Charges in Affine Toda Theories

The aim of this chapter is to find, if possible, the S-matrices for the affine Toda theories described above. Higher spin conserved charges played a very important part in the considerations of chapter two, and so the first step must be to look at these. This first section will describe the results of such a study, using the bootstrap consistency conditions (2.24):

$$\gamma_s^{\bar{c}} = \gamma_s^a e^{-is\bar{U}_{ac}^b} + \gamma_s^b e^{is\bar{U}_{bc}^a}. \quad (4.1)$$

For the Toda theories it turns out to be possible to obtain the complete solution to these equations.

In some senses this section is still dealing with classical issues: the process leading to (4.1), illustrated in figure 12, is at tree level when the non-vanishing three point couplings C^{abc} are the lowest order couplings obtained in the last chapter. It is important to realize that in the quantum theory the consistency conditions may be modified. First, the masses will renormalize, and this may change the fusing angles. This will be discussed to one loop in a subsequent section, with the conclusion that while for the simply-laced theories the angles do not change, there are difficulties for all non simply-laced cases. Secondly, all vertices should be ‘dressed’ since loop diagrams coupling three particles also contribute, and there may be extra couplings arising from such diagrams even when the direct three point couplings vanish, giving further consistency conditions. Such a possibility will be ignored below — only ‘classical’ three point couplings will be used — but for the quantum theory to be consistent with the results presented, some form of ‘topological’ non-renormalization theorem is needed, stating that couplings zero to lowest order in the coupling constant remain zero at higher orders where loop diagrams are present. (Note that for the consistency conditions (4.1) it is only the fact that a coupling is non-vanishing that is relevant.) This has now been checked in a few cases,^[57, 58] but for now the only general statement that can be made is that any extra vertices arising

from quantum corrections would be felt in the S-matrix in the appearance of 'unexpected' simple poles in the physical strip. Below it will be shown that for the simply-laced theories, consistent S-matrices can be postulated which do not have any extra simple poles beyond those predicted by the classical data.* The consistency conditions (2.23) for S-matrices *do* seem to be essentially quantum mechanical — this was remarked on at the end of chapter two and can be given intuitive justification from the fact that the diagram in figure 11 involves a loop. Thus for the simply-laced models, the conserved charges are involved in a circle of consistency checks which at least at some stages involves the quantum aspects of the problem. These theories will be treated first and in some detail, with the non-simply laced cases receiving a mention at the end of the section.

Thus the initial concern will be with the affine Toda theory based on a simply-laced affine diagram g , itself the extension of one and only one non-affine diagram G by the highest root. Two features of the affine Toda theories will be relevant, and will be restated here.

The first is given by equation (3.10). The non-zero three point couplings are such that the angles $U_{ab}^{\bar{c}}$ are always 'nice' numbers: for all allowed fusions $ab \rightarrow c$,

$$U_{ab}^{\bar{c}} = \frac{\pi}{h} \cdot \text{integer}, \quad (4.2)$$

where h is the Coxeter number of G . Together with (4.1), this implies that a solution $\{\gamma_s^a\}$ at spin s will also satisfy the consistency conditions pertaining to spin $s + 2h$. Since this set of numbers also solves the equations for $-s$ (true independently of (4.2)), this demonstrates that all solutions to (4.1) are known once spins in the range 1 to h have been examined.

The second feature to note is (3.8), that if the particle masses are arranged into a vector (m_1, m_2, \dots, m_r) , this turns out to be an eigenvector of the Cartan matrix of G , the eigenvector of lowest eigenvalue, $2 - 2 \cos \frac{\pi}{h}$.

Given that the particle masses are just the numbers $\{\gamma_1^a\}$ (equation (2.4)), it is natural to hope that the higher spin conserved charges might have a similar characterization, and this is indeed the case. The result (independently noted for the simply-laced cases in [14]) is that the spin s , modulo the Coxeter number of G , must be an exponent of G

* For reasons to be described later, the simple poles are occasionally masked by higher order odd poles; a fuller statement is that no odd-order poles ever occur at rapidities other than those predicted from the fusing angles given in the last chapter.

for there to be a nontrivial solution to (4.1), and for such an s the vector $(\gamma_s^1, \gamma_s^2, \dots, \gamma_s^r)$ is the eigenvector of the Cartan matrix of G with eigenvalue $2 - 2 \cos \pi s/h$. Together with the observation above that only the first h spins need to be examined, this serves to characterize the ratios of conserved quantities at all possible values of spin. This is the most one can hope for, (4.1) being a set of homogeneous equations. Information on overall normalization would probably need more specific details of the theory concerned.

The result will be established for each algebra in turn, though obviously it would be preferable to have a general understanding. Also, while every relation implied by (4.1) could be checked for consistency, without this general understanding this would not be very edifying. Rather, a convenient route through the bootstrap will be indicated for each case. Different choices often lead to apparently very different expressions; it is interesting to check that for s an exponent of G the values of these expressions are indeed the same.

It is convenient to take real and imaginary parts of (4.1). This yields:

$$\gamma_s^c = \gamma_s^a \cos s\bar{U}_{ac}^b + \gamma_s^b \cos s\bar{U}_{bc}^a \tag{4.3}$$

$$\gamma_s^a \sin s\bar{U}_{ac}^b = \gamma_s^b \sin s\bar{U}_{bc}^a \tag{4.4}$$

All angles appearing in these equations will be integer multiples of $\theta_s \equiv \pi s/h$, by (4.2). The spin s will be taken in the range $1 \dots h$, and to be an exponent of G .

$A_n, \theta_s = \pi s/(n + 1)$

This case is particularly simple as

$$1 \ a \rightarrow a+1$$

is always an allowed fusing. Equation (4.4) becomes

$$\gamma_s^a \sin \theta_s = \gamma_s^1 \sin a\theta_s$$

so picking $\gamma_s^1 = \sin \theta_s$ gives $\gamma_s^a = \sin a\theta_s$ and the eigenvectors of the A_n Cartan matrix are reproduced for $s = 1, 2, \dots, n$.

$$D_n, \theta_s = \pi s/2(n-1)$$

The cases n even and n odd are slightly different.

(a) n odd:

Let a be an odd integer between 1 and $n-2$. Equation (4.3) for

$$s s \rightarrow a \quad \text{and} \quad \bar{s} \bar{s} \rightarrow a$$

is

$$\begin{aligned} \gamma_s^a &= 2\gamma_s^s \cos(n-1-a)\theta_s \\ &= 2\gamma_s^{\bar{s}} \cos(n-1-a)\theta_s. \end{aligned}$$

Hence for $s \neq n-1$, $\gamma_s^s = \gamma_s^{\bar{s}}$, while for $s = n-1$, $\gamma_s^a = 0$ and the 'crossed' process $s a \rightarrow \bar{s}$ is sufficient to show that $\gamma_{n-1}^s = -\gamma_{n-1}^{\bar{s}}$. Next let b be an even integer. The fusing

$$s \bar{s} \rightarrow b$$

together with equation (4.3) shows that

$$\gamma_s^b = (\gamma_s^s + \gamma_s^{\bar{s}}) \cos(n-1-b)\theta_s.$$

So for $s = 1, 3, \dots, 2n-3$ the conserved quantities are

$$(2 \cos(n-2)\theta_s, \dots, 2 \cos \theta_s, 1, 1)$$

while for $s = n-1$, the result is

$$(0, 0, \dots, 1, -1).$$

(b) n even:

The story is much the same here. The fusings $s s \rightarrow \text{even}$, $s' s' \rightarrow \text{even}$ and $s s' \rightarrow \text{odd}$ give, for $s \neq n-1$,

$$\begin{aligned} \gamma_s^{s'} &= \gamma_s^s, \\ \gamma_s^a &= 2\gamma_s^s \cos(n-1-a)\theta_s, \end{aligned}$$

where a is any integer from 1 to $n-2$. There turns out to be no constraint between γ_{n-1}^s and $\gamma_{n-1}^{s'}$ (this reflects the doubling up of the D_n exponent at $n-1$ for even n). It is convenient to take them to be $(1, 1)$ and $(1, -1)$, in which case the pattern of conserved quantities already found for n odd is reproduced.

$E_6, \theta_s = \pi s/12$

Setting $\gamma_s^1 = \sin \theta_s$,

$$1 \bar{3} \rightarrow 4 \Rightarrow \gamma_s^3 = \sin 2\theta_s,$$

$$1 4 \rightarrow 3 \Rightarrow \gamma_s^4 = \sin 9\theta_s = \sin 3\theta_s,$$

(the last equality holding for all relevant values of s)

$$1 3 \rightarrow \bar{1} \Rightarrow \gamma_s^3 = \sin 10\theta_s,$$

$$\bar{1} 3 \rightarrow 4 \Rightarrow \gamma_s^{\bar{1}} = \sin 11\theta_s,$$

$$4 4 \rightarrow 2 \Rightarrow \gamma_s^2 = \sin 8\theta_s - \sin 2\theta_s.$$

Equation (4.3) is needed for the final equality, (4.4) being used for all the rest.

$E_7, \theta_s = 18$

Take $\gamma_s^1 = \sin \theta_s$. Using (4.4),

$$1 4 \rightarrow 6 \Rightarrow \gamma_s^4 = \sin 2\theta_s,$$

$$1 6 \rightarrow 4 \Rightarrow \gamma_s^6 = \sin 15\theta_s = \sin 3\theta_s,$$

$$1 6 \rightarrow 7 \Rightarrow \gamma_s^7 = \sin 14\theta_s = \sin 4\theta_s,$$

the second equalities in the last two equations holding for all odd s . Next (4.3) is used, as follows:

$$4 4 \rightarrow 5 \Rightarrow \gamma_s^5 = \sin 7\theta_s - \sin 3\theta_s,$$

$$1 1 \rightarrow 2 \Rightarrow \gamma_s^2 = \sin 6\theta_s - \sin 4\theta_s,$$

$$5 6 \rightarrow 3 \Rightarrow \gamma_s^3 = \frac{1}{2}(\sin 9\theta_s - \sin 7\theta_s + \sin 5\theta_s - \sin \theta_s).$$

$E_8, \theta_s = 30$

Again, set $\gamma_s^1 = \sin \theta_s$. Using (4.4), and assuming s to be odd since this is true of all the E_8 exponents,

$$1 3 \rightarrow 5 \Rightarrow \gamma_s^3 = \sin 2\theta_s,$$

$$1 5 \rightarrow 3 \Rightarrow \gamma_s^5 = \sin 3\theta_s,$$

$$1 7 \rightarrow 8 \Rightarrow \gamma_s^7 = \sin 4\theta_s,$$

$$1 8 \rightarrow 7 \Rightarrow \gamma_s^8 = \sin 5\theta_s.$$

For the final cases, (4.3) is simpler.

$$3\ 3 \rightarrow 6 \Rightarrow \gamma_s^6 = \sin 8\theta_s - \sin 4\theta_s,$$

$$1\ 1 \rightarrow 2 \Rightarrow \gamma_s^2 = \sin 7\theta_s - \sin 5\theta_s,$$

$$5\ 5 \rightarrow 4 \Rightarrow \gamma_s^4 = \sin 14\theta_s - \sin 8\theta_s.$$

Reference should be made to table 8 for the full set of results. Note that these are in agreement with the result (2.27) for charge-conjugation properties — in particular, the even-spin charges are always zero on self-conjugate particles. Either by explicit calculation or by comparison with the table in [59], it is easy to check the claimed result that these are the eigenvectors of the relevant Cartan matrices, each with eigenvalue $2 - 2\cos\theta_s$.

Non simply-laced theories

The nature of these cases has already been mentioned in the discussion of folding. Briefly, the situation is that for the untwisted theories, the folding increases the number of couplings among the remaining particles and the consequently more stringent consistency conditions reduce the set of conserved spins down to the exponents of the non simply-laced algebra. The twisted theories have no new consistency conditions among the remaining particles, as their couplings are the same as those of the parent theory, but as the conserved charges are realized on a smaller set of particles, some become trivial. Thus the set of spins is again reduced, this time down to the set of exponents relevant for the twisted affine diagram. This has not been mentioned before, but in fact exponents can be defined directly for the affine diagrams.^[51] For the untwisted affine diagrams, these exponents are the same as those of the corresponding non-affine diagram listed in table 3. For reference, the exponents for the twisted diagrams are given in figure 13, and for the classical twisted affine Toda theories, these are known to be the spins of the conserved charges. Thus the conclusion is that in all cases the bootstrap consistency conditions (4.1), when used with the tree level three point couplings, give results in accordance with those known for the classical theories.

The remainder of this section deals with the non simply-laced theories in turn. In all cases, the actual values of the charges may be extracted from those for the parent theory shown in table 8.

Diagram	Coxeter Number	Exponents
$a_{2n-1}^{(2)}$	$4n - 2$	$1, 3, 5, \dots, 4n - 3.$
$d_{n+1}^{(2)}$	$2n + 2$	$1, 3, 5, \dots, 2n + 1.$
$d_4^{(3)}$	12	$1, 5, 7, 11.$
$e_6^{(2)}$	18	$1, 5, 7, 11, 13, 17.$
$a_{2n}^{(2)}$	$4n + 2$	$1, 3, 5, \dots, 2n - 1, 2n + 3, \dots, 4n + 1.$

Figure 13 : Exponents for the twisted diagrams.

First, the untwisted theories. For these, the eigenvalue result for the masses generalizes to the higher spin charges just as for the simply-laced theories.

$$b_n^{(1)}, \theta_s = \pi s / 2n$$

This theory descends from $d_{n+1}^{(1)}$, the only changes being that rather than two degenerate particles s, s' there is now a single particle n , of the same mass, with rather more couplings than either s or s' individually (see (3.30)). The effect of these changes is to remove the 'extra' conserved charge of spin n possessed by the $d_{n+1}^{(1)}$ theory (the second vector of the D entry in table 8). The mechanism is slightly different for n odd or even.

When n is odd, there are two independent charges of spin n in the $d_{n+1}^{(1)}$ theory. However they are both zero on particles $1, 2, \dots, n - 1$, being distinguished only by their values for the s and s' particles. With only a single particle (n) remaining of these two in the $b_n^{(1)}$ theory, this distinction vanishes and the two charges become identical.

For n even, the 'extra' charge has even spin. All particles in the $b_n^{(1)}$ theory are self-conjugate, so the result (2.27) can be used to see that this charge must vanish in the folded theory. Alternatively, the fact that the fusings $n n \rightarrow a$ and $n a \rightarrow n$ both occur

establishes the result directly.

$$c_n^{(1)}, \theta_s = \pi s / 2n$$

This case comes from $a_{2n-1}^{(1)}$, which has charges at spins $1, 2, \dots, 2n - 1$. All particles in the folded theory are self-conjugate so (2.27) can be used again to see that the even spins in this list must be lost, leaving the charges with spins $1, 3, \dots, 2n - 1$, the exponents of C_n .

$$f_4^{(1)}, \theta_s = \pi s / 12$$

The same reasoning applies here: all particles are self-conjugate, so spins 4 and 8 of the parent $e_6^{(1)}$ theory are removed leaving 1, 5, 7 and 11, the F_4 exponents.

$$g_2^{(1)}, \theta_s = \pi s / 6$$

The parent theory is $d_4^{(1)}$ here, which has three mass-degenerate light particles. These three are replaced by a single particle ϕ^1 in the $g_2^{(1)}$ theory, which now has the ' ϕ^3 property': there is a three-point coupling C^{111} , in contrast to the situation in the original theory. The other, heavy, particle is unchanged from that in the parent and also has the ϕ^3 property. The bootstrap equation (4.3) for such a particle becomes

$$(1 - 2 \cos \frac{\pi}{3} s) \gamma_s^1 = 0,$$

from which it is clear that conserved charges can only be non-trivial on the $g_2^{(1)}$ particles if $s = 1$ or 5 modulo 6 , precisely the G_2 exponents.

Finally, the twisted theories.

$$a_{2n-1}^{(2)}, \theta_s = \pi s / (4n - 2)$$

This comes from $d_{2n}^{(1)}$, with particles $2, 4, \dots, 2n - 2$ and s surviving from the original set $\{1, 2, \dots, 2n - 2, s, s'\}$. The extra charge of spin $2n - 1$ is lost in the same way as happened for $b_{odd}^{(1)}$ above, leaving spins $1, 3, 5, \dots, 4n - 3$.

$$d_{n+1}^{(2)}, \quad \theta_s = \pi s/2(n+1)$$

The parent here is $d_{n+2}^{(1)}$, with *both* mass-degenerate particles being lost. Again, this removes the extra charge at spin $n+1$ so the spectrum of spins is $1, 3, 5, \dots, 2n+1$.

$$d_4^{(3)}, \quad \theta_s = \pi s/12$$

Only the two self-conjugate particles 2 and 4 remain from the $e_6^{(1)}$ parent. As is easily checked from table 8, the even spin charges P_4 and P_8 vanish on these (as of course they should, given (2.27)). The remaining charges, which *are* non-vanishing here, have spins 1, 5, 7 and 11, the exponents of $d_4^{(3)}$.

$$e_6^{(2)}, \quad \theta_s = \pi s/18$$

Particles 2, 4, 5 and 7 remain from the parent theory, $e_7^{(1)}$. This theory had charges of spin 1, 5, 7, 9, 11, 13 and 17, but from the explicit expression in table 8, the charge of spin 9 vanishes for these particles leaving the exponents of $e_6^{(2)}$ shown in figure 13. Alternatively, note that all four remaining particles have the ϕ^3 property, and so can only support charges of spin 1 or 5 modulo 6, which rules out the spin 9 charge.

$$a_{2n}^{(2)}, \quad \theta_s = \pi s/(4n+2)$$

This theory comes from $d_{2n+2}^{(1)}$, or alternatively by a further folding of $a_{2n+1}^{(2)}$. This removes the remaining particle of mass $\sqrt{2}m$, and the charge at spin $2n+1$ becomes trivial. The conserved spins are thus $1, 3, 5, \dots, 2n-1, 2n+3, \dots, 4n+1$, as required.

4.2 Fundamental S-Matrix Elements

Assuming that the results of the last section hold good when vertices receive their quantum corrections, it is easily checked from table 8 that the conserved charges distinguish all particles in the Toda theories, even when there are mass degeneracies. Hence, in the absence of any further subtleties the scattering theories are expected to be of the purely elastic type described at the end of chapter two. At this stage, such a claim rests on only a small amount of evidence, none of which probes the quantum aspects of the

problem, and so it is best thought of as a working hypothesis to be justified or otherwise later, by the consistency of its consequences. In fact, there turn out to be difficulties for the non simply-laced theories, indicating that the claim that all scattering is purely elastic is indeed non trivial. These problems will be commented on as they arise, and are most apparent for the untwisted non simply-laced cases.

However, if the scattering *is* purely elastic, it should be possible to postulate a 'fundamental' S-matrix element between two suitably chosen particles of the theory, and then deduce the rest by use of the S-matrix bootstrap equations, (2.23). The object of this section is to obtain the fundamental S-matrix elements, while in the next the remainder of the S-matrices will be computed, a process which will provide numerous consistency checks.

The first question is which S-matrix elements are fundamental, in the sense of fully determining the complete S-matrix via the bootstrap. It is helpful to think of the rather better-understood situation of the conserved charges first. Given that the bootstrap determines the values of a given charge Q_s on all particles up to an overall normalization, specifying the value of Q_s on any single particle a for which it is not identically zero serves to fix that charge completely — the value of γ_s^b for any other particle b must follow from γ_s^a via the bootstrap, and can be found using table 8. In view of the close correspondence between the S-matrix and conserved charge bootstraps, a reasonable hypothesis is that the S-matrix element S_{aa} of any particle possessing the full set of conserved charges will be fundamental. For example, in the $e_7^{(1)}$ theory, only particles 1, 3 and 6 have a non-vanishing value for the spin 9 conserved charge, but any one of these should do as a starting point for the bootstrap. The only subtlety comes when there is a repeated exponent, say r , and only arises for the $d_{\text{even}}^{(1)}$ theories. In such cases, knowledge of the single fourier component t_r^{aa} (see (2.26)) of the logarithmic derivative of the S-matrix does not fix the value of t_r^{ab} for all the other particles, since there are two independent solutions to the spin r bootstrap equations, one for each exponent. Hence it would be expected that a single S-matrix element, even involving a fundamental particle, does not contain sufficient information. For these theories it is better to view the situation as there being two fundamental particles, a and b say, with $\gamma_s^a = \gamma_s^b$ when $s \neq r$, while γ_r^a and γ_r^b are independent. The algebraic structure of the bootstrap then permits S_{aa} , S_{ab} and S_{bb} to be postulated with some degree of independence, corresponding to the freedom to specify certain fourier components of their logarithmic derivatives independently. In fact the two fundamental particles for the $d_{\text{even}}^{(1)}$ theories are s and s' , and it is interesting to

see that from a purely algebraic point of view, there is indeed some freedom to specify the corresponding S-matrix elements independently. However, physically it is always clear what should be postulated, so there are no problems arising from this extra freedom.

Having chosen a particular fundamental particle, a say, a hypothesis must be made for the meromorphic function $S_{aa}(\theta)$. The key idea here is to use both perturbative and non-perturbative information for this — the perturbative input coming in the form of low-order Feynman graphs which are expected to dominate for small values of the coupling constant, the non-perturbative information being the requirements of crossing and unitarity. As explained in the final section of chapter two, crossing and unitarity together imply that purely elastic S-matrices are built from quotients of hyperbolic functions, the basic block (x) being defined in equation (2.18).

Simple poles with positive residue in the physical strip are expected to correspond to bound states, themselves possible asymptotic states, and in perturbation theory such poles may be found in tree level diagrams as drawn in figure 8. The pole is at $\theta = iU_{aa}^c$, where U_{aa}^c is the fusing angle and c is the intermediate bound state. Cross-channel poles are also to be expected, with opposite residue. If perturbation theory is valid then at least for small values of the coupling constant it should be possible to predict the positions of all physical poles in S_{aa} , by examining a finite number of Feynman diagrams.

As will be explained in more detail later, there is also a possibility of higher order physical poles. These have a straightforward explanation in perturbation theory, but are rather harder to spot. For this reason it is most convenient to choose the lightest of the fundamental particles as a base for the bootstrap, as a simple argument shows that the S-matrix elements of such particles are never expected to have higher physical poles of this type.

Assuming this to be the situation, the physical pole structure is easy to predict, and can be encoded into a 'minimal' S-matrix element possessing no further poles, even off the physical strip. There will be one building block (x) for each pole, (x) having a single simple pole in θ , at $i\pi x/h$. (The reason for the appearance of the factor π/h in the definition (2.18) should now be clear — the poles occur at the relevant fusing angles, themselves integer multiples of π/h by (3.10). Inserting this factor ensures that x is an integer.)

For example, particle 1 in the $a_n^{(1)}$ theories can be taken as fundamental. From (3.16), there is a fusing $1\ 1 \rightarrow \overline{n-1} = 2$, with fusing angle $2\pi/h$, and no further poles are

expected in either forward or crossed channels. Hence the postulated minimal S-matrix element for 1 1 scattering in the $a_n^{(1)}$ theory is

$$S_{11}^{\min} = (2),$$

an S-matrix which was examined independently of Toda theory by K\"oberle and Swieca.^[60] The residue here *is* of the correct sign — this follows immediately from the correctness of the residues in the modification of this S-matrix to take account of the coupling constant, a result to be established in a later section.

A more complicated case is the s s scattering in the $d_n^{(1)}$ theories (for which $h = 2(n-1)$). If n is even, there are fusings s $s \rightarrow a$ for $a = 2, 4, \dots, n-2$ at fusing angles $2(n-3)\pi/h, 2(n-5)\pi/h, \dots, 6\pi/h$ and $2\pi/h$ respectively. All particles are self-conjugate so the crossed channel poles occur at $i\pi$ minus the forward channel rapidity, *ie* with angles $4\pi/h, 8\pi/h, \dots, 2(n-2)\pi/h$. Note the neat way in which forward and crossed channels mesh together, their poles alternating across the physical strip. This means that the signs of the residues of a simple product of building blocks will behave correctly:

$$S_{ss}^{\min} = - \prod_{k=1}^{n-2} (2k).$$

The same form (although without the minus sign) turns out to be correct when n is odd, noting that s is no longer self-conjugate so the fusings relevant to the crossed channel in s s scattering are between s and \bar{s} .

When the untwisted non simply-laced theories are considered, difficulties start to emerge. Rather than going through each case, the $b_n^{(1)}$ theory, which descends from the $d_{n+1}^{(1)}$ theory treated in the last paragraph, will serve as an example of the problems found. Particle n , the folded remnant of s and s' , should still be taken as fundamental (no other particle has all conserved quantities nonvanishing). Referring to (3.30), this couples to all the other particles, so forward channel poles are expected at $2(n-1)\pi/h, 2(n-2)\pi/h, \dots, 4\pi/h$ and $2\pi/h$. The problem becomes clear when the crossed channel is considered, as the *same* set of angles appears, this time requiring poles with opposite residues. Thus the forward and crossed channels 'clash', and the simple reasoning given above cannot be used to postulate a minimal S-matrix. There are other reasons why the non simply-laced theories are expected to have difficulties, to be mentioned below.

For now, suffice it to say that similar problems of clashing channels occur in all untwisted cases. The twisted theories, their particle contents being simple truncations of those of the parent theory, do not run into the same immediate trouble, and their S-matrices can be postulated to be suitable sub-matrices of the simply-laced ones. However other problems, in particular renormalization difficulties, occur here also. Hence for the time being, discussion will be restricted to the simply-laced cases.

Minimal S-matrices can be found for the e series theories in a similar fashion to that described above for a and d . By (2.17), they are (up to a sign) fully determined by the locations of their poles and zeroes in the physical strip, and this information is most simply given in pictorial form. Figure 14 collects together the results for all simply-laced theories, showing representative examples for a , d_{odd} and d_{even} . The complex plane has been rotated by 90 degrees, the imaginary axis being marked in units of π/h in each case. Double arrows denote forward channel poles, single ones crossed channel poles with the opposite residue. The crosses above the imaginary axis show zeroes in the physical strip which are not present in the minimal S-matrices, since by the unitarity equation (2.17) a zero on the physical strip must be accompanied by a pole on the 'unphysical strip', while the minimal S-matrices have been specified to have *no* additional poles. The zeroes are relevant to a correction factor incorporating the coupling constant, to be introduced below.

The bootstrap equations (2.23) may now be used for each forward channel pole to deduce further S-matrix elements, and from these more still. This will be described in detail in the next section, the result being that the whole process closes on a finite set of S-matrix elements, revealing the presence of exactly the expected number of particles on the basis of the Toda theory, with precisely the classical mass ratios and fusing structure. This is an important consistency check.

The minimal S-matrices, with no further poles or zeroes over those demanded by the bound state fusings, are precisely those that have been linked with perturbations of conformal field theories — for example, the minimal $e_8^{(1)}$ S-matrix for the magnetic perturbation of the Ising model,^[2] or the minimal $a_2^{(1)}$ S-matrix for the ϕ_{21} perturbation of the three-state Potts model.^[39] Since the fusing structure implied by the poles of each minimal S-matrix is exactly that following from the three point couplings in the classical Toda theory, the calculations in the last section demonstrate that these theories can indeed have conserved charges with spins at the exponents of the relevant algebra. Thus they form perfectly acceptable candidates for the S-matrices of the particular perturbed

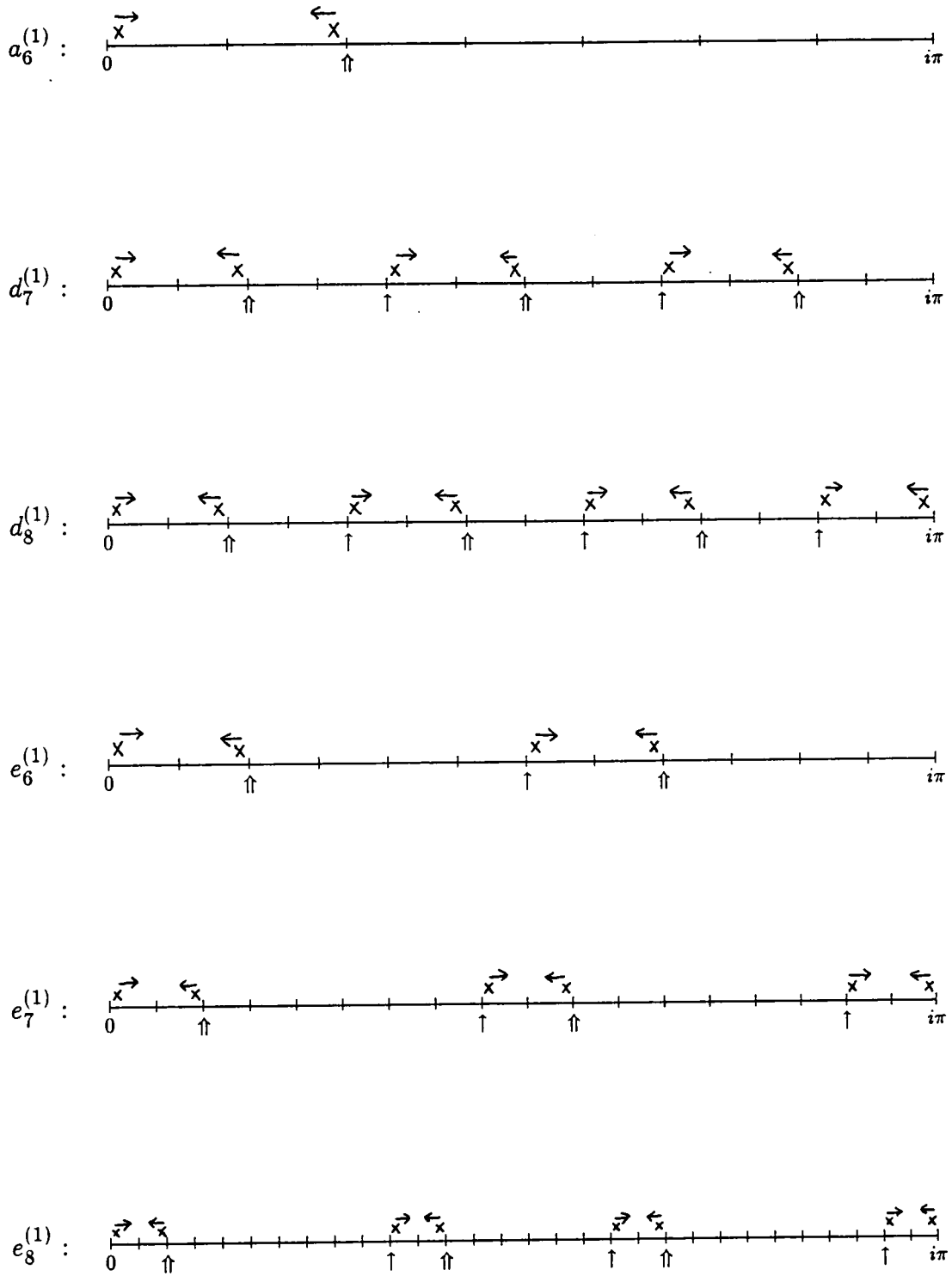


Figure 14 : Poles and zeroes of $S_{11}(\theta)$ in the physical strip.

$\uparrow\uparrow$: forward pole; \uparrow : crossed pole; x : zero; \rightarrow : movement of the zero for small β .

conformal theories discussed at the end of chapter one.

However they cannot be quite right for the Toda theories, as they contain no mention of the coupling constant. The perturbative approach adopted here requires that as $\beta \rightarrow 0$, the theory becomes free and the S-matrix trivial. It might also be expected that quantum corrections would give the mass ratios some coupling-constant dependence, and hence that the positions of the physical poles would change from that encoded in S^{\min} . It seems that this does not occur—for example, a one-loop check of the mass corrections for the simply-laced Toda theories reveals that the masses renormalize together in such a way that their ratios are unchanged (this will be described in a later section). The algebraic structure of the bootstrap equations (2.24) and (2.23) appears to be so tight that any continuous change in their parameters (ie the numbers \bar{U}_{bc}^a , determined from the mass ratios) destroys their solubility, and so the mass ratios are ‘frozen’ at their classical values even in the quantum theory (this situation can be compared with that in conformal field theory where the scaling dimension of the energy-momentum tensor does not renormalize). Hence, it is natural to assume^[61] that the full S-matrix element can be written as:

$$S(\theta; \beta) = S^{\min}(\theta)F(\theta, \beta) \quad \text{where} \quad F(\theta, 0) = (S^{\min}(\theta))^{-1},$$

the condition on F arising from the requirement that $S(\theta, 0) = 1$. There are a number of further conditions on F which turn out to determine it almost completely.

First, the unitarity and crossing equations holding for S^{\min} must also hold for F , so that they hold for the full S-matrix. This means that F is also built from the (x) functions.

Next, note that S^{\min} already contains all the bound state poles required by perturbation theory. Hence $F(\theta, \beta)$ should not have any physical strip poles in θ , at least for β small enough that perturbation theory applies.

Furthermore, the signs of the pole residues in S^{\min} identify forward and crossed channel poles correctly, so F must not change these. In particular F can never introduce an odd number of zeroes into any segment of the physical strip between two physical poles.

F must respect the bootstrap. Since it has no physical poles, it does not give rise to any new bootstrap equations, but once F_{11} has been proposed, the correction factors for all other S-matrix elements follow via the existing bootstrap, in an overdetermined fashion which must be consistent. The other factors so deduced must then respect all the consistency conditions already given.



Finally, for small β perturbative checks can be made against tree level Feynman diagram calculations. Details of this will be given later — the area formula (3.9) turns out to be important.

Now let S^{\min} have poles at $i\omega_1, i\omega_2, \dots, i\omega_p$. F is expected to introduce a set of zeroes into the physical strip, with positions that vary continuously with β . At $\beta = 0$, there must only be zeroes at $i\omega_1, \dots, i\omega_p$, cancelling the poles of S_{\min} . Hence as $\beta \rightarrow 0$, the zeroes of F must either tend to these points, or migrate to the edge of the physical strip, where they will cancel against unphysical poles implied by (2.17). Thus at least for small β , $F(\theta, \beta)$ has zeroes at $i(\omega_1 + b_1(\beta)), \dots, i(\omega_p + b_p(\beta))$, where each $b_i(\beta)$ tends to zero with β , together with some number of zeroes near 0 and $i\pi$. To preserve the signs of the residues, the signs of the derivatives of the b_i 's at $\beta = 0$ must alternate. In fact cancellations needed for the consistency of the bootstrap require that the zeroes at different locations behave consistently, with $b_1 = b_3 = \dots = -B(\beta)$, say, and $b_2 = b_4 = \dots = C(\beta)$. Tree-level perturbation theory confirms this, and establishes that $C'(0) = B'(0)$. (Actually, since the theory is unchanged by sending β to $-\beta$, there is no linear term in B or C , and the derivatives here are with respect to β^2 .) Once the crossed channel process has been deduced via the bootstrap, the additional input of crossing symmetry (2.17) implies that $C(\beta) = B(\beta)$. The fact that the first pole (at ω_1) is forward channel in each case means that $B'(0) > 0$.

The bootstrap also determines the positions of any zeroes which leave the physical strip as $\beta \rightarrow 0$, using the fact that each fundamental S-matrix element has a forward channel pole at $2i\pi/h$. The bootstrap equations (2.23) appropriate to this fusing angle yield an S-matrix element with a cross-channel pole at $i\pi/h$. The logic of the last paragraph also applies to this new function and requires that the pole at $i\pi/h$ be accompanied by a zero at $i\pi/h + iB$, which in turn implies that the original, fundamental, S-matrix must have had a single zero near 0, at $iC(\beta)$. For self-conjugate theories, there must also be a zero at $i(\pi - B)$, but that is all — anything more would violate the restrictions on F given above.

These results are shown for each theory in figure 14, the zeroes being marked by crosses above the imaginary axis together with their direction of travel as β^2 increases from zero. A particularly simple structure is visible in the completed picture, namely that the zeroes of F always occur in pairs, $2\pi i/h$ apart when $\beta = 0$. When following through the bootstrap it turns out that these pairs are always preserved, cancelling against each other as single units; this is where the requirements that $b_1 = b_3 = \dots = -B$ and

$b_2 = b_4 = \dots = C$ came from. Once these conditions have been met, the bootstrap will work for any value of B and C , and hence for all β . Note that for the coupling-constant dependent piece F to be consistent with the bootstrap in this way, pole structure of the minimal S-matrix, derived before the coupling constant was mentioned, had to be of just the right form.

This pairing of the zeroes motivates the introduction of a new building block for the Toda S-matrices, defined in terms of (x) as follows:

$$\{x\} = \frac{(x-1)(x+1)}{(x-1+B)(x+1-B)}. \tag{4.5}$$

(For convenience, the normalization of B has been changed by a factor of $1/h$ from that of the last paragraph.) This block seems to be more than a mere book-keeping device — it has many useful properties, and is the largest portion of the S-matrix which maintains its integrity throughout the bootstrap.

As a function of θ , $\{x\}$ has poles in the physical strip at $i\pi(x-1)/h$ and $i\pi(x+1)/h$, though recall that $(0) = 1$, $(h) = -1$, and so $\{1\}$ has only a single physical pole at $2i\pi/h$, and $\{h-1\}$ a single physical pole at $(h-2)i\pi/h$. Thus the full (coupling-constant dependent) S-matrix element for 1 1 scattering in the a theories is simply $\{1\}$. $\{x\}$ crosses to $\{h-x\}$, and using (2.19) it is possible to gather together other useful properties:

$$\{0\} = \{h\} = 1 \quad \{x\}^{-1} = \{-x\} \quad \{x\} = \{x \pm 2h\}. \tag{4.6}$$

One more property of this block will be remarked on here: in obvious notation,

$$\{x\}_B = \{x\}_{2-B}. \tag{4.7}$$

This feature is inherited by any S-matrix built from these blocks, and is easy to see for the fundamental S-matrices in the pictures of figure 14. It has a bearing on the one remaining ambiguity in the proposed S-matrices: the dependence of B on β . If there are to be no extra physical poles for any real β , then it is easily seen that $B(\beta)$ must lie between 0 and 2. Given (4.7), it is tempting to suppose that $B(\beta) \rightarrow 2$ as $\beta \rightarrow \infty$, so that the theory becomes free again in the strong coupling limit. The function

$$B(\beta) = \frac{1}{2\pi} \frac{\beta^2}{1 + \beta^2/4\pi} \tag{4.8}$$

has the desired property, ‘duality’ between strong and weak couplings appearing as

$$B\left(\frac{4\pi}{\beta}\right) = 2 - B(\beta)$$

so that

$$\{x\}_{4\pi/\beta} = \{x\}_\beta. \quad (4.9)$$

The overall factor $1/2\pi$ in (4.8) is fixed by tree level diagrams (its universality for all Toda theories is a curious fact), but beyond this the hypothesis is highly non-perturbative and rather hard to check. For the a theories it was proposed years ago by Arinshtein, Fateev and Zamolodchikov,^[10] and this section concludes with a description of one of the motivations for their hypothesis.

In the initial discussion of the a_n theories, it was stated that the a_1 theory (the sinh-Gordon model) appeared to be special in that there were no three point couplings in the model. However it is possible to consider the a_n S-matrix proposed above for $n = 1$, at least formally. For $h = 2$ (the Coxeter number of A_1), $\{1\}$ has no physical poles, just a pair of zeroes at $i\pi B/2$ and $i\pi(1 - B/2)$. This is certainly consistent with the absence of three point couplings, and indeed has been postulated independently to be the S-matrix for the sinh-Gordon model (see, for example, [62]). The coupling-constant dependence proposed there agrees with that given in (4.8). One other interesting remark is that the sinh-Gordon model can be thought of as the analytic continuation of the sine-Gordon theory to imaginary values of the coupling constant. The natural candidate to correspond to the single sinh-Gordon particle is the lowest sine-Gordon breather, and the analytic continuation of this breather-breather S-matrix element is exactly $\{1\}$, with the hypothesised coupling-constant dependence. This is an example where ‘naive’ analytic continuation of S-matrix elements in the coupling constant seems to be valid. Things are not always this simple.

4.3 Following Through the Bootstrap

This section contains the full results for the simply-laced Toda S-matrices. These provide many checks on the fundamental S-matrices proposed above, since each individual S-matrix element can be compared against predictions coming directly from perturbation

theory with the original Toda lagrangian. These other S-matrix elements are found by use of the bootstrap equations (2.23):

$$S_{d\bar{c}}(\theta) = S_{da}(\theta - i\bar{U}_{ac}^b)S_{db}(\theta + i\bar{U}_{bc}^a).$$

For practical calculations, it is convenient to develop the notation somewhat. First, define a shift operator \mathcal{T}_y acting in the space of functions on \mathbb{C} as

$$(\mathcal{T}_y f)(\theta) = f\left(\theta + \frac{i\pi y}{h}\right),$$

the factor $i\pi/h$ being inserted for later convenience. The bootstrap equations can now be rewritten, without explicit mention of θ :

$$S_{d\bar{c}} = (\mathcal{T}_{-h\bar{U}_{ac}^b} S_{da})(\mathcal{T}_{h\bar{U}_{bc}^a} S_{db}). \tag{4.10}$$

A slight subtlety arises here in that \mathcal{T}_y does not preserve the unitarity property (2.17), and so does not map the functions (x) to other such functions. To get round this problem, define

$$(x)^+ = \sinh\left(\frac{\theta}{2} + \frac{i\pi x}{2h}\right),$$

so that

$$(x) = \frac{(x)^+}{(-x)^+}.$$

Then

$$\mathcal{T}_y(x)^+ = (x + y)^+.$$

Similarly define $\{x\}^+$, exactly as $\{x\}$ but built from $(x)^+$ instead of (x) . Clearly

$$\{x\} = \frac{\{x\}^+}{\{-x\}^+} \quad \text{and} \quad \mathcal{T}_y\{x\}^+ = \{x + y\}^+.$$

Note also that

$$(x)^+ = -(x \pm 2h)^+ \quad , \quad \{x\}^+ = \{x \pm 2h\}^+. \tag{4.11}$$

Bearing in mind that \mathcal{T}_y acts distributively on products and quotients, it is now straightforward to use these deconstructed blocks to check any given bootstrap relation (4.10). The left-hand side of (4.10), $S_{d\bar{c}}$, always turns out to be unitary (as has to be), but this relies on sometimes quite involved cross-cancellations between the two individually non-unitary terms on the right-hand side of the equation.

The $a_n^{(1)}$ case will be used to illustrate the use of the above, while for the other theories only the final results will be given.

$a_n^{(1)}$

As stated earlier, the fundamental S-matrix element here is $S_{11} = \{1\}$. This has a forward channel pole at $i\pi/h$, corresponding to the $1\ 1 \rightarrow 2$ fusing. Since $\bar{U}_{12}^1 = \pi/h$, (4.10) becomes

$$\begin{aligned} S_{12} &= (\mathcal{T}_{-1}\{1\})(\mathcal{T}_1\{1\}) \\ &= (\mathcal{T}_{-1}\frac{\{1\}^+}{\{-1\}^+})(\mathcal{T}_1\frac{\{1\}^+}{\{-1\}^+}) \\ &= \frac{\{0\}^+ \{2\}^+}{\{-2\}^+ \{0\}^+} \\ &= \frac{\{2\}^+}{\{-2\}^+} = \{2\}. \end{aligned}$$

This has a forward channel pole at $3i\pi/h$, and a cross channel pole at $i\pi/h$, exactly as expected given that the Toda lagrangian predicts fusings $1\ 2 \rightarrow 3$ and $1\ \bar{2} \rightarrow \bar{1}$ with fusing angles $3\pi/h$ and $\pi - \pi/h$ respectively.

Next, the same $1\ 1 \rightarrow 2$ fusing can be used to find S_{22} :

$$\begin{aligned} S_{22} &= (\mathcal{T}_{-1}S_{12})(\mathcal{T}_1S_{12}) \\ &= (\mathcal{T}_{-1}\frac{\{2\}^+}{\{-2\}^+})(\mathcal{T}_1\frac{\{2\}^+}{\{-2\}^+}) \\ &= \frac{\{1\}^+ \{3\}^+}{\{-3\}^+ \{-1\}^+} \\ &= \{1\}\{3\}. \end{aligned}$$

The simple pole at $4i\pi/h$ is again as expected, given the $2\ 2 \rightarrow 4$ fusing, but note that this S-matrix element also has a double pole in the physical strip, at $2i\pi/h$. This is also predicted by perturbation theory, as will be explained in the final section of this chapter.

One more example should make the method clear. The $1\ 2 \rightarrow 3$ fusing can be used

to deduce S_{23} . $\bar{U}_{13}^2 = 2\pi/h$, $\bar{U}_{23}^1 = \pi/h$, so

$$\begin{aligned} S_{23} &= (\mathcal{T}_{-2}S_{12})(\mathcal{T}_1S_{22}) \\ &= (\mathcal{T}_{-2}\frac{\{2\}^+}{\{-2\}^+})(\mathcal{T}_1\frac{\{1\}^+\{3\}^+}{\{-1\}^+\{-3\}^+}) \\ &= \frac{\{0\}^+ \{2\}^+\{4\}^+}{\{-4\}^+ \{0\}^+\{-2\}^+} \\ &= \{2\}\{4\}. \end{aligned}$$

Note the intricate way in which the terms on the right-hand side of the equation gather themselves up into unitary combinations.

Eventually, additional cancellations occur owing to the periodicity of $\{x\}^+$ in x , equation (4.11), and the bootstrap closes, on exactly n particles. The general S-matrix element is

$$\begin{aligned} S_{ab} &= \{|a-b|+1\}\{|a-b|+3\}\dots\{|a+b|-1\} \\ &= \prod_{\substack{a+b-1 \\ |a-b|+1 \\ \text{step } 2}}^{\dots} \{p\}. \end{aligned} \tag{4.12}$$

The closing of the bootstrap can be seen in the cancellations that occur within this expression if both a and b are larger than $n/2$. For example, consider $S_{\bar{1}\bar{1}} = S_{nn}$. The expression (4.12) gives this to be

$$\{1\}\{3\}\dots\{2n-3\}\{2n-1\},$$

but, recalling that $h = n + 1$, (4.11) (or, in this case, (4.6)) implies that

$$\{2n-p\} = \{2n-p-2(n+1)\} = \{-p-2\} = (\{p+2\})^{-1}.$$

Hence all terms but the first cancel in pairs, leaving

$$S_{nn} = \{1\} = S_{11},$$

the result expected on the basis of CT invariance.

The minimal S-matrices are obtained from (4.12) simply by omitting the B -dependent part, that is by substituting

$$\{x\}' = (x-1)(x+1) \tag{4.13}$$

for $\{x\}$ throughout.

$d_n^{(1)}$

The fundamental matrix element shown in figure 14 for $d_n^{(1)}$ can be re-expressed in terms of the new building block. The result is slightly different for n even or odd:

$$S_{ss}^{(\text{even})} = \{1\}\{5\}\{9\} \dots \{2n-3\}$$

$$= \prod_{\substack{p=1 \\ \text{step } 4}}^{h-1} \{p\}$$

$$S_{ss}^{(\text{odd})} = \{1\}\{5\}\{9\} \dots \{2n-5\}$$

$$= \prod_{\substack{p=1 \\ \text{step } 4}}^{h-3} \{p\}.$$

If n is even, it turns out *not* to be possible to deduce all the rest of the S-matrix from this information and the bootstrap alone. As remarked earlier, this is a reflection of the doubled up exponent of D_{even} . However, physically there is no doubt what the answers should be. Exactly the same reasoning as led to $S_{ss}^{(\text{even})}$ can be used to derive

$$S_{s's'}^{(\text{even})} = S_{ss}^{(\text{even})},$$

$$S_{s's'}^{(\text{even})} = \{3\}\{7\}\{11\} \dots \{2n-5\}$$

$$= \prod_{\substack{p=3 \\ \text{step } 4}}^{h-3} \{p\}.$$

In contrast, for n odd the fusings $s s \rightarrow 1$ and $1 s \rightarrow \bar{s}$ allow the bootstrap to determine the corresponding two matrix elements with no further physical input. The results of this are:

$$S_{\bar{s}\bar{s}}^{(\text{odd})} = S_{ss}^{(\text{odd})},$$

$$S_{s\bar{s}}^{(\text{odd})} = \{3\}\{7\}\{11\} \dots \{2n-3\}$$

$$= \prod_{\substack{p=3 \\ \text{step } 4}}^{h-1} \{p\}.$$

In fact, both of these could have been predicted in advance. The first follows from CT invariance, while the second is just the crossed version of $S_{ss}^{(\text{odd})}$ (recall that $\{x\}$ crosses

to $\{h - x\}$, in agreement with the charge conjugation properties already assigned to s and \bar{s} .

Whatever the value of n , the above three matrix elements are sufficient to deduce the rest of the S-matrix. The results are of the same form for n even or odd. Letting \hat{s} stand for s' or \bar{s} as appropriate,

$$S_{sa} = S_{\hat{s}a} = \{n - a\}\{n - a + 2\} \dots \{n + a - 2\}$$

$$= \prod_{\substack{h/2+a-1 \\ h/2-a+1 \\ \text{step } 2}} \{p\},$$

$$S_{ab} = \prod_{\substack{a+b-1 \\ |a-b|+1 \\ \text{step } 2}} \{p\}\{h - p\}.$$

Note that the last S-matrix element is just the crossing symmetric version of (4.12).

As above, the minimal S-matrix can be obtained by substituting $\{x\}'$, defined by (4.13), for $\{x\}$ in all expressions. A point which will not be expanded on here is that these minimal S-matrix elements are very nearly those of the sine-Gordon model at specific values of the coupling constant.^[4, 8, 6]

$e_6^{(1)}, e_7^{(1)}$ and $e_8^{(1)}$

The results for these theories can be found in tables 9a,10a and 11a. To ease the comparison of the physical pole structure of these theories with the classical data given in tables 9,10 and 11, the minimal S-matrices are shown in the upper right halves of the tables, along with the full object in the lower left. All of the e_7 and e_8 S-matrix elements are self-conjugate (as are many in e_6), and in order to save space, crossing symmetric versions of the two basic blocks have been used whenever possible. These are:

$$[x] \equiv (x)(h - x) \quad \text{and} \quad x \equiv \{x\}\{h - x\}.$$

4.4 Perturbative Checks of the Proposed S-Matrices

This section describes some of the progress that has been made in checking the results of the last section against perturbation theory based on the affine Toda lagrangian. Such calculations will never provide a complete proof of the ansätze made above, but they do provide strong evidence for their correctness, as well as revealing many interesting features.

The first task is to justify some of the claims made in earlier sections by checking the residues of the simple poles. The exact S-matrices above predict these to be particularly simple, as can be seen from the following nice feature of the building block $\{x\}$: from the definitions (2.18) and (4.5), it is immediate that

$$\{x\}(\theta) = 1 + \frac{i\beta^2}{2h} \left(\frac{-1 + o(\beta^2)}{\theta - i\pi(x-1)/h} + \frac{1 + o(\beta^2)}{\theta - i\pi(x+1)/h} + \dots \right), \quad (4.14)$$

the dots standing for terms which are regular when θ is in the physical strip. Thus to lowest order in β , the poles in $\{x\}$ at $i\pi(x \pm 1)/h$ have residues $\pm i\beta^2/2h$, independent of x , and furthermore within an S-matrix $\{x\}$ has no effect on the residues of any other poles.

In perturbation theory, the lowest-order contributions to these residues must come from tree level diagrams; any corrections will be of higher order in β . In the forward channel, the internal propagator and vertices of a diagram such as that shown in figure 8 will contribute, by the standard Feynman rules, an amount

$$\hat{S}_{ab} = (iC^{abc})^2 \frac{i}{p_c^2 - m_c^2}$$

where, using equations (2.10) and (2.20),

$$\begin{aligned} p_c^2 - m_c^2 &= s - m_c^2 = m_a^2 + m_b^2 + 2m_a m_b \cosh \theta_{ab} - m_c^2 \\ &= 2m_a m_b (\cosh \theta_{ab} - \cos U_{ab}^{\bar{c}}) \\ &= -4m_a m_b \sin \frac{i}{2}(\theta + iU) \sin \frac{i}{2}(\theta - iU) \\ &\sim 2im_a m_b \sin U_{ab}^{\bar{c}} (\theta_{ab} - iU_{ab}^{\bar{c}}) \quad \text{as } \theta_{ab} \rightarrow iU_{ab}^{\bar{c}}. \end{aligned} \quad (4.15)$$

Before comparison with the S-matrix is made, the normalization of the external wavefunctions and the flux factor must be taken into account. Near $\theta_{ab} = iU_{ab}^{\bar{c}}$ this yields an

overall factor

$$\frac{1}{4im_a m_b \sin U_{ab}^{\bar{c}}} \quad (4.16)$$

and so the correctly normalized contribution is

$$S_{ab} = \frac{i(C^{abc})^2}{8m_a^2 m_b^2 \sin^2 U_{ab}^{\bar{c}}} \frac{1}{\theta_{ab} - iU_{ab}^{\bar{c}}}.$$

Now the area formula (3.9) can be used, to find

$$S_{ab} = \frac{i\beta^2}{2h} \frac{1}{\theta_{ab} - iU_{ab}^{\bar{c}}}, \quad (4.17)$$

in perfect agreement with (4.14). The crossed residue turns out to be the same same in magnitude, but of opposite sign. This justifies the claim made in the discussion of the fundamental S-matrix elements that the zeroes associated to forward and crossed channel poles moved by equal but opposite amounts for small β (*ie* $C'(0) = B'(0)$), while the correct normalization of the above residues verifies the leading β -dependence of $B(\beta)$ implied by the hypothesis (4.8).

This provides a ‘universal’ proof of the correctness of the leading-order residues of the simple poles in all Toda theories. The situation for the higher poles is much more complicated, involving the evaluation of loop diagrams in perturbation theory, and discussion of the relevant issues will be postponed until the next section.

However there remains one question at tree level. Above it was verified that for diagonal scattering, the residues of the poles agree with tree level calculations. It should also be checked that the amplitudes for non-diagonal (*ie* inelastic) scattering do indeed vanish. It is often possible to find Feynman diagrams contributing to such processes, and a check should be made (at least at tree level) that the sum of all relevant contributions is zero. Verification of this in all cases would give a ‘tree level no-production theorem’ and, if achieved in a similarly universal way to the above ‘residue theorem’, would probably be very illuminating. Unfortunately, the kinematics becomes much more complicated when the outgoing particles are of different masses to those incoming, and furthermore the cancellations rely on precise relationships among the different non-zero couplings, and so such a universal understanding of non-production is lacking. However in all cases that have been checked to date (including all the $A_n^{(1)}$ theories^[58]) the theorem holds,

so there seems little reason to doubt its truth. In fact, it also holds in non simply-laced theories, perhaps implying that this, like the solution to the conserved charges bootstrap, is essentially a classical result.

Rather than go into details, the $d_4^{(1)}$ theory will be used to illustrate some features found in all cases. This is a theory with three light particles, and one heavy. There is complete symmetry between the light particles and so, in contrast to the usual notation for d theories, these will be labelled l, l' and l'' . They each have mass $\sqrt{2}m$, while h , the single heavy particle, has mass $\sqrt{6}m$. The non-vanishing three-point couplings are:

$$\begin{aligned}
 C^{llh} &= C^{l'l'h} = C^{l''l''h} = -\sqrt{2}\beta m^2, \\
 C^{l'l''} &= \sqrt{2}\beta m^2, \quad C^{hhh} = 3\sqrt{2}\beta m^2.
 \end{aligned}
 \tag{4.18}$$

(The discrepancy with the set of couplings quoted in [7] and [8] is explained by the fact that combinatorial factors have been omitted in the definition (3.7) of the Toda couplings — if such factors had been included, they would have been reabsorbed into symmetry factors when evaluating Feynman graphs, so the conventions chosen here are simpler in practice.) The fusing angles are all multiples of $\pi/h = \pi/6$; a representative subset is:

$$U_{hh}^h = U_{l'l''}^l = \frac{2}{3}\pi, \quad U_{ll}^h = \frac{1}{3}\pi, \quad U_{lh}^l = \frac{5}{6}\pi.
 \tag{4.19}$$

This data is illustrated in figure 15.

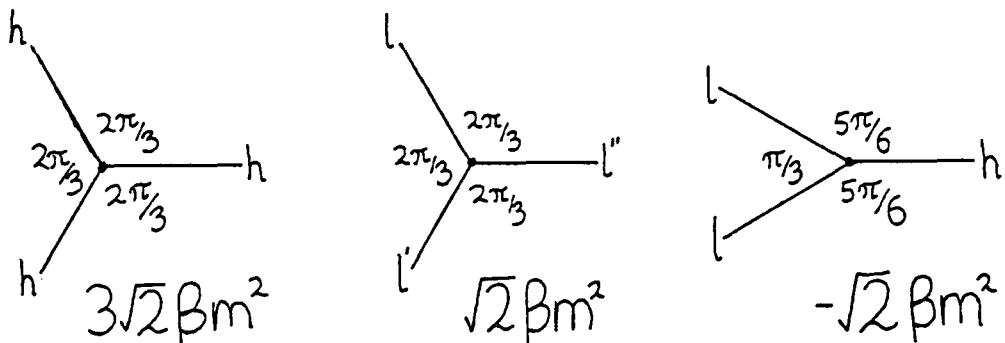


Figure 15 : $d_4^{(1)}$ couplings and fusing angles.

For a full tree level calculation of $2 \rightarrow 2$ scattering, diagrams involving a four point coupling should also be included, contributing a constant factor. These are found in the

order β^2 term in the expansion (3.7), and the results that will be needed below are:

$$C^{ll'l'} = \beta^2 m^2, \quad C^{hhll} = \beta^2 m^2. \quad (4.20)$$

The scattering of two light particles is described by the matrix element $S_{ll} = \{1\}\{5\}$, with a pole in the forward channel at $i\pi/3$, and in the crossed channel at $2i\pi/3$. These appear in perturbation theory in the two diagrams shown in figure 16.

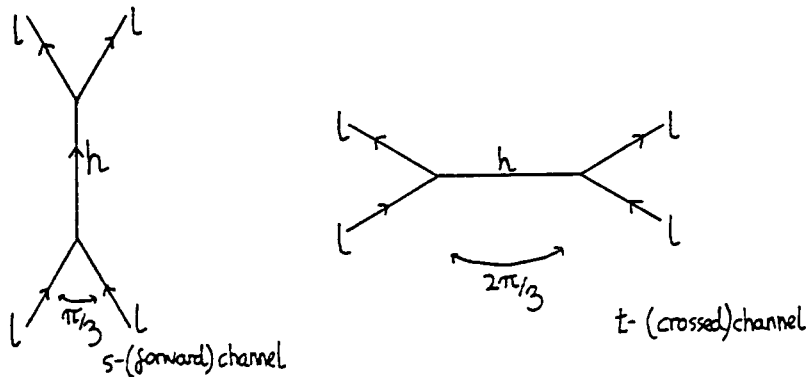


Figure 16 : $ll \rightarrow ll$ scattering.

This much is perfectly satisfactory, but it might appear that there should also be a forward channel pole in $ll \rightarrow l'l'$ scattering, given that the upper vertex in the first diagram could be replaced by the $C^{l'l'h}$ coupling. This would imply a non-zero amplitude for a supposedly disallowed process, so certainly ought to cancel against something. In fact it does: the $C^{ll'l'}$ coupling implies that there is a crossed channel pole at exactly the same location. This cancels the forward pole, since $(C^{ll'l'})^2 = C^{llh}C^{l'l'h}$, and the crossed nature of the pole negates its residue relative to the forward channel. The diagrams are drawn in figure 17.

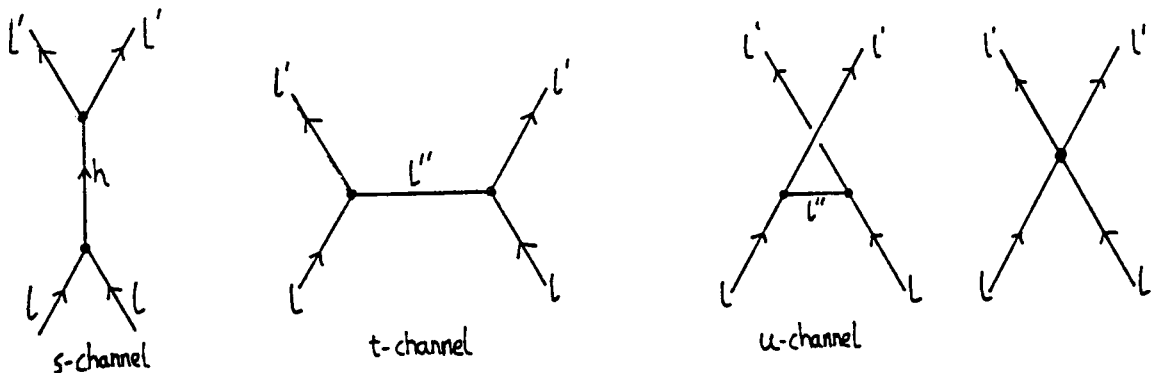


Figure 17 : $ll \rightarrow l'l'$ scattering.

The figure also includes the two other contributions to the $l l \rightarrow l' l'$ scattering to order β^2 . Neither of these is singular (note that the u-channel momentum is identically zero), which is why they were ignored before, but of course even a constant term would violate the no-production theorem. Note that the kinematics here is exactly that of an elastic process, since l and l' are of equal mass. For this reason it is easy to see that the first two diagrams of figure 17 cancel exactly (not even a constant term is left). Hence the last two diagrams should also cancel. This is easily verified: the u-channel process contributes

$$\frac{(C^{ll'l'})^2}{p_{l'}^2 - m_{l'}^2} = \frac{2\beta^2 m^4}{-2m^2}$$

which is exactly cancelled by the contribution of $C^{ll'l'} = \beta^2 m^2$ coming from the last diagram.

The crossed process to that shown in figure 17 is the scattering $l l' \rightarrow l' l$ involving the reflection of particles l and l' , and rotating all the diagrams by 90 degrees shows that this amplitude also vanishes to order β^2 , as expected.

An interesting feature of the above, apart from the implied interrelationship between the various three-point couplings, is the necessity of the four-point coupling to cancel an unwanted amplitude completely. One could envisage starting with just the three-point couplings and then generating the higher order terms iteratively, an n point coupling being needed to cancel the constant term remaining after all other tree level contributions to a (forbidden) $2 \rightarrow (n - 2)$ process had been summed. Such a mechanism has been claimed to work for the sine-Gordon model^[63]; its detailed verification would of course be much more complicated for a general Toda theory.

Useful though the above example was, it misses most of the complexities that beset the cancellation of a general amplitude, since the kinematics was that of a diagonal process and the u-channel diagram consequently trivial. A more representative example is easily found: rather than have the heavy intermediate particle of the first process in figure 16 decay into two further light particles, it can decay into a pair of heavy particles. This gives a diagram contributing to $l l \rightarrow h h$ scattering, with a pole at $i\pi/3$ in the forward channel rapidity. The other diagrams involved in this process are shown in figure 18.

It is easy to verify geometrically (using the fusing angle data illustrated in figure 15) that there is indeed a candidate to cancel the undesirable pole, namely the u-channel process with another particle of type l as the intermediate state. (Note that the fusing

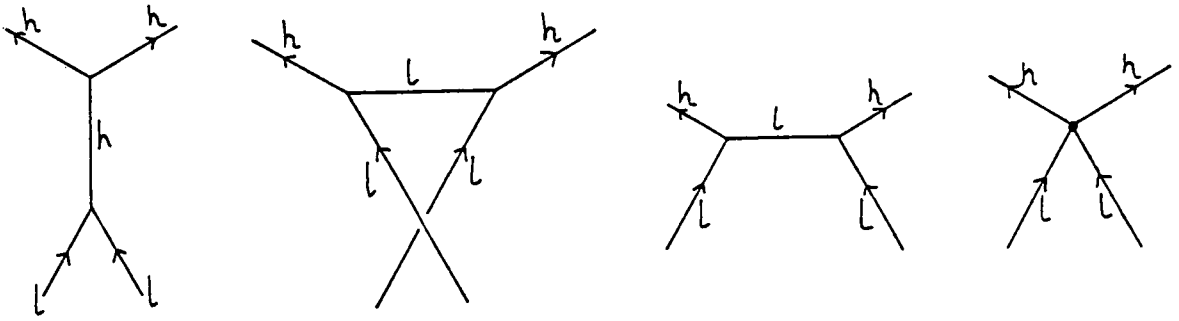


Figure 18 : $ll \rightarrow hh$ scattering.

angles give precisely the relative rapidity at which the propagator is singular, the intermediate (fused) particle then being on shell.) To say more is much harder, since there is no longer a simple relation such as (2.14) to fix the Mandelstam variable t (and hence u) in terms of s . A detailed calculation shows that the full amplitude *does* vanish, but is not very instructive, and it would be very useful to obtain a more general understanding of how the cancellation comes about. (In fact in this particular case the ‘classical’ tree level cancellation is in any case masked in the quantum theory by a higher pole arising from a loop diagram; more will be said on this in the next section.) However one general point can be made, which will turn out to be important in the discussion of higher poles. Assuming that the tree level no-production theorem does hold, then every forward channel diagram corresponding to a disallowed process must be accompanied by one in the u - or t - channels which has a pole at exactly the same place, for there to be any chance of a cancellation. It is helpful to think of this in terms of ‘on-shell diagrams’, that is diagrams constructed by gluing together vertices with legs at the relevant fusing angles, of the type shown in figure 15. Such diagrams correspond to Feynman graphs with all external and internal lines on-shell. For tree diagrams there is only one internal line, and it is on-shell exactly when the diagram has a pole in the relative rapidity of the incoming particles. The pairs of on-shell diagrams relevant to the cancellations already seen are shown in figure 19, together with their duals (made up of triangles with sides the corresponding masses). The deficit in the second dual diagram can be traced to the crossing of two particle tracks in the corresponding on-shell picture.

On the basis of a somewhat tenuous analogy with string theory, the process of swapping between two on-shell diagrams with the same external momenta will be called ‘dualising’ (not, of course, to be confused with the geometrical procedure of drawing the dual

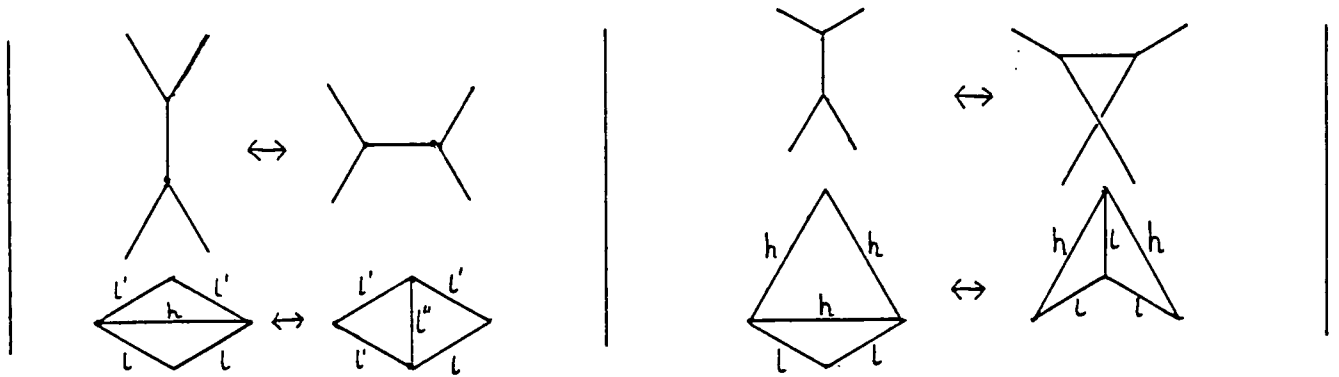


Figure 19 : Dualising forbidden tree level processes.

diagram). It is important to realize that it must be possible to find the dualised diagram for *any* non-diagonal tree level diagram, if the tree level no-production theorem is true. The procedure has been checked in many cases, but just as for the full theorem, no general proof exists as yet. Indeed it is possible that the full theorem will be proved by an entirely different route, in which case this 'dualising theorem' would be an interesting corollary. More will be said on the potential uses of this theorem in the next section.

The final subject to be mentioned here is that of renormalization. So far the perturbative treatment has been at tree level only, and the consistency checks on conserved charges and non-production have failed to distinguish between the simply-laced and non simply-laced theories. It is only when the tree level data is used with the S-matrix bootstrap equations that differences emerge, in the difficulties mentioned above for the non simply-laced theories. It would be helpful to see these differences directly within perturbation theory, and for this reason it is worth pushing the perturbative treatment one stage further. This involves the calculation of diagrams containing loops, and so questions of renormalization, avoided up to now, must be addressed.

Perturbation theory in β takes the free part of the lagrangian (3.1) to be the kinetic term plus the mass term (3.6) extracted from the expansion of the potential $V(\phi)$; the remainder of the potential is then the sum of higher order interaction terms (a different point of view, having more in common with the ideas of perturbed conformal field theories, will be mentioned in the next chapter). In two dimensions the only ultraviolet divergences come from tadpole diagrams, and are removed by normal-ordering. In [12] it is shown that any finite parts of these tadpoles that might remain after normal-ordering will respect the classical mass ratios, for both simply and non-simply laced theories (a discussion of the tadpoles in the simpler situation of the sine-Gordon model can be found in [64], [65]).

However there are still finite wave function and mass renormalizations required owing to other propagator insertions.

These mass renormalizations allow an immediate check to be made on the validity of many of the assumptions made above. For example, in the quantum theory the bootstrap equations (2.24) for conserved charges should use fusing angles U_{ab}^c derived from the renormalized masses. For the set of conserved quantities derived above to survive quantization, these angles should retain their classical values, and hence the mass ratios should not renormalize.

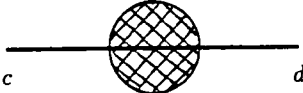
The renormalized masses are found by considering the corrections to the propagator. The bare propagator is

$$\text{---}_c \text{---}_d = \frac{i}{(2\pi)^2} \left(\frac{1}{p^2 - M^2} \right)_{cd}$$

Here M^2 is the (mass)² matrix, given by (3.6); in the basis of classical mass eigenstates it is simply

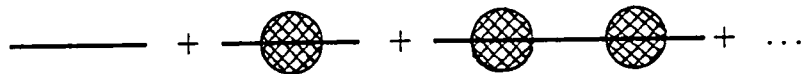
$$(M^2)_{cd} = m_c^2 \delta_{cd}.$$

There are corrections to the bare propagator from all (amputated) 1PI diagrams; the sum of these will be denoted by the matrix $\Sigma(p^2)$:



$$= \Sigma_{cd}(p^2).$$

Some of these diagrams will connect particles of different types, so Σ has off-diagonal entries. The full propagator is



$$= \frac{i}{(2\pi)^2} \frac{1}{p^2 - M^2} \left[1 + \Sigma(p^2) \frac{i}{(2\pi)^2} \frac{1}{p^2 - M^2} + \left(\Sigma(p^2) \frac{i}{(2\pi)^2} \frac{1}{p^2 - M^2} \right)^2 + \dots \right]$$

$$= \frac{i}{(2\pi)^2} \frac{1}{p^2 - M^2 - \frac{i}{(2\pi)^2} \Sigma(p^2)},$$

and it should be remembered that the denominator is again a matrix. The renormalized

masses and mass eigenstates are found by looking for the zeroes of this denominator, that is by solving

$$p^2 I - M^2 = \frac{i}{(2\pi)^2} \Sigma(p^2)$$

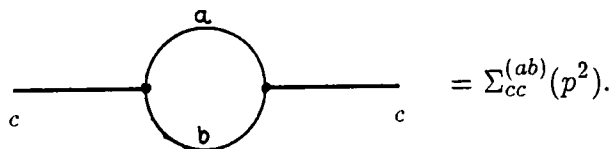
for p^2 . In perturbation theory this can be done iteratively, since Σ is of order β^2 , while M^2 is of order β^0 . For particle c , $p^2 = m_c^2$ to lowest order, and substituting this into the right-hand side, the renormalized mass to order β^2 is the eigenvalue of

$$M^2 + \frac{i}{(2\pi)^2} \Sigma(m_c^2)$$

which as $\beta^2 \rightarrow 0$ tends to m_c^2 . Off-diagonal entries in Σ only contribute at the next order, so the simple result for the first correction to the particle masses is

$$\hat{m}_c^2 = m_c^2 + \frac{i}{(2\pi)^2} \Sigma_{cc}(m_c^2)$$

where Σ_{cc} should only be evaluated to order β^2 . Higher corrections are much harder to evaluate, as the re-diagonalization of the (mass)² matrix needs to be taken into account, but all that remains for the current calculation is to find the order β^2 contributions to Σ_{cc} . These are just bubble diagrams containing a pair of three point couplings, with intermediate particles a and b , say:



The value of this elementary bubble (computed after a Wick rotation) is given by the formula

$$\Sigma_{cc}^{(ab)}(p^2) = |C^{abc}|^2 \frac{i\pi}{p\Delta} \tan^{-1} \left[\frac{2p\Delta}{m_a^2 + m_b^2 - p^2} \right]$$

where

$$\Delta^2 = \frac{2p^2(m_a^2 + m_b^2) - (m_a^2 - m_b^2)^2 - p^4}{4p^2}$$

Substituting $p^2 = m_c^2$ simplifies the result considerably:

$$\Sigma_{ab}(m_c^2) = \frac{i\pi |C^{abc}|^2 \bar{U}_{ab}^c}{m_a m_b \sin U_{ab}^c} \tag{4.21}$$

Recalling the area rule (3.9) for the magnitude of the coupling constant, for all but the

untwisted non simply-laced theories this becomes

$$\begin{aligned}\Sigma_{cc}^{(ab)}(m_c^2) &= \frac{4i\pi\beta^2}{h} \bar{U}_{ab}^c m_a m_b \sin U_{ab}^c \\ &= \frac{4i\pi\beta^2}{h} m_c^2 \bar{U}_{ab}^c \frac{\sin U_{ac}^b \sin U_{bc}^a}{\sin U_{ab}^c}.\end{aligned}\tag{4.22}$$

This form turns out to be the most convenient.

In general, there will be many intermediate contributions a, b to the bubble^{*}, and the calculation is quite involved. Remarkably, for all the simply-laced theories the final result is very simple, and leads to a universal formula for δm_c^2 , the one-loop correction to m_c^2 :

$$\frac{\delta m_c^2}{m_c^2} = \frac{-\beta^2}{4h} \cot \frac{\pi}{h}.\tag{4.23}$$

Thus to one loop in the simply-laced theories, the mass ratios do *not* renormalize, the fusing angles retain their classical values and the bootstrap equations used earlier remain valid.

For the non simply-laced theories, no such result is found — even to order β^2 the masses do not renormalize together. This is an important result, confirming the difficulties that were found above for the untwisted cases. For the twisted theories, it demonstrates that simply truncating the appropriate simply-laced S-matrix, a prescription that up to now has seemed perfectly consistent, cannot be correct. The problem with the truncation is that while the twisted particles form a subalgebra in the couplings, thus forbidding their fusing to form one of the omitted ('untwisted') particles, this does not prevent one twisted particle splitting into two untwisted ones, which might then recombine to form a bubble and contribute to the mass renormalization, for example. Hence the quantum properties of a theory containing *just* the twisted particles and those of the parent may be very different, even when one tries to restrict attention to the subset of twisted particles in the parent theory.

For the simply-laced theories the result is also very significant, providing strong evidence for the quantum integrability of these models. Unfortunately there is no universal understanding of the final result (4.23), the summation of contributions differing in details from case to case. The nature of the calculation will be illustrated with the a_n theory.

* In fact $h - 2$, counting a, b and b, a separately when a and b are different.

In this case, the coupling rule (3.16) shows that for given c the allowed choices for a, b are

$$k, n + 1 - c - k \quad \text{for } k = 1, \dots, n - c$$

$$n + 1 - k, n + 1 - c + k \quad \text{for } k = 1, \dots, c - 1,$$

a total of $n - 1 \equiv h - 2$ possibilities. Summing (4.22) over all these possibilities yields (setting $\lambda = 4i\pi\beta^2 m_c^2/h$ and $\theta = \pi/(n + 1)$),

$$\Sigma(m_c^2) = \frac{1}{2} \lambda \theta \left[\sum_{k=1}^{n-c} c \frac{\sin(c+k)\theta \sin k\theta}{\sin c\theta} - \sum_{k=1}^{c-1} (n+1-c) \frac{\sin(c-k)\theta \sin k\theta}{\sin c\theta} \right]$$

$$= \frac{1}{2} \frac{\lambda \theta}{\sin c\theta} \left[c \sum_{k=0}^n \sin(c+k)\theta \sin k\theta - (n+1) \sum_{k=0}^c \sin(c-k)\theta \sin k\theta \right]$$

where in the last expression some extra (zero) terms have been added for convenience. The factor of $1/2$ comes about in one of two ways: if $a \neq b$ then the a, b bubble is otherwise counted twice, while if $a = b$, $1/2$ is the required symmetry factor for the bubble graph. (Note, the normalization of the three point couplings adopted in (3.9) is such that extra combinatorial factors are only ever required for graphs having such additional symmetry.) The sums are performed using the identity

$$\sum_{k=0}^m \cos(c + 2k)\theta = \frac{\cos(c + m)\theta \sin(m + 1)\theta}{\sin \theta},$$

to yield

$$\Sigma(m_c^2) = \frac{i\pi^2 \beta^2}{h} m_c^2 \cot \frac{\pi}{h},$$

from which the formula (4.23) for the mass shift follows immediately.

For d_n the calculation is much the same, if a little more involved, and the details can be found in [6]. For e_6 the result has also been obtained analytically, while for e_7 and e_8 it has been verified numerically by computer. Clearly, a universal understanding would be highly desirable, as would some understanding of how the result generalizes to higher orders.

4.5 Higher Poles

A feature of the S-matrices derived above is the frequent occurrence of higher order poles. This phenomenon was first observed in the exact S-matrix of the sine-Gordon model and was initially unexplained, thought maybe to be connected with the integrability of the model. However Coleman and Thun^[66] showed that the higher sine-Gordon poles, surprising to those accustomed to dealing with scattering in 3+1 dimensions, have a straightforward field-theoretic explanation in 1+1 dimensions as ordinary Landau singularities, and indeed would be seen in the perturbative treatment of *any* 1+1 dimensional field theory with suitable mass spectrum.

At generic values of the coupling constant the sine-Gordon model has poles only up to the second order, while the poles in Toda S-matrices can be of much higher order, in fact up to 12 in the case of 8 8 scattering in the $e_8^{(1)}$ theory. This section will explain how the mechanism of Coleman and Thun generalizes to these cases, and the possible implications of this for the bootstrap equations. A very rich structure will be seen to emerge, only small parts of which are currently understood.

Singularities in Feynman integrals are identified by the Landau rules. These rules are equivalent to the intuitively appealing criterion that a singularity in the external momenta is expected when the relevant Feynman diagram can be viewed as an energy- and momentum- conserving process occurring in spacetime with all internal particles on shell.^[67] In other words a large amplitude occurs when the intermediate particles are all long-lived, an idea that is the natural generalization of the tree level situation. (To be more precise, an internal particle may be off shell, but then its line should be contracted to a point when drawing the space-time diagram, corresponding to the short lifetime of such a state. When all such lines have been contracted, the resulting 'short-circuited' diagram *will* have all particles on shell.)

As stated, these rules apply to poles occurring for physical values of the external momenta — the diagram to be drawn involves real particles in Minkowski space-time — and so should not be directly relevant to scattering in integrable theories such as the sine-Gordon or Toda models. However just as happened with the simple poles, the singularities are still found, but pushed to unphysical values of momenta below the two-particle threshold. The positions of the singularities are still given by the Landau rules, but now the relative momenta in the on-shell diagram are all euclidean. For a graph constructed from the Toda three-point couplings this is easily seen: at any vertex, the

conditions that momentum be conserved and that all three particles be on-shell are exactly those that went into the derivation of formula (2.20) for the fusing angles. These always correspond to euclidean relative momenta, as has to be the case given that all particles are stable. Being true at each vertex, the same conclusion must hold across the entire diagram, with the result that the figure can be drawn using straight lines in Euclidean space, with the angles at each vertex being the appropriate fusing angles. Sometimes it is more helpful to draw the corresponding dual diagram, but in any event, the location of singularities is reduced to a question of plane geometry.

Note how naturally all the above generalizes the discussion of the simple poles, where the on-shell diagram is just the tree level Feynman diagram of figure 8 with the single intermediate particle on shell, exactly the point at which the propagator has a pole. It is natural to ask whether the bootstrap ideas associated to the simple poles can also be extended, and this question will be addressed towards the end of this section.

Before discussing such general issues, some specific cases will be examined starting with one of the simplest, the $d_4^{(1)}$ theory. The fusing angles for this model have already been given in figure 15, and are sufficiently small in number that it is perfectly feasible to enumerate all the possible on-shell diagrams that can be formed. However it is easier to start with the S-matrix, to find when such diagrams might be expected to occur. To facilitate the location of poles in S-matrix elements, it is helpful to introduce a streamlined version of the pictorial notation used in figure 14. The building block $\{x\}$ is represented by a rectangle above the imaginary axis, stretching from $(x - 1)\pi i/h$ to $(x + 1)\pi i/h$:

$$\{x\} \equiv \begin{array}{c} \begin{array}{ccc} [-i\beta^2/2h] & & [+i\beta^2/2h] \\ \hline & \text{rectangle} & \\ \hline \end{array} \\ \text{---} \frac{(x-1)\pi i/h}{} \qquad \qquad \qquad \frac{(x+1)\pi i/h}{} \text{---} \end{array}$$

The residues of the poles at $(x \pm 1)\pi i/h$, given by equation (4.14) to lowest order in β , are shown above the block. A product of blocks making up an S-matrix element is represented by stacking the rectangles; for example,

$$\{3\}^2\{5\} \equiv \begin{array}{c} \text{rectangle} \\ \text{---} \frac{2\pi i/h}{} \qquad \qquad \qquad \frac{4\pi i/h}{} \qquad \qquad \qquad \frac{6\pi i/h}{} \text{---} \end{array}$$

Poles occur at the ends of the blocks, and higher order poles where the ends of blocks coincide. Thus in the above example there is a pole of order three at $\theta = 4i\pi/h$, coming

from the two blocks to the left and one to the right. A feature of the notation is the ease with which the residue* in θ can be read off the diagrams: the residues from each contributing block multiply, and furthermore the contribution from two directly abutting blocks (one to the left and one to the right of the pole) is

$$\frac{i\beta^2}{2h} \times \frac{-i\beta^2}{2h} = \frac{\beta^4}{4h^2}.$$

Hence the sign of the residue is determined solely by the difference in the number of blocks immediately to the left and right of the pole, that is by the change in height of the wall of blocks at the position of the pole. In fact the change in the height is never by more than plus or minus one, though I know of no explanation for this fact. It is clear that, travelling from left to right, an 'uphill' pole has residue proportional to $-i$, while for a 'downhill' pole the residue is proportional to $+i$:

$$\begin{array}{c} \text{---} \\ \{x-1\} \end{array} \Bigg| \begin{array}{c} \overline{\{x+1\}} \\ \{x+1\} \end{array} \sim \left(\frac{\beta^2}{2h}\right)^m \frac{-i}{(\theta - ix/h)^m}. \quad (4.24)$$

$$\begin{array}{c} \overline{\{x-1\}} \\ \{x-1\} \end{array} \Bigg| \text{---} \{x+1\} \sim \left(\frac{\beta^2}{2h}\right)^m \frac{+i}{(\theta - ix/h)^m}, \quad (4.25)$$

Note that m , the total number of blocks to left and right of the pole, is odd in both of these cases. These odd order poles always seem to have an interpretation in terms of the production of a bound state. More will be said on this below: it turns out that the second case above, the downhill pole with a positive residue, is always forward channel, while the first, uphill, case is crossed channel. For the simple poles this is immediate from the field theory, as (4.17) shows, but for the higher poles it is far from clear why such a simple rule should hold.

Even order poles occur if (and only if, given that height changes of two or more never occur) the height of the wall remains constant at the pole position, and thus always have positive (real) residue.

The $d_4^{(1)}$ theory is so simple that all this notation may seem to be unnecessary, but it becomes useful when more complicated theories are examined. As an example, appendix

* The term residue is being used somewhat loosely here to mean the coefficient of the highest-order term in the Laurent expansion about the pole.

involving the couplings C^{lh} , $C^{l'h}$ and $C^{l''l''}$ for S_{ll} , $S_{l'l'}$ and $S_{l''l''}$ respectively. The S-matrix elements between these two and the other light particle, l'' , follow by the bootstrap, or alternatively can be deduced from the complete symmetry between the light particles. Thus the poles are again simple, and are also explained by tree diagrams.

There are essentially only two further S-matrix elements, and both have higher poles. First, the heavy particle scatters with any light particle as:

$$S_{lh} = \int_0^{i\pi} \dots$$

The forward channel pole at $5\pi i/6$ can be seen in a tree diagram with l appearing as a bound state, but the double pole at $\pi i/2$ is new. It is explained by an on-shell box diagram, shown together with its dual in figure 20.

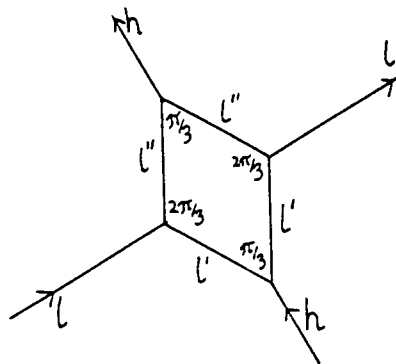


Figure 20 : the double pole in S_{lh} .

There is also a similar diagram with l' and l'' exchanged, but these are the only diagrams expected to contribute to the double pole to the relevant order in β^2 . Note that an m^{th} order pole always has a residue proportional to β^{2m} in the S-matrix, and for topological reasons, no diagram involving four or more point couplings can have sufficiently many on-shell loops to contribute at this order in β^2 . This justifies restricting attention to on-shell diagrams with only three point couplings when seeking a perturbative explanation for the higher poles. Coleman and Thun used on-shell box diagrams in their explanation of the sine-Gordon poles, and in two dimensions they do indeed have a double pole. For the d_4 Toda theory the total residue from the relevant two diagrams has been calculated,^[69, 58] and it is found to agree with the order β^4 prediction coming from the exact S-matrix. One other point with reference to the double pole: note that figure 20 gives no support

to the idea that this might be connected with a single bound state, a fact consistent with the absence of any classical fusing between l and h at $\pi i/2$, the position of the pole.

Finally there is the heavy-heavy S-matrix element:

$$S_{hh} = \int_0^{i\pi} \dots$$

This only has triple poles, at $\pi i/3$ and $2\pi i/3$, with residues proportional to $-i$ and $+i$ respectively. The most obvious contribution to these residues comes from on-shell diagrams obtained from the tree level graph with an h intermediate state by replacing the C^{hhh} couplings by a pair of 'vertex corrections'. One of the resulting expanded graphs is shown in figure 21, together with its dual; each vertex can be made from l , l' , or l'' propagators so there are nine such graphs in all.

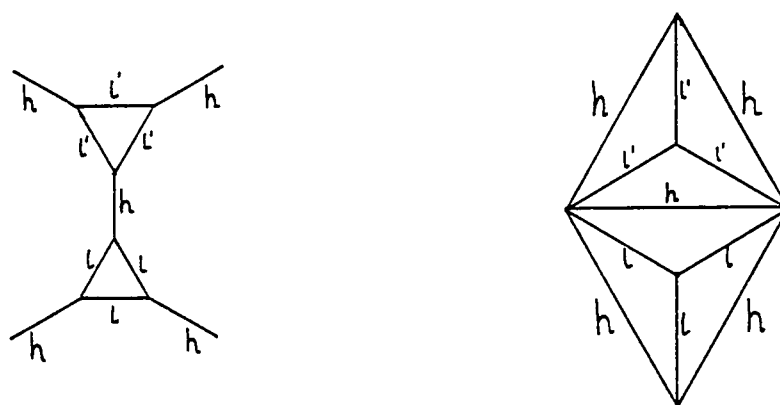


Figure 21 : the double vertex part of the S_{hh} triple pole.

Note that in this case there *is* a sense in which this pole has an associated bound state, namely a particle of type h , and furthermore the forward channel pole for this particle has residue $+i\beta^6/(2m)^3$, in agreement with the 'uphill/downhill' rule formulated above for the identification of the forward channel. No new consistency checks are implied by this pole over those already checked, though, since the classical fusing implied by the C^{hhh} coupling occurs at exactly the same angle as the new fusing. Of course, this had to be the case given that the diagrams arose via vertex corrections to the tree level picture. In fact it will be argued later that a reverse situation holds, in that a higher pole tends to be the sign of a reduction in the number of independent consistency conditions.

However this cannot be the whole story for the third order pole. The structure of the double vertex Feynman integral is sufficiently simple that it is possible to see this without

any detailed calculations. The double integral over the two free internal momenta of any graph with the topology shown in figure 21 separates into two independent parts, one for each vertex, together with the propagator for the intermediate particle, fixed by the external momenta. Let the contribution to the whole coming from just one corrected vertex with, say, particle l propagating round the loop be denoted by $iV_l(s)$, a function of s , the squared rapidity difference of the two (incoming or outgoing) on-shell particles at the corrected vertex. Now $V_l(s)$ must be real, since in the integral each propagator has a factor of i , as does each vertex, and there is an additional i coming from the Wick rotation which takes care of the i in the definition of V . The Landau rules state that a singularity in this integral is expected when s is such that all the internal propagators in the integral can be simultaneously on shell; in the case at hand this happens when the corresponding rapidity difference is $2\pi i/3$. A first order pole in s is expected; let the residue of this pole be iR_l . The fact that the entire diagram goes on-shell together means that the other vertex, involving say particle l' , is also on-shell at this value of s , as is the propagator for the intermediate h particle (so the pole actually occurs at $s = m_h^2$). Thus the total order of the pole is three (as predicted by the S-matrix), and the contribution to the residue in the s variable from the l, l' vertex-corrected graph is $iR_l \cdot iR_{l'} \cdot i/(2\pi)^2$ (the last piece coming from the h propagator). Adding all nine such graphs together, the total contribution due to the vertex graphs, near to the pole at $s = m_h^2$, is

$$\hat{S}^{(\text{vert})} \sim -i \frac{(R_l + R_{l'} + R_{l''})^2}{(2\pi)^2 (s - m_h^2)^3} .$$

Just as at tree level this must be multiplied by the normalization factor (4.16) before comparison with the S-matrix is made, yielding

$$S^{(\text{vert})} \sim \frac{-R^2}{(s - m_h^2)^3} ,$$

where R is some real number. The residue in s is of the same sign as at tree level; this is expected since the vertex correction is proportional to $i/(s - m_h^2)$, and the original vertex was proportional to i . However in θ , the third-order residue must therefore be of the opposite sign to the tree-level residue, since (4.15) shows that near the pole θ is a purely imaginary multiple of s (this fact is also obvious from looking at the pictures of

the complex s - and θ - planes, figures 5 and 7). Thus

$$S^{(\text{vert})} \sim \frac{-i\mathcal{R}^2}{(\theta - iU_{ll}^h)^3},$$

where \mathcal{R} is another real constant. This is in conflict with the residue found in the S-matrix at $2\pi i/3$, which, in agreement with the general rule (4.25) for forward channel S-matrix poles, is a positive real multiple of i .

The above reasoning is perfectly general, and applies to any third order pole. The conclusion is that if the S-matrix is correct, there have to be further graphs in addition to the vertex corrections, to remedy the sign of the residue. Even more generally, it is possible to see that any pole of order $4m+3$ cannot be accounted for by vertex corrections alone, given that (4.25) always gives the residue for a forward channel fusing angle.

For the third order poles, the residues of the vertex corrections have been evaluated explicitly, and using this information the contributions of the double vertex diagrams to many third-order poles have been evaluated. The surprising result^[69] is that the magnitude of this contribution is always exactly the desired amount — it is only the sign that is incorrect. Thus the other diagrams must yield precisely twice the residue of the S-matrix pole for agreement to be found. There is no explanation as yet for this observation, but in a number of the simplest cases it has been found that other diagrams do indeed conspire to give the correct contribution.

There remains the question of identifying these extra diagrams, and it is here that the dualising idea can be employed. Consider an off-diagonal double vertex diagram, for example the d_4 diagram involving particle l in one vertex correction, particle l' in the other. Now remove the central portion of this diagram, containing the C^{llh} and $C^{l'l'h}$ couplings. This by itself forms an on-shell diagram for the non-diagonal scattering process $ll \rightarrow l'l'$, and so by the tree level no-production theorem it must be possible to dualise it, yielding another tree diagram with the same external momenta as the original subdiagram. This was discussed in the last section, and is illustrated in figure 19; the dualised diagram involves particle l'' in the crossed channel. Since the external momenta are unchanged, it must be possible to fit this new diagram back into the double vertex picture, into the space left by the old subdiagram. The result is a double-box diagram, also expected to contribute to the third-order pole. The whole process is illustrated in figure 22.

This idea is very general, and can be tried at every internal line of a given on-shell diagram. There are two situations when it may fail to yield another on-shell diagram.

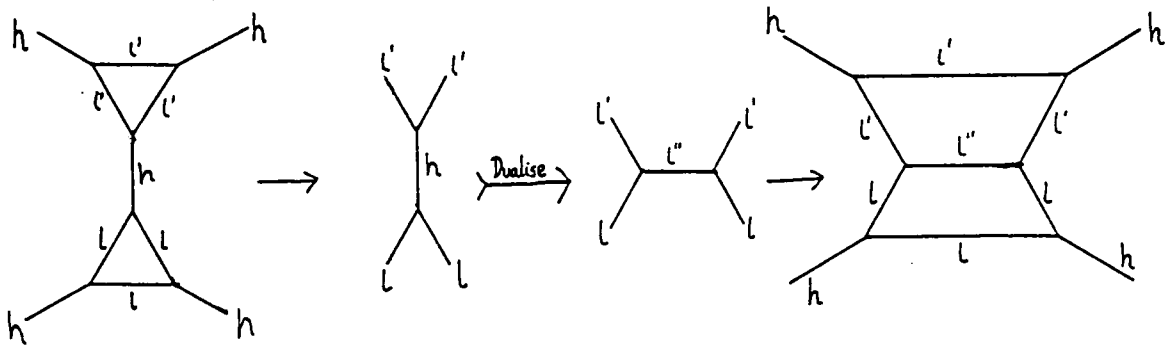


Figure 22 : Dualising within a higher diagram.

First, the tree level subdiagram containing the chosen internal line may in fact be an allowed scattering, so that no dualised diagram is expected — this would happen when considering the h internal line of one of the diagonal double vertex diagrams, for example. The second situation occurs when the momenta of the dualised diagram are wrongly ordered for a fit to be possible. An example is the attempt to dualise the lowest l internal line in the double vertex shown in figure 21; the tree level scattering process involved is $h h \rightarrow l l$. This scattering was also discussed in the last section, and the dualised diagram involves another h particle, in the forward channel. However the two outgoing l particles from this dualised diagram are diverging, while they must be converging if the picture is to be fitted back into the larger diagram. The problem is illustrated in figure 23. Also shown are the dual diagrams, which gives an alternative interpretation of the difficulty, namely that the dual of the dualised diagram is larger than the original dual diagram, and so cannot fit into the space left by removing that diagram. The problem is also related to the fact that the relevant forbidden tree level process in this case is masked by a higher pole, an issue that will be mentioned below.

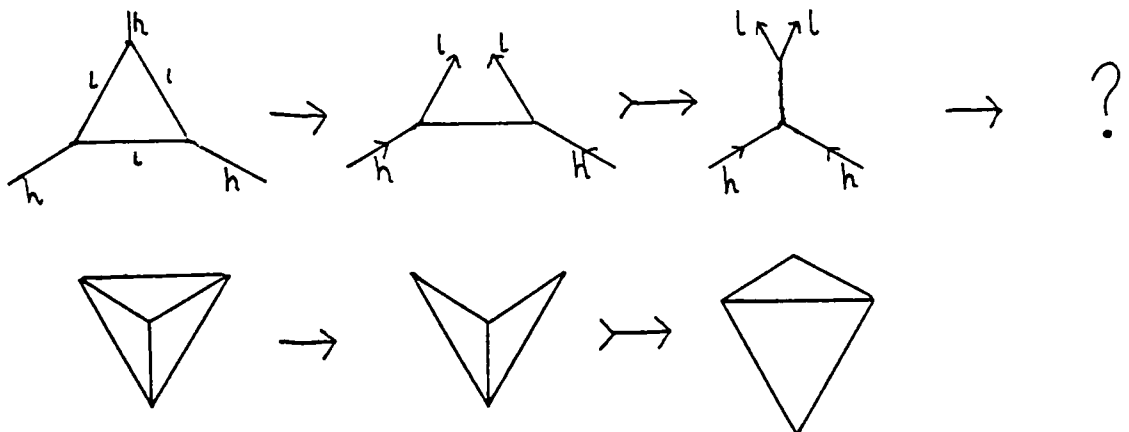


Figure 23 : A situation where dualising fails.

The one remaining subtlety to mention is that occasionally the outgoing particles in a forbidden process may be travelling in parallel, in which case the dualised process involves the two particles swapped over, and a complementary dualising will be needed somewhere else in the larger picture to ensure that everything matches up. This occurs in the d_4 double box diagrams, for example.

Thus starting from a given on-shell diagram it is possible to generate a whole set of further diagrams, all with the same external momenta and all expected to contribute to the higher pole. The network for d_4 is shown in figure 24.

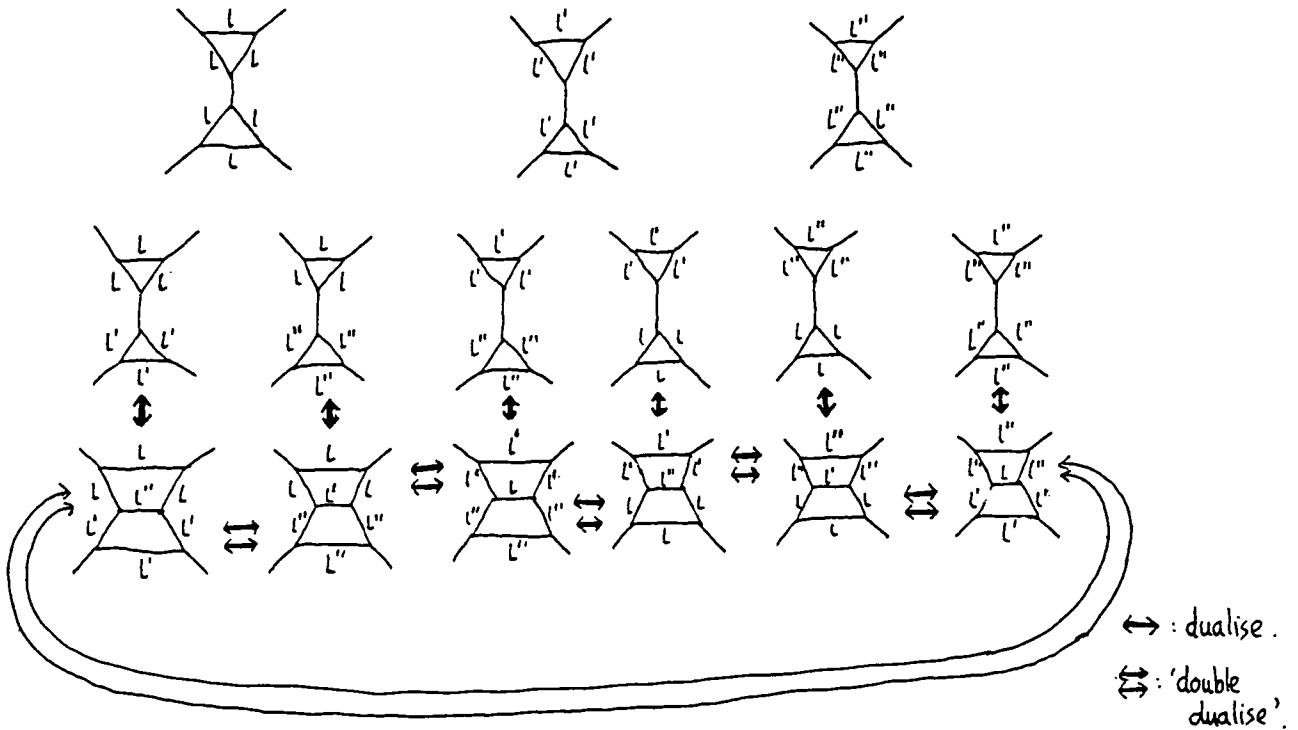


Figure 24 : The network of diagrams for the d_4 third order pole.

The diagonal double vertex diagrams are isolated points, but all the rest may be generated starting from any one of their number. An explicit calculation^[69, 58] has shown that the six double box diagrams give a total contribution of twice the S-matrix residue, so after adding all fifteen diagrams together, perturbation theory is in complete agreement with the hypothesised exact result. The double lines mark occasions where some relevant particle tracks are parallel, the subtlety referred to above occurs, and two simultaneous dualisings are required. This has the effect of closing the network off on fewer diagrams than is found for other third-order poles; a more general situation will be encountered below in the e_3 theory, when the network for 3 4 scattering is exhibited.

There is one more point that can be examined within the example of the $d_4^{(1)}$ theory, though, and that is the question of higher-level non-production. Just as was the case at tree level, it is often possible to draw on-shell diagrams for off-diagonal scattering processes. By the Landau rules these certainly should contribute poles to the relevant amplitudes, and if the proposed S-matrices are correct these poles must cancel amongst themselves to enable the total amplitude for the forbidden process to be zero. Thus without getting into the full complexities of higher-loop non-production, it should at least be checked that candidate on-shell diagrams are available to give such cancellations a chance. This can be illustrated with an example already considered, that of $ll \rightarrow hh$ scattering. Referring back to figure 18, it should now be clear that the diagram drawn there is masked by at least one on-shell diagram with a higher pole, obtained by 'correcting' the upper C^{hhh} vertex with a triangle containing three l, l' or l'' propagators, just as was done for both vertices in the $hh \rightarrow hh$ scattering. If scattering is purely elastic, there must therefore be some further diagrams to cancel this one. As before, the dualising idea can be used to find them. The resulting network (which is a subset of the network for hh diagonal scattering) is shown in figure 25.

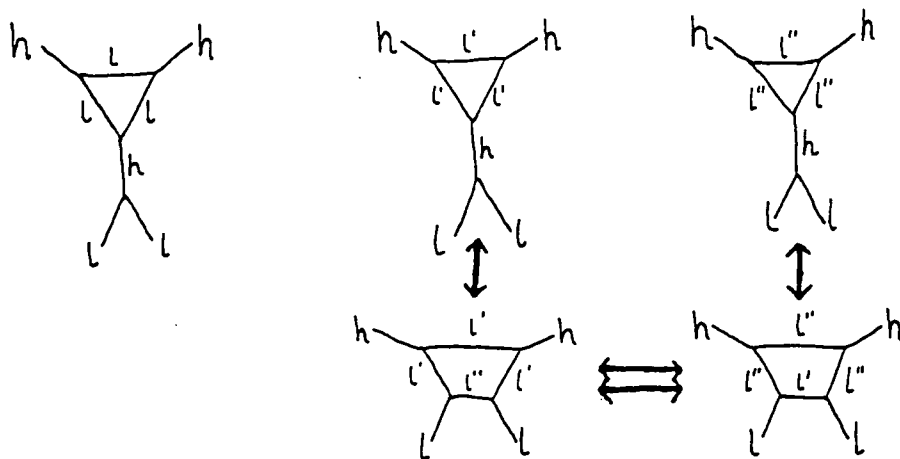


Figure 25 : The network of diagrams contributing to a disallowed process.

This particular calculation has yet to be performed, but should not present any great difficulties. However, the general question of higher loop non-production, even in the simplified form of requiring the leading order poles to cancel, is much harder to check than at tree level, and a general understanding is absent.

Returning to allowed scattering, for the a and d series the poles are of sufficiently low order that it should be possible to obtain general results on the correctness of their residues. For $a_n^{(1)}$, the highest poles are in fact only of second order. In the S_{ab} S-matrix element they are found where the blocks in (4.12) adjoin, that is at

$$\theta = \frac{i\pi}{n+1}(a+b-2k), \quad k = 1, \dots, \min(a, b) - 1.$$

(a and b are taken to be less than or equal to $h/2$, results for other values following via crossing. If either a or b is 1, there are no double poles.) Generically there are four diagrams to explain this pole, as shown in figure 26.

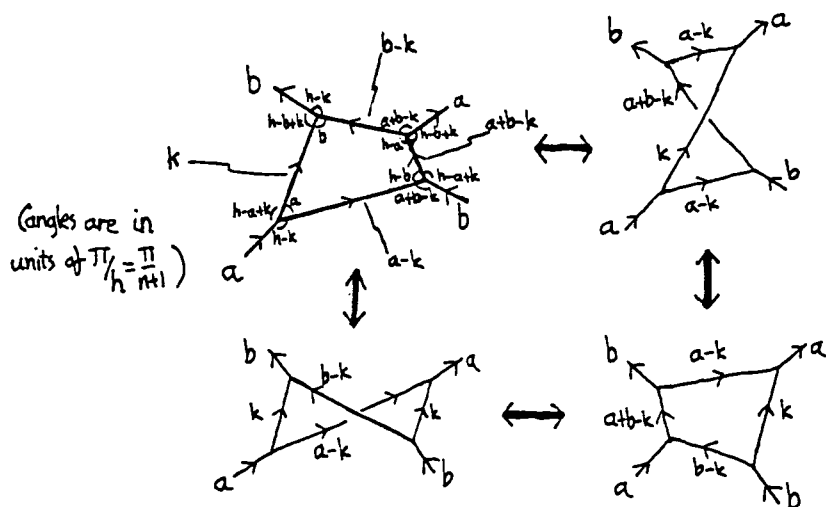


Figure 26 : The double poles of the a_n S-matrices.

Sometimes the exceptional situation referred to above occurs, in that one of the crossed boxes above fails to work, the relevant two particle tracks being parallel, forcing a double dualising. From the angles on the diagrams, this happens either when $a = b$ or when $a + b = h$ (note, the second case is just the crossed version of the first). Thus the S_{22} double pole mentioned in the bootstrap discussion only involves three diagrams, shown in figure 27.

When n is odd, the heaviest particle, $(n+1)/2$, is a singlet and for $a = b = (n+1)/2$, both possibilities occur. The other diagram with a cross-over is also lost, the two remaining diagrams involving rectangular boxes.

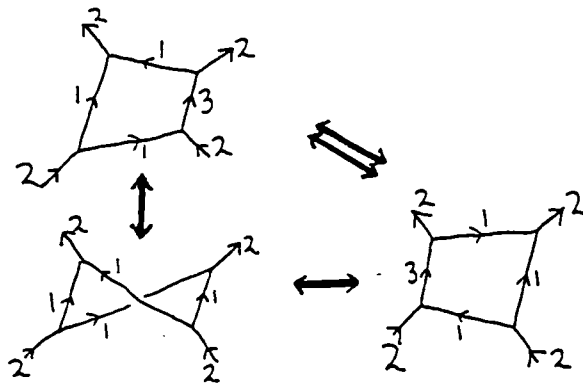
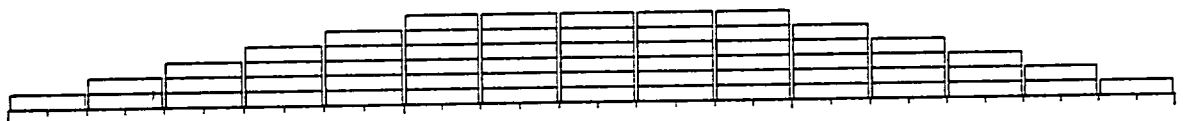


Figure 27 : The double pole in the $a_n S_{22}$ S-matrix.

For the d series the situation is a bit more complicated, as poles up to order 4 arise (d_4 was a special case, with the highest pole of order three). Rather than going into details of this, the $e_8^{(1)}$ theory will be briefly touched on to show how much more involved things can become.

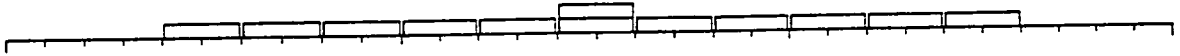
Appendix 2 lists the block structure of all the e_8 S-matrix elements, and it is clear that poles of much higher order are found, up to order twelve for 8 8 scattering. For these very high order poles it is something of a challenge to find even one candidate on-shell diagram, let alone to classify and evaluate all the relevant contributions. To show that candidates do always seem to be present, appendix 3 shows some examples for the higher poles in the S_{88} S-matrix element, the block structure of which is:



This had a sequence of odd-order higher poles, with those at $20, 22, 24, 26$ and $28 \pi/30$ expected to be forward channel. This expectation is supported by the fact that these poles mask forward channel tree level fusings involving particles 8, 7, 5, 3 and 1 respectively (reference should be made to table 11, showing the classical fusing data for this theory). It is natural to start by looking for the corresponding vertex corrections, and examples for each case are given in the appendix. Note that once a single example is known, many more can be constructed by the dualising idea. The other poles are all twelfth order, and the final picture shows that candidates for these can also be found. Again, once this on-shell diagram is known it is relatively easy to construct a whole string of further examples by dualising (in particular, the cross-over in the middle of the diagram can be removed, at the expense of some loss of symmetry). However the systematics of this are

not yet worked out in general, and this discussion of the e_8 theory concludes with another example which does at least seem to exhibit the generic behaviour for third order poles.

The block structure of S_{34} in the e_8 theory is:



There is a single forward channel third order pole, at $8\pi i/15$, which masks the classical fusing $3\ 4 \rightarrow 5$. Three on-shell vertex corrections to the C^{345} coupling can be found, and their dual diagrams are shown in figure 28.

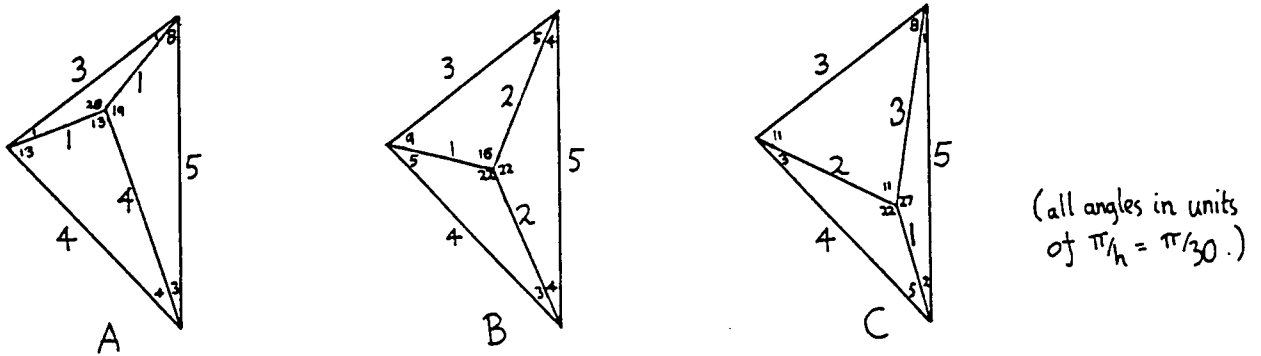


Figure 28 : On shell corrections to C^{345} .

Nine double vertex graphs result directly from these, all contributing to the triple pole. Just as happened in the d_4 case, the six non-diagonal pairings of vertex corrections can each be dualised, yielding six double box diagrams. However further dualising is possible here, leading to new graphs involving the crossing of particle tracks. The complete network is shown in figure 29.

The structure seems clearest when the dual diagrams are used. The labelling scheme adopted is based on the observation that couplings involving an external particle are always drawn from the set appearing in the vertex corrections. For the dual diagrams, this means that any triangle bordering on the edge of a diagram must be one of the six subtriangles which border on particles 3 or 4 in figure 28, and can be uniquely specified by the label A , B or C of the particular vertex correction where it can be found. These labels are marked round the edge of each dual diagram of figure 29. Thus in the top left diagram, the upper left triangle borders on particle 3 and comes from vertex correction A , so must be made up of particles 1, 1 and 3, while the lower left triangle again comes

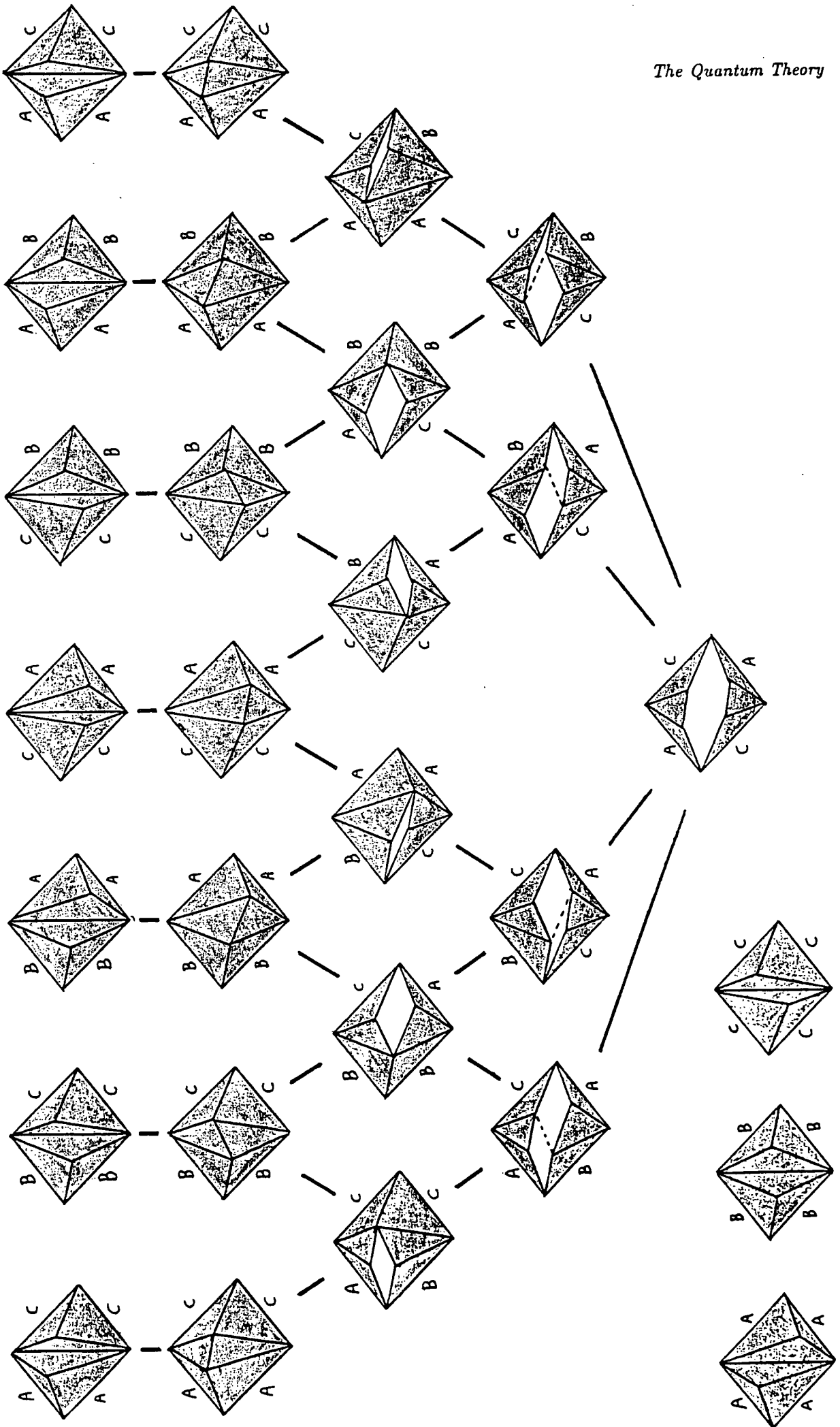


Figure 29 : The network of dual diagrams for an e_8 third order pole.

from the A vertex correction but this time involves particle 4, so consists of particles 1, 4 and 4. Using the dualising relationships between diagrams, it is straightforward to work out the remaining internal particles in each case, so this information is omitted.

Diagrams related by dualising are linked by a solid line, and for clarity the leftmost diagram in the top two rows is repeated on the right, so the figure shows a total of 26 distinct diagrams. The three isolated diagrams are diagonal double vertex corrections, the top row shows the non-diagonal double vertex corrections, and the second row the double boxes that are found by dualising these. The extra diagrams over those found for d_4 make up the rest of the network. Their dual diagrams all contain holes, corresponding to the crossing of particle tracks in the space-time diagram of the relevant process – one crossing for the diagrams in the third row, two for those in the fourth and three for the single diagram in the fifth row.

The symmetry properties of the network are explained once it is noticed that there is a natural ordering on the dual diagrams of the three initial vertex corrections. Refer back to figure 28, and consider the intermediate particle which couples with the incoming 3 and 4 particles, corresponding to the leftmost internal line in each dual diagram. The angle that this line makes with the vertical provides the ordering, diagram B being distinguished from the other two as the middle case. The effect that this has on the dualising possibilities can be seen on examining figure 29.

Given that third order poles always seem to have just three vertex corrections,^[69] figure 29 should give the generic situation for third order poles. Of course, the network may occasionally be truncated, as happened in the d_4 theory.

The residues of all these graphs have now been evaluated,^[69] and the total has been found to be in agreement with the S-matrix prediction. However the calculation is very laborious, and it seems likely that there is a more elegant way to understand how perturbation theory conspires to give such a simple result. Certainly, some form of systematics will have to be uncovered for there to be any hope of checking the higher poles shown in appendix 3, and in fact the initial motivation behind the dualising idea was the hope that the residues of any two diagrams related by dualising would cancel (this would be the direct generalization of the tree-level situation). Unfortunately this turns out not to be the case, but it is still possible that dualising will be of use to uncover some more subtle cancellations, and thus have implications for the calculation of residues as well as for the classification of contributing diagrams. The dualising networks for the higher poles will

be very complicated, and understanding their general structure remains an interesting problem.

Finally, to a couple of more general questions. First, some of the considerations of section 4.2 should be re-examined, since many of the classical three point couplings have been seen to receive on-shell vertex corrections (which should not be ignored, even for small β). It is natural to wonder whether this possibility should have been taken into account when postulating the fundamental S-matrix elements. However it is easily seen that if the chosen fundamental particle is also the lightest particle in the model, then there is no need to worry. Consider first the situation where all external particles couple separately with internal lines in the on-shell diagram, so thinking of all four particles as ingoing, each initially splits into two. Each lightest particle can only split into two others with a (de-) fusing angle of at least $2\pi/3$, and so there is no possibility of the particles so produced meeting to form the outer edges of an on-shell diagram. (The situation is even worse if the trajectories of these particles head inside the diagram.) Similarly, the angles fail to work if two external particles couple separately before interacting with the others, leaving only the possibility of the external particles fusing in pairs to form a common bound state, which is exactly the tree level situation already taken into account. For the d series this argument cannot be applied directly, since the fundamental particle is not the lightest in the theory. However on noticing that there are no couplings in the d theories involving just a single s or s' particle, it is clear that the defusing angle referred to above must be greater than $\pi/2$, after which the argument goes through as before.

The last question to be discussed here is the meaning that should be given to the bootstrap equations in the presence of higher poles. The initial argument in chapter 2 assumed there to be only a simple pole in the S-matrix element S_{ab} at the fusing angle U_{ab}^c where the bootstrap was to be applied. The reasoning then was that at that angle, the process would be dominated by the tree-level Feynman graph of figure 8. There would therefore be a long-lived intermediate state $|c\rangle$, and after suitable analytic continuation the bootstrap equations (2.23) and (2.24) followed from the requirement that this state should reproduce quantities found in terms of the state $|ab\rangle$, as depicted in figures 11 and 12. However if there is a higher order pole, then the dominant diagram is no longer at tree level. Rather, it is a loop diagram in which all internal lines may be simultaneously on shell. As stated above, this can be viewed as the production of a variety of long-lived intermediate particles, which scatter off each other in complicated ways, the totality of their trajectories forming the on-shell diagram. There will therefore be a variety

of (multiparticle) intermediate states, depending on how many rescatterings have taken place, each of which will dominate the wavefunction for a time. (As at tree level, it is helpful to think in terms of wavepackets here, so that some meaning can be given to the particle trajectories.) The natural generalization of the tree-level bootstrap argument to this situation is to require consistency of the S-matrix and conserved quantities with *all* of the possible long-lived intermediate states. The reasoning is best illustrated with an example, taken from the d_4 theory already discussed. Consider a three body scattering process, as illustrated in figure 3, with two of the particles being heavy. Repeating the arguments of chapter 2, when the relative rapidity of these two particles is $2\pi i/3$ the point in figure 3(a) corresponding to their scattering can be expanded to show the long-lived intermediate particles. However this expansion process can now go rather further than before. Figure 30 shows one possibility for the expansion of figure 3(a) in this situation, replacing figure 11.

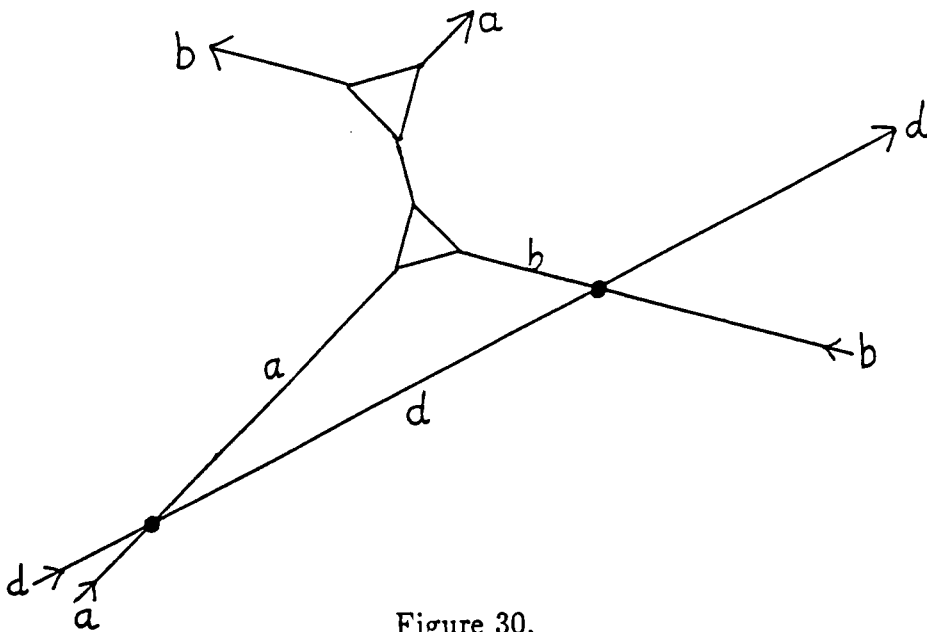


Figure 30.

As before, the conserved charges should allow the impact parameter of the third particle to be changed continuously, so that it interacts with some of the intermediate particles drawn in figure 30, a scattering process corresponding to figure 3(b). There are now a variety of different consistency conditions that can be deduced, depending on the particular value of the impact parameter. These possibilities are shown in figure 31, the replacement for figure 12.

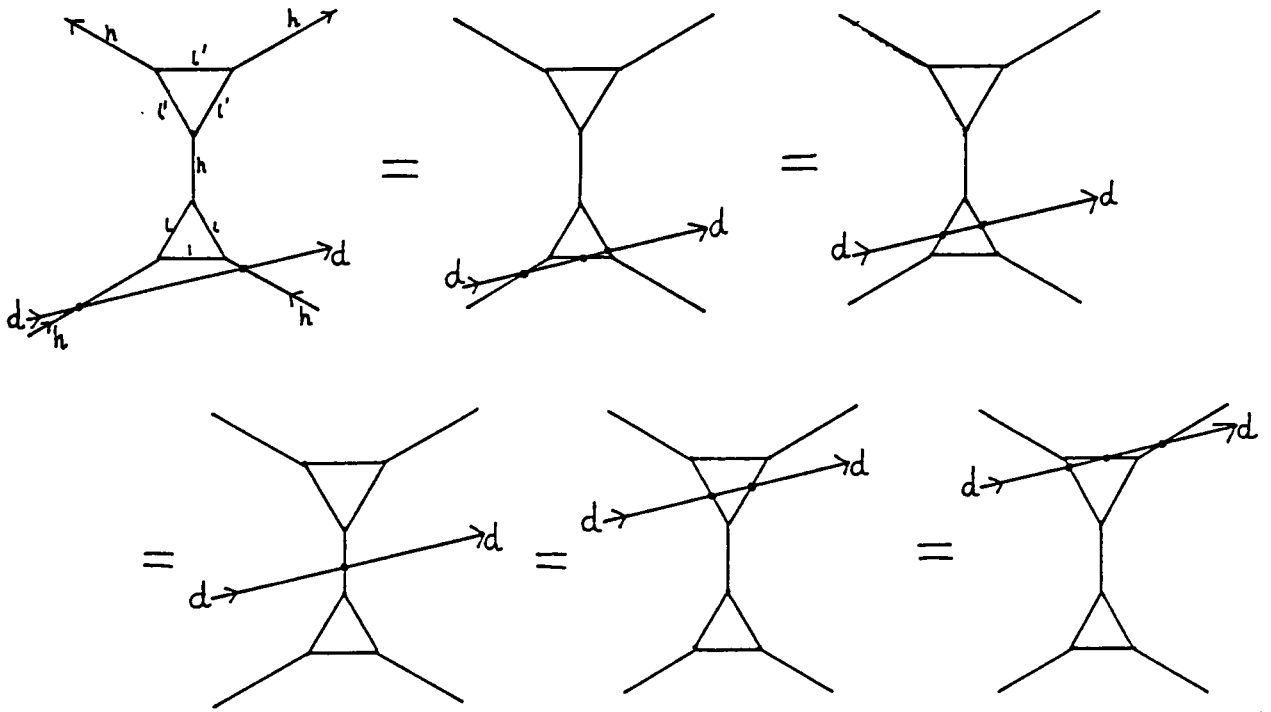


Figure 31.

Making use of the d_4 fusing angle data of equation (4.19), the full set of equalities implied by these diagrams is:

$$\begin{aligned}
 S_{dh}(\theta - i\pi/3)S_{dh}(\theta + i\pi/3) &= S_{dh}(\theta - i\pi/3)S_{dl}(\theta + i\pi/2)S_{dl}(\theta + i\pi/6) \\
 &= S_{dl}(\theta - i\pi/6)S_{dl}(\theta + i\pi/6) \\
 &= S_{dh}(\theta) \\
 &= S_{dl}(\theta + i\pi/6)S_{dl}(\theta - i\pi/6) \\
 &= S_{dl}(\theta + i\pi/2)S_{dl}(\theta - i\pi/6)S_{dh}(\theta - i\pi/3).
 \end{aligned}
 \tag{4.26}$$

It should be clear that a similar set of conditions can be read off any on-shell diagram in any of the theories under consideration, sometimes leading to a very large number of identities to be satisfied — recall for example some of the diagrams shown in appendix 3.

Considering these other diagrams exhibits one subtlety that has so far been ignored, namely that figure 30 showed only one possibility for the expansion of the $h h$ scattering at the $2\pi i/3$ pole, while nine are shown in figure 24. All such diagrams contribute a third order pole at the same location, and so no one can be said to dominate over the others. This might cast some doubt on the derivation of (4.26), where only the single on-shell diagram was examined. However if the analogous equations to (4.26) were to hold for each on-shell diagram individually, then the S-matrix would certainly be consistent with any

superposition of multiparticle states coming from a combination of the different diagrams. Thus the (at this stage possibly over-stringent) requirement for the higher-pole bootstrap, corresponding to the tree level requirements of (2.23), is that for every on-shell diagram that can be drawn at the pole under consideration, all consistency conditions derived from that diagram should hold. The corresponding set of equations for the conserved charges emerge in exactly the same way, and generalize (2.24). All the following applies in equal measure to the conserved charge equations.

This associates to every higher pole a large set of new identities, and a worry might be that this would invalidate some of the earlier work. However *all* of these identities are automatically satisfied once the tree-level bootstrap has been verified, as will now be shown. The key idea is to consider changing the impact parameter of particle d in suitably small steps. The trajectory of particle d will then be swept slowly across the picture, passing over one three-point vertex in the on-shell diagram at each step. The full set of identities for that diagram will be obtained when the sweep is complete. In the above example, the steps are the successive diagrams of figure 31, and generate the equations of (4.26) in turn. Now the desired result follows on noting that two ‘neighbouring’ equations, a single step apart, differ only by a single three-point coupling and their equality follows from the tree-level result involving that coupling. The more involved equalities then follow automatically, as the result of several steps each of which uses a tree-level result. For example, consider the d_4 case again. The step between the first two diagrams of figure 31 involves passing the trajectory of particle d over a single C^{llh} coupling, and the first equality of (4.26) follows from the tree-level fusing $l l \rightarrow h$, with bootstrap equation

$$S_{dh}(\theta) = S_{dl}(\theta - i\pi/6)S_{dl}(\theta + i\pi/6),$$

on shifting θ by an amount $i\pi/3$. The next step again involves a C^{llh} coupling, but this time the equation following from the $l h \rightarrow l$ fusing,

$$S_{dl}(\theta) = S_{dh}(\theta - i\pi/6)S_{dl}(\theta + 2i\pi/3),$$

should be used, and θ shifted by $-i\pi/6$.

The way in which the process continues should now be obvious, but it is worth pressing on one more step, to see that the third equality follows from the second via the bootstrap

equation for the $l l \rightarrow h$ fusing,

$$S_{dh}(\theta) = S_{dl}(\theta - i\pi/6)S_{dl}(\theta + i\pi/6).$$

This is interesting, because the ‘composite’ equality that has been deduced by putting these three stages together is just

$$S_{dh}(\theta) = S_{dh}(\theta - i\pi/3)S_{dh}(\theta + i\pi/3),$$

which is the tree-level bootstrap constraint following from the $h h \rightarrow h$ fusing. Previously this had been considered to be an independent restriction on the S-matrix elements, but the above has shown that it follows identically from a suitable combination of the $l l \rightarrow h$ and $l h \rightarrow l$ constraints.

Thus in contrast to initial expectations, the higher pole has actually led to a reduction in the number of independent bootstrap equations. This is clearly a rather general situation: whenever a classical three-point coupling is masked by an on-shell vertex correction, the bootstrap equations for that coupling can be deduced from those for the couplings that make up the vertex correction. Hence there is a direct link between higher order poles in the S-matrices and algebraic degeneracies among the bootstrap equations.

Previously, the bootstrap consistency conditions were checked for every classical coupling, even when in the S-matrix its amplitude was masked by a higher (odd) order pole. It might now be wondered whether this was necessary. Certainly if it could be shown that all odd-order poles involve at least one on-shell diagram with a pair of vertex corrections masking the classical coupling for that fusing angle, then the above arguments would show that the corresponding bootstrap equations were redundant. While there is no reason to doubt the truth of this hypothesis, I have been unable to find a general proof. If the hypothesis failed, and a situation did arise in which there were no double vertex graph, it might be argued that there would be no need on physical grounds to impose the bootstrap conditions for the classical coupling anyway, its tree-level on-shell diagram being masked by the higher-order process. However the classical coupling might appear singly within some other on-shell diagram, and so it is possible that there is some dominant physical process for which these bootstrap conditions *are* required. Hence a proof of the ‘double-vertex’ hypothesis does seem to be required before the higher poles can be completely disregarded when checking the bootstrap.

Chapter 5

Conclusions

One of the initial motivations for studying the Toda theories was the hope that they would provide explicit lagrangian models for the perturbed conformal field theories discussed in chapter 1, and this question will be examined first. As seen in section 4.2, the full Toda S-matrices are a product of two pieces: a ‘minimal’ part containing all the physical pole structure, together with an extra factor which encodes the coupling-constant dependence. The minimal and the full S-matrices are both consistent solutions of the bootstrap equations, and share the same set of conserved spins, namely the exponents of the relevant Lie algebra. Hence they provide two distinct candidates for each perturbed coset conformal theory of the type discussed in the final sections of chapter 1, and it is important to decide which one is correct.

The most direct evidence on this issue comes from work by Klassen and Melzer.^[14] A method known as the thermodynamic Bethe Ansatz, developed in this context by Al. Zamolodchikov,^[70] allows the central charge of the ultraviolet limit of a theory to be computed solely from its S-matrix. Since the ultra-violet limit of a relevant perturbation of a conformal theory is the original theory again, this enables a direct check to be made on the various proposals. This approach was used by Klassen and Melzer, who computed the central charges arising from both the minimal and the full S-matrices for each simply-laced Toda theory. They found that the central charge for the $g^{(1)} \times g^{(1)}/g^{(2)}$ coset was reproduced in each case by the minimal candidate, while the full S-matrix yielded a central charge equal to the rank of the corresponding finite algebra. This is strong evidence that the original proposals of Zamolodchikov in certain cases^[39, 2] were indeed correct, and the S-matrices for the perturbed conformal field theories are the minimal rather than the full candidates.

Hence the affine Toda field theories with real coupling constant do *not* provide a straightforward lagrangian framework for the perturbed minimal conformal field theories. As remarked at the beginning of chapter 3, this is perhaps not too surprising given the absence of such a formulation for the unperturbed models. In fact, the value of the central charge found by Klassen and Melzer for the full S-matrices, namely the rank r of the algebra, is not unexpected. Recall that r is also equal to the number of bosonic

fields in the theory. The perturbative approach used in this thesis to derive the Toda S-matrices implicitly assumed the Hilbert space structure of the theory to be that of a theory with the same number of free massive bosons. Given that the central charge is in some senses a measure of the number of degrees of freedom in the model, the Toda theory might therefore be expected to share the same ultraviolet central charge as a theory of r massive bosons, and this is certainly given by r . However the nature of the ultraviolet limit seems to be rather puzzling for the Toda theories with real coupling constant. It might be thought that at very short distances the effect of the exponential term in the Toda lagrangian would be lost, leaving just the kinetic term describing a (conformal) theory of r massless bosons for which the central charge is indeed r . However if this were correct, then it would be possible to view affine Toda theory as a perturbation of the theory of r massless bosons by an operator corresponding to the exponential potential. The problem is that from the point of view of the free massless boson theory, the exponential with real coupling constant has negative scaling dimension, so it is hard to see how it can be considered as a sensible local interaction term. This could be viewed as a particularly extreme case of the infra-red problems that afflict even the attempt to view a free massive theory in 1+1 dimensions in terms of a perturbation of a massless model. Note this problem does not arise in the more-studied case of the sine-Gordon model,^[65, 71] where the corresponding exponential involves an imaginary multiple of the basic field, and the scaling dimension of the perturbation is therefore positive. Recently there has been some work on renormalization group flows in Toda theories,^[72] but again for imaginary values of the coupling constant. The rather different situation for real values of the coupling constant will require independent investigation.

Even if the Toda theories are not perturbations of minimal models, there are still many things to be learnt from them, and they are certainly interesting in their own right. The structure of the bootstrap is not well understood, and it is helpful to have simple models available which allow many of the bootstrap axioms to be checked. A number of features of the bootstrap equations have already emerged from the studies of Toda theory which turn out to have more general applicability. In particular the conserved charge result of section 4.1 relies only on the physical pole structure and hence also holds for the minimal S-matrices, and much of the discussion of the implications of higher poles in section 4.5 was of a very general nature, and should apply to any purely elastic scattering theory.

In fact, no other unitary purely elastic S-matrices seem to be known beyond those

already described in this thesis. It is possible that if the bootstrap is to close on a finite number of particles in a unitary theory with only elastic scattering, then a minimal or full simply-laced Toda S-matrix is the only option. If no further conditions were imposed, then the sub-S-matrices identified by the twisted foldings would also be permitted, but the physical requirement that all higher poles be explicable in terms of suitable on-shell diagrams may well be enough to rule these out. For example, consider the twisted foldings of the $d_4^{(1)}$ theory, the higher poles of which were extensively discussed in section 4.5. The twisted folding to $a_3^{(2)} \equiv d_3^{(2)}$ preserves a light and a heavy particle, l and h say, and so the sub-S-matrix consists of the elements S_{ll} , S_{lh} and S_{hh} from the parent theory. These form a closed set under the bootstrap equations, but the double pole in S_{lh} , accounted for in the $d_4^{(1)}$ theory by two diagrams of the type shown in figure 20, both involving the other two light particles, cannot be explained in terms of particles l and h alone. Similarly, the folding to $a_2^{(2)}$, leaving just the heavy particle, results in an S-matrix element S_{hh} with a third-order pole that has no explanation within the particle spectrum of the model. Encouraged by such examples, a conjecture can be made that unitary purely elastic scattering theories for which the bootstrap closes on finitely many particles, with all higher physical S-matrix poles having an explanation in terms of on-shell diagrams involving three-point couplings already deduced from the simple poles, can only be of the simply-laced Toda type. This differs from an earlier proposal^[12, 16] in the imposition of the higher pole condition and consequent hypothesised restriction to the simply-laced theories. This restriction, if correct, has the appealing feature that the physical pole structure of the allowed S-matrices would then be uniquely characterized by the spectrum of conserved spins, confirming a conjecture of Zamolodchikov.^[73] An examination of table 3 and figure 13 shows that this would fail to be the case if any of the non simply-laced theories were permitted (recall, in all cases the spins repeat modulo the Coxeter number). A general proof of this conjecture would provide an interesting alternative characterization of the ubiquitous ADE series of simply-laced Dynkin diagrams.

Finally, it is worth recalling that the bootstrap idea has applicability beyond the purely elastic scattering theories: it is also found in theories which possess non-trivial multiplets.^[47] The Yang-Baxter structure of these models may shed light on aspects of the bootstrap; conversely, it would be interesting to see how many of the ‘pure bootstrap’ ideas contained in the last chapter can be generalized. Given an initial solution to the Yang-Baxter equation, the bootstrap (or fusion) procedure is often used to generate further solutions, with multiplets transforming under higher representations, and is hence of

considerable practical importance. One question to be answered concerns the extent to which the algebraic structure of the 'singlet' bootstrap found in Toda theory is repeated in these more complicated situations, and in particular whether the algebraic degeneracy induced by higher poles has any rôle to play. In addition, the fact that the mass ratios found in the group-invariant S-matrices of Ogievetsky and Wiegmann^[56] are the same as those for the Toda theories is perhaps a hint that there is a generalization of the result in section 4.1 relating higher Toda conserved charges to eigenvectors of Cartan matrices. In fact these sets of numbers seem to be of rather general significance, and it is possible that the conjecture of the previous paragraph can be widened, the hope being that an appropriate finiteness condition on the bootstrap in *any* scattering theory would always select a mass and conserved charge spectrum related to one of the simply-laced Lie algebras.

Appendix 1

REDUCE Listings for Character Calculations

```

procedure h(r,s,m);
begin
  return (((m+1)*r - m*s)**2 - 1) / (4*m*(m+1))
end;

procedure c(m);
begin
  return 1- 6/(m*(m+1))
end;

procedure p(b);
begin
  q**(b+1):=0;
  return for k:= 1:b product ( for l:= 0:b sum q**(k*l) )
end;

procedure tmp(k,r,s,m);
begin
  return q**(k*(k*m*(m+1)+(m+1)*r-m*s))-q**((k*m+r)*(k*(m+1)+s))
end;

procedure char(r,s,m,b);
begin
  q**(b+1):=0;
  l:= 0;
  tot:= tmp(l,r,s,m);
  while ((m+1)*l)**2-1 < b do
  begin
    l:= l+1;
    tot:= tot+ tmp(l,r,s,m)+tmp(-1*l,r,s,m)
  end;
  return p(b) * tot
end;

```



```

procedure negpart(w);
begin
  res:=0;
  for nl:= 0:deg(w,q) do
    if coeffn(w,q,nl)<0 then res:=res-coeffn(w,q,nl)*(q**nl);
  return res
end;

procedure poly(w);
begin
  nn:= deg(den(w),q);
  if nn=0 then return w else
  begin
    ptmp:=num(w);
    for pl:= 0:nn-1 do ptmp:=ptmp-coeffn(ptmp,q,pl)*q**pl
  end;
  return ptmp/den(w)
end;

procedure charges(l,u,b);
begin
  off allfac;
  b:=b+1;
  for m:= 1:u do
  begin
    write;
    write "=====";
    write "m = ",m,"      c = ",c(m);
    w0:= ((1-q)*char(1,1,m,b)+q-1)/q;
    for s:=2:m do for r:=1:s-1 do
      if h(r,s,m) neq 0 then
      begin
        w1:=(1-q)*char(r,s,m,b); q**b:=0; w3:=negpart(w1-w0);
        if deg(w3,q)>1 then
          begin
            write "-----";
            write "r,s = ",r," ",s," ;   m-r,m+1-s = ",m-r," ",m+1-s;
            write "h = ",h(r,s,m);
            write w3;
          end;
        end;
      end;
    end;
  end;
end;

```

```

procedure extracharges(l,u,b);
begin
  off allfac;
  b:=b+1;
  for m:= 1:u do
    if remainder(m-1,4)=0 or remainder(m-2,4)=0 then
      begin
        write;
        write "=====";
        write "m = ",m; write "Spin of first extra charge = ",h(1,m,m)-1;
        w0:=(1-q)*char(1,m,m,b)*q**(h(1,m,m)-1);
        if remainder(m-1,4)=0 then << ls:=3;ss:=2;sr:=1 >>
          else << ls:=2;ss:=1;sr:=2 >>;
        for s:= ls step ss until m do for r:= 1 step sr until s-1 do
          if h(r,s,m) neq 0 then
            begin
              w1:=(1-q)*char(r,m+1-s,m,b)*q**(h(r,m+1-s,m)-h(r,s,m));
              q**b:=0; w3:=negpart(poly(w1-w0));
              if deg(w3,q)>1 then
                begin
                  write "-----";
                  write "r,s = ",r,",",s," ;   m-r,m+1-s = ",m-r,",",m+1-s;
                  write "h = ",h(r,s,m);
                  write w3;
                end;
            end;
          end;
        end;
      end;
end;
end;
end;

```

In the above, `charges(1,u,b)` lists the polynomials of interest for the calculation described in section 1.5, for $m = 1 \dots u$, with b specifying the degree of the polynomial, while `extracharges` performs a similar function for the particular candidate higher-spin charges discussed in a section 1.8.

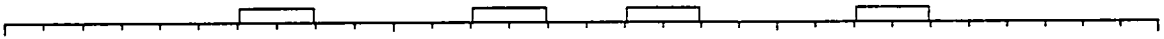
Appendix 2

Block Structure of the $e_8^{(1)}$ S-Matrix

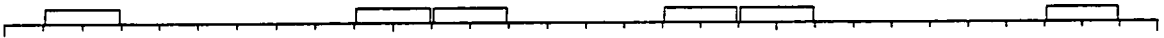
S_{11} :



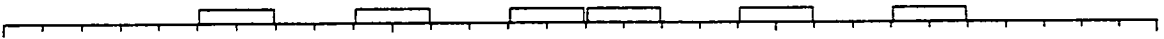
S_{12} :



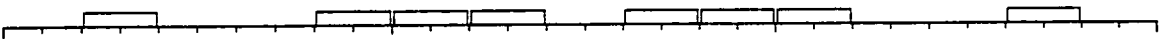
S_{13} :



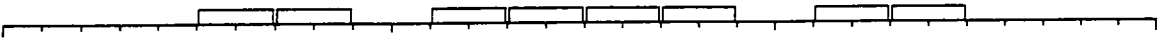
S_{14} :



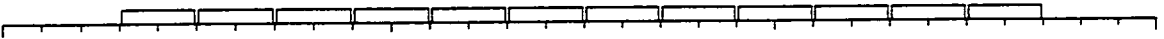
S_{15} :



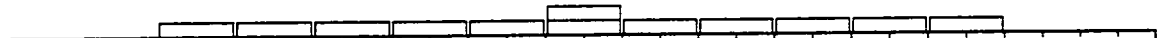
S_{16} :



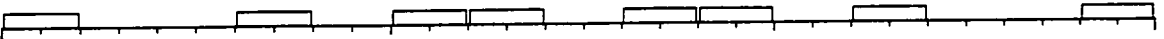
S_{17} :



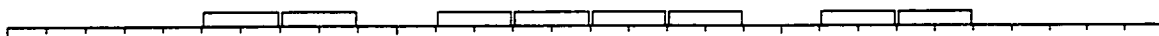
S_{18} :



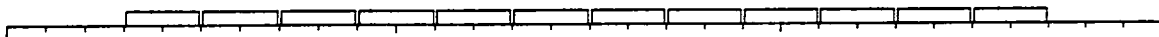
S_{22} :



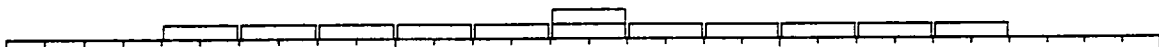
S_{23} :



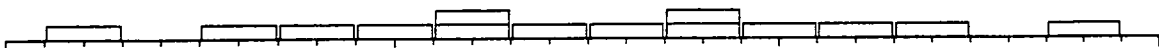
S_{24} :



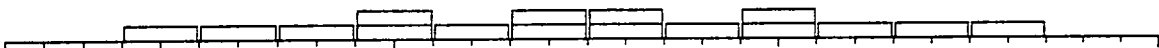
S_{25} :



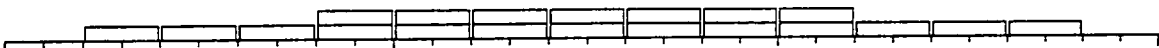
S_{26} :



S_{27} :



S_{28} :



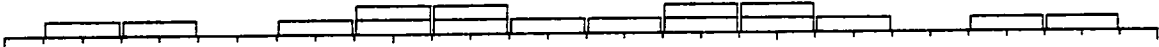
S_{33} :



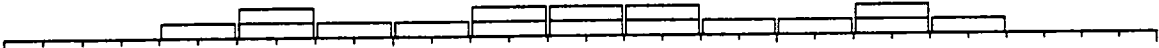
S_{34} :



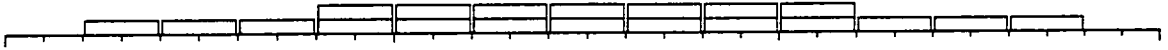
S_{35} :



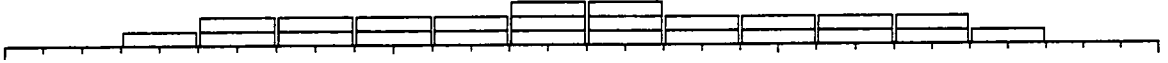
S_{36} :



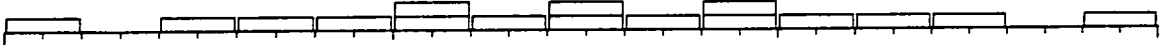
S_{37} :



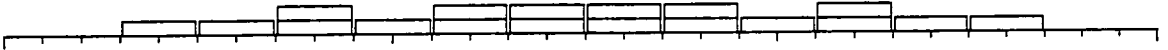
S_{38} :



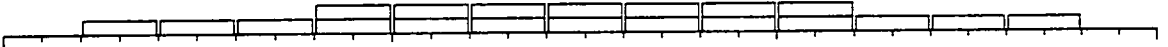
S_{44} :



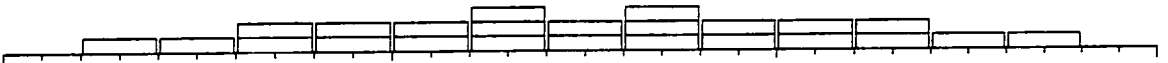
S_{45} :



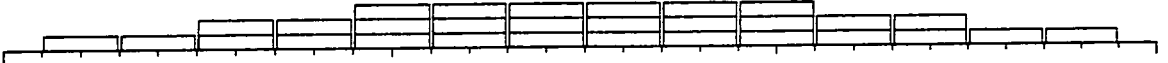
S_{46} :



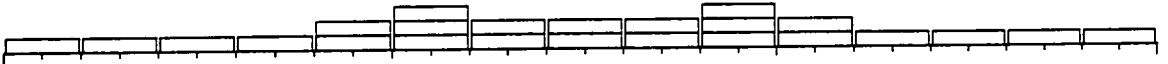
S_{47} :



S_{48} :



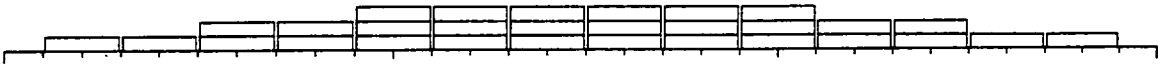
S_{55} :



S_{56} :



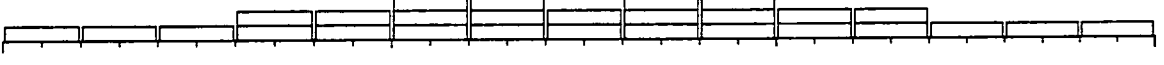
S_{57} :



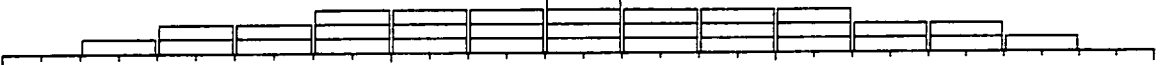
S_{58} :



S_{66} :



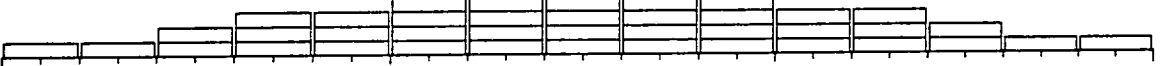
S_{67} :



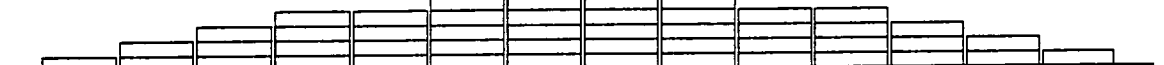
S_{68} :



S_{77} :



S_{78} :

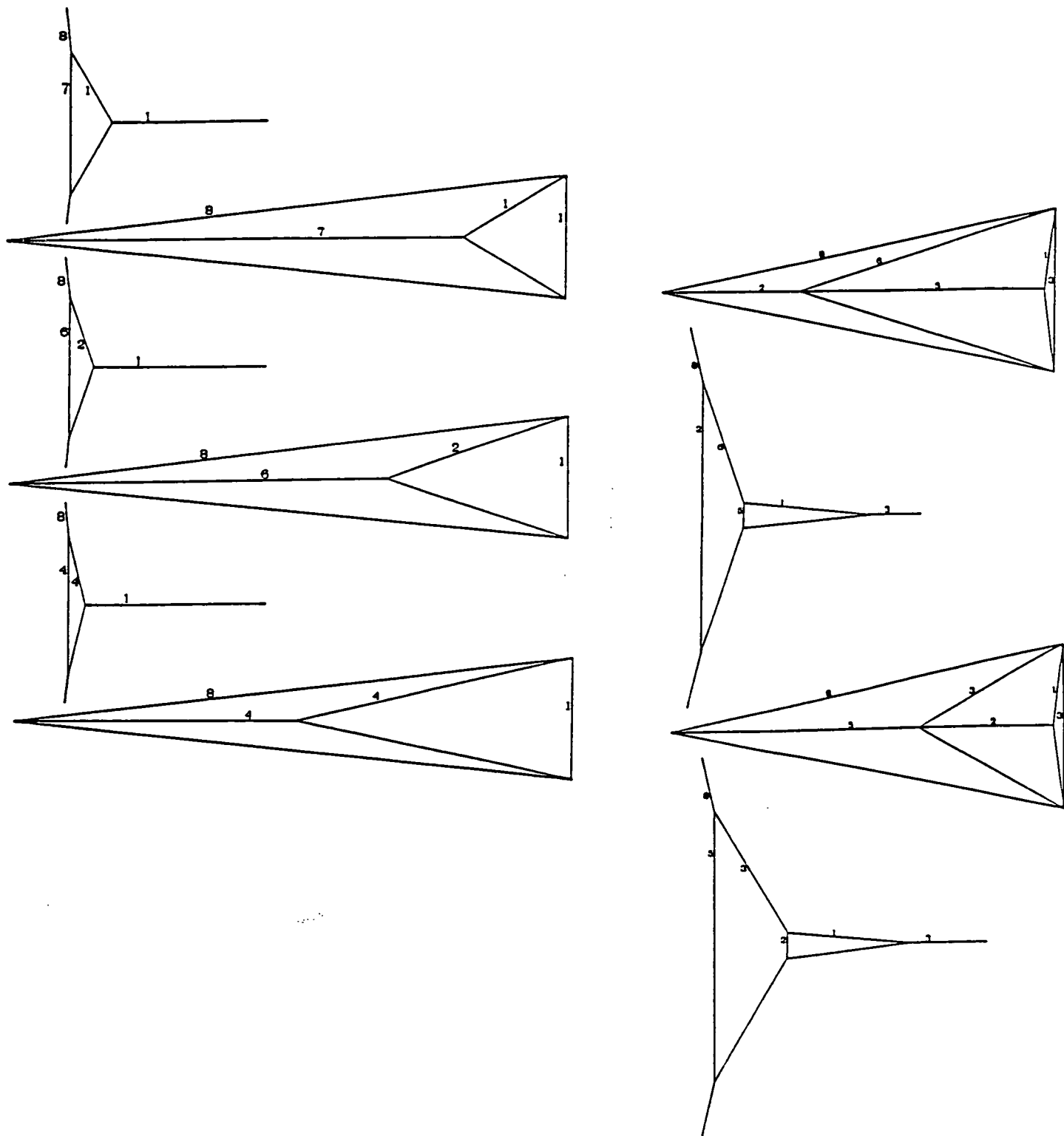


S_{88} :

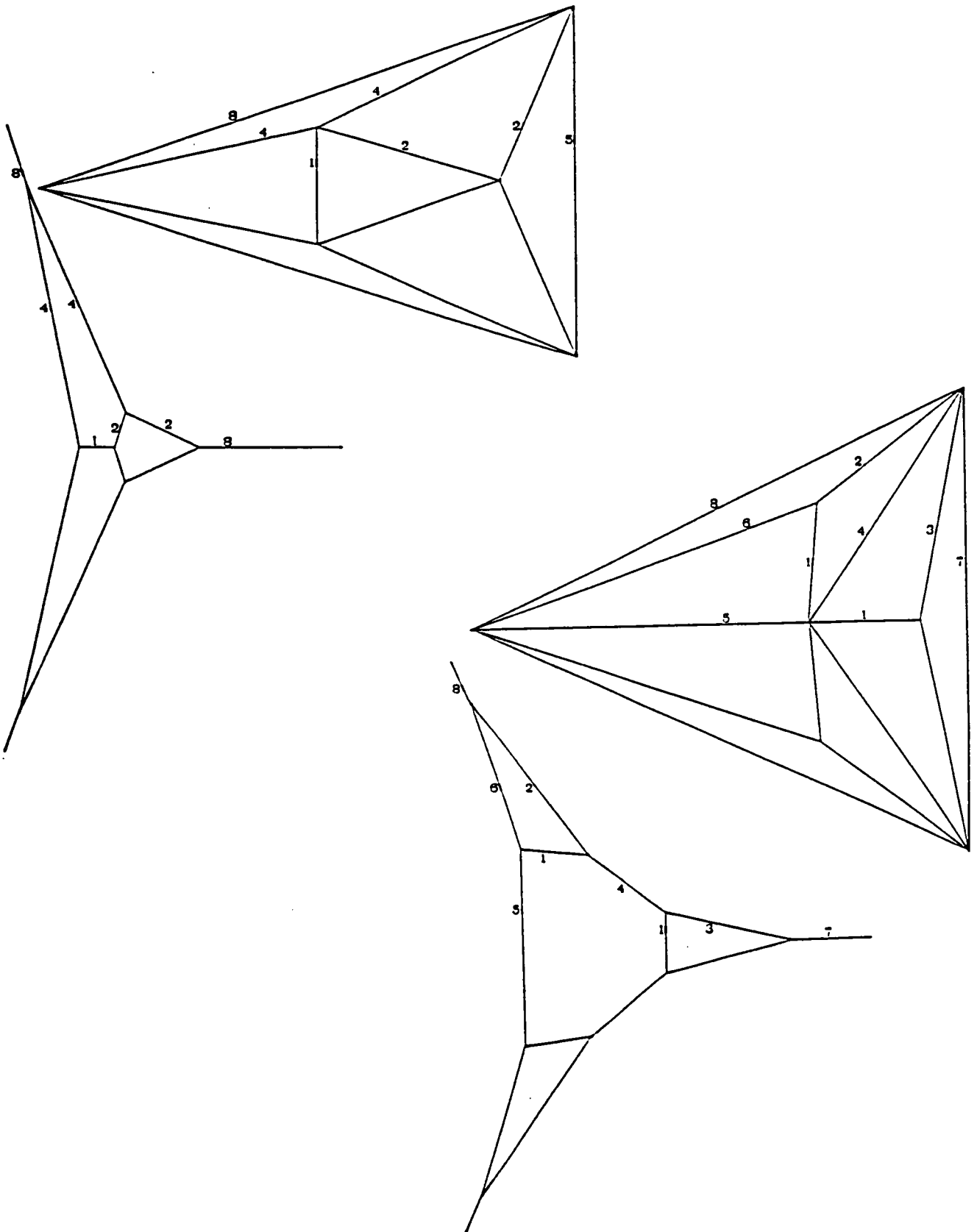


Appendix 3

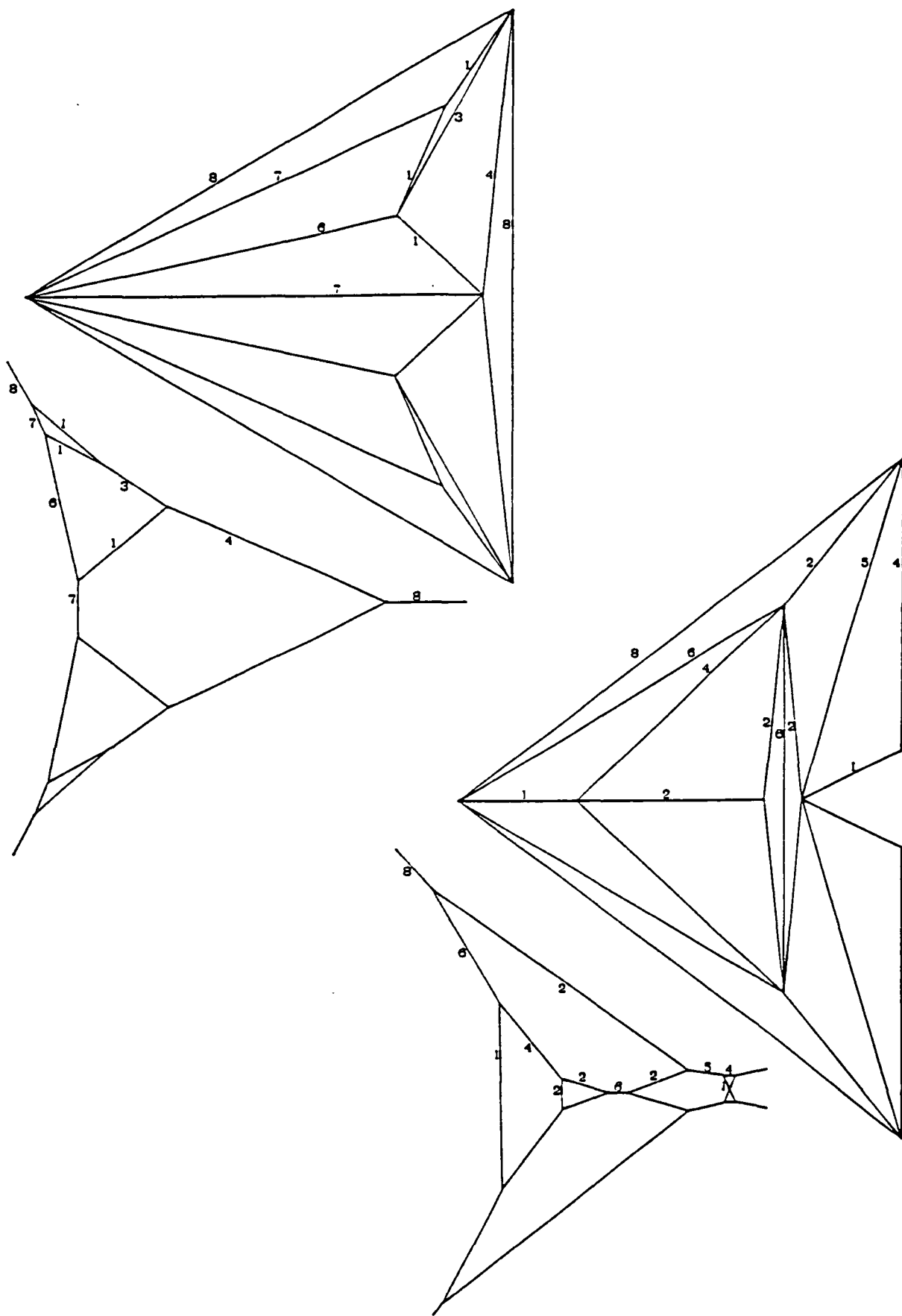
On-shell Diagrams for Scattering in the $e_8^{(1)}$ Theory



Third and fifth order poles



Seventh and ninth order poles



Eleventh and twelfth order poles

m	c	Perturbing Field	Dimension	Spins of Conserved Charges
3	$\frac{1}{2}$	$\phi_{12} = \phi_{22}$	$\frac{1}{16}$	1, 7, 11, 13, 17, 19.
		$\phi_{13} = \phi_{21}$	$\frac{1}{2}$	1, 3, 5, 9, 11 ² , ... (see text)
4	$\frac{7}{10}$	$\phi_{12} = \phi_{33}$	$\frac{1}{10}$	1, 5, 7, 9, 11, 13.
		$\phi_{21} = \phi_{24}$	$\frac{7}{16}$	1, 5, 7, 11, 13.
		$\phi_{13} = \phi_{32}$	$\frac{3}{5}$	1, 3, 5, 7, 9, 11.
		$\phi_{31} = \phi_{14}$	$\frac{3}{2}$	1, 3, 5, 7 ² , ... (see text)
5	$\frac{4}{5}$	$\phi_{12} = \phi_{44}$	$\frac{1}{8}$	1, 5, 7, 11.
		$\phi_{21} = \phi_{35}$	$\frac{2}{5}$	1, 5, 7, 11.
		$\phi_{13} = \phi_{43}$	$\frac{2}{3}$	1, 3, 5, 7.
		$\phi_{31} = \phi_{25}$	$\frac{7}{5}$	1, 3, 5, 7.
		$\phi_{15} = \phi_{41}$	3	1, 5, 7.
6	$\frac{6}{7}$	$\phi_{12} = \phi_{55}$	$\frac{1}{7}$	1, 5, 7, 11.
		$\phi_{21} = \phi_{46}$	$\frac{3}{8}$	1, 5, 7, 11.
		$\phi_{13} = \phi_{54}$	$\frac{5}{7}$	1, 3, 5, 7.
		$\phi_{31} = \phi_{36}$	$\frac{4}{3}$	1, 3, 5, 7.
		$\phi_{15} = \phi_{52}$	$\frac{22}{7}$	1, 5.
		$\phi_{51} = \phi_{16}$	5	1, 5.

Table 1

Fields ϕ_{ab} and spins s for which $\dim(\hat{\Lambda}_{s+1}) > \dim(\hat{\Phi}_s^{ab})$

m	c	Perturbing Field	Dimension	Spins of Conserved Charges
7	$\frac{25}{28}$	$\phi_{12} = \phi_{66}$	$\frac{5}{32}$	1, 5, 7, 11.
		$\phi_{21} = \phi_{57}$	$\frac{5}{14}$	1, 5, 7, 11.
		$\phi_{13} = \phi_{65}$	$\frac{3}{4}$	1, 3, 5, 7.
		$\phi_{31} = \phi_{47}$	$\frac{9}{7}$	1, 3, 5, 7.
		$\phi_{15} = \phi_{63}$	$\frac{13}{4}$	1, 5.
		$\phi_{51} = \phi_{27}$	$\frac{34}{7}$	1, 5.
8	$\frac{11}{12}$	$\phi_{12} = \phi_{77}$	$\frac{1}{6}$	1, 5, 7, 11.
		$\phi_{21} = \phi_{68}$	$\frac{11}{32}$	1, 5, 7, 11.
		$\phi_{13} = \phi_{76}$	$\frac{7}{9}$	1, 3, 5, 7.
		$\phi_{31} = \phi_{58}$	$\frac{5}{4}$	1, 3, 5, 7.
		$\phi_{15} = \phi_{74}$	$\frac{10}{3}$	1, 5.
		$\phi_{51} = \phi_{38}$	$\frac{19}{4}$	1, 5.
9	$\frac{14}{15}$	$\phi_{12} = \phi_{88}$	$\frac{7}{40}$	1, 5, 7, 11.
		$\phi_{21} = \phi_{79}$	$\frac{1}{3}$	1, 5, 7, 11.
		$\phi_{13} = \phi_{87}$	$\frac{4}{5}$	1, 3, 5, 7.
		$\phi_{31} = \phi_{69}$	$\frac{11}{9}$	1, 3, 5, 7.
		$\phi_{15} = \phi_{85}$	$\frac{17}{5}$	1, 5.
		$\phi_{51} = \phi_{49}$	$\frac{14}{3}$	1, 5.

Table 1, continued

m	c	Perturbing Field	Dimension	Spins of Conserved Charges
10	$\frac{52}{55}$	$\phi_{12} = \phi_{99}$	$\frac{2}{11}$	1, 5, 7, 11.
		$\phi_{21} = \phi_{8.10}$	$\frac{13}{40}$	1, 5, 7, 11.
		$\phi_{13} = \phi_{98}$	$\frac{9}{11}$	1, 3, 5, 7.
		$\phi_{31} = \phi_{7.10}$	$\frac{6}{5}$	1, 3, 5, 7.
		$\phi_{15} = \phi_{96}$	$\frac{38}{11}$	1, 5.
		$\phi_{51} = \phi_{5.10}$	$\frac{23}{5}$	1, 5.
11	$\frac{21}{22}$	$\phi_{12} = \phi_{10.10}$	$\frac{3}{16}$	1, 5, 7, 11.
		$\phi_{21} = \phi_{9.11}$	$\frac{7}{22}$	1, 5, 7, 11.
		$\phi_{13} = \phi_{10.9}$	$\frac{5}{6}$	1, 3, 5, 7.
		$\phi_{31} = \phi_{8.11}$	$\frac{13}{11}$	1, 3, 5, 7.
		$\phi_{15} = \phi_{10.7}$	$\frac{7}{2}$	1, 5.
		$\phi_{51} = \phi_{6.11}$	$\frac{50}{11}$	1, 5.
12	$\frac{25}{26}$	$\phi_{13} = \phi_{11.10}$	$\frac{11}{13}$	1, 3, 5, 7.
		$\phi_{12} = \phi_{11.11}$	$\frac{5}{26}$	1, 5, 7, 11.
		$\phi_{21} = \phi_{10.12}$	$\frac{5}{16}$	1, 5, 7, 11.
		$\phi_{13} = \phi_{11.10}$	$\frac{11}{13}$	1, 3, 5, 7.
		$\phi_{31} = \phi_{9.12}$	$\frac{7}{6}$	1, 3, 5, 7.
		$\phi_{15} = \phi_{11.8}$	$\frac{46}{13}$	1, 5.
		$\phi_{51} = \phi_{7.12}$	$\frac{9}{2}$	1, 5.

Table 1, continued

m	h_{1m}	Perturbing Field	Dimension	Spins of Conserved Charges
5	3	$\phi_{21} = \phi_{35}$	$\frac{2}{5}$	2, 4, 8.
		$\phi_{15} = \phi_{41}$	3	2, 4, 8, 10.
6	5	$\phi_{12} = \phi_{55}$	$\frac{1}{7}$	4, 8.

Table 2

Fields ϕ_{ab} and spins s for which $\dim(\hat{\Phi}_{s+1-h_{1m}}^{1m}) > \dim(\hat{\Phi}_{s+h_{ab}-h_{a,m+1-b}}^{a,m+1-b})$

Lie Algebra	Coxeter Number	Exponents
A_n	$n + 1$	$1, 2, \dots, n.$
B_n	$2n$	$1, 3, \dots, 2n - 1.$
C_n	$2n$	$1, 3, \dots, 2n - 1.$
D_n	$2(n - 1)$	$1, 3, \dots, 2n - 1, n.$
E_6	12	$1, 4, 5, 7, 8, 11.$
E_7	18	$1, 5, 7, 9, 11, 13, 17.$
E_8	30	$1, 7, 11, 13, 17, 19, 23, 29.$
F_4	12	$1, 5, 7, 11$
G_2	6	$1, 5$

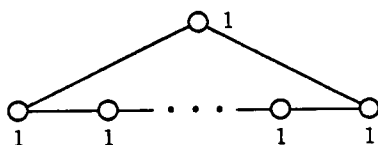
Table 3
Exponents of the simple Lie algebras

Coset	m	c
$a_1^{(1)} \times a_1^{(k)} / a_1^{(k+1)}$	$k + 2$	$1 - \frac{1}{(k+2)(k+3)}$
$e_8^{(1)} \times e_8^{(1)} / e_8^{(2)}$	3	$\frac{1}{2}$
$e_7^{(1)} \times e_7^{(1)} / e_7^{(2)}$	4	$\frac{7}{10}$
$a_2^{(1)} \times a_2^{(1)} / a_2^{(2)}$	5	$\frac{4}{5}$
$e_6^{(1)} \times e_6^{(1)} / e_6^{(2)}$	6	$\frac{6}{7}$
$g_2^{(1)} \times g_2^{(1)} / g_2^{(2)}$	9	$\frac{14}{15}$
$f_4^{(1)} \times f_4^{(1)} / f_4^{(2)}$	10	$\frac{52}{55}$
$e_8^{(1)} \times e_8^{(2)} / e_8^{(3)}$	11	$\frac{21}{22}$

Table 4

$g^{(1)} \times g^{(k)} / g^{(k+1)}$ cosets for which $c < 1$

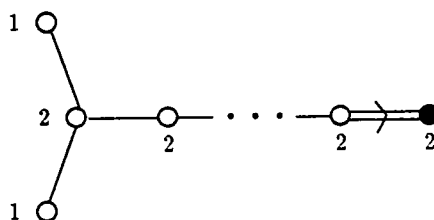
$$a_n^{(1)} \equiv \bar{D}(A_n)$$



$$a_1^{(1)} \equiv \bar{D}(A_1)$$



$$b_n^{(1)} \equiv \bar{D}(B_n)$$



$$c_n^{(1)} \equiv \bar{D}(C_n)$$



$$d_n^{(1)} \equiv \bar{D}(D_n)$$

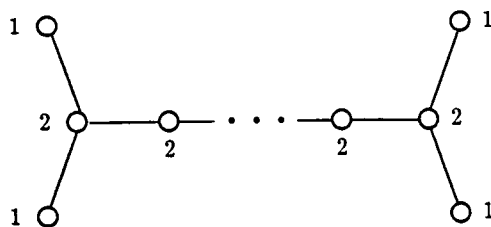
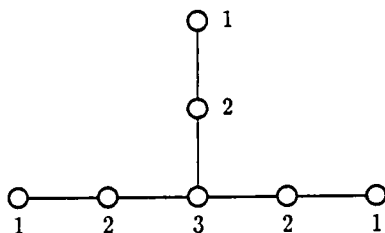
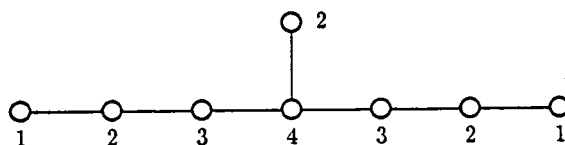


Table 5
Untwisted affine Dynkin diagrams

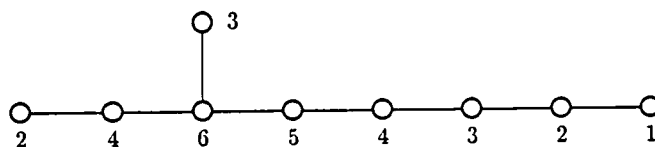
$$e_6^{(1)} \equiv \bar{D}(E_6)$$



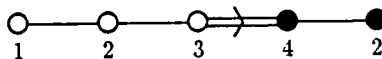
$$e_7^{(1)} \equiv \bar{D}(E_7)$$



$$e_8^{(1)} \equiv \bar{D}(E_8)$$



$$f_4^{(1)} \equiv \bar{D}(F_4)$$



$$g_2^{(1)} \equiv \bar{D}(G_2)$$

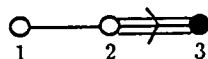
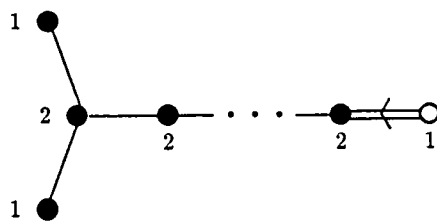
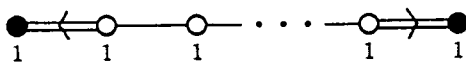


Table 5, continued

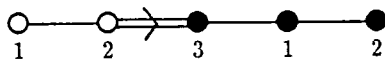
$$a_{2n-1}^{(2)} \equiv \bar{D}^T(B_n)$$



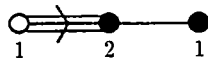
$$d_{n+1}^{(2)} \equiv \bar{D}^T(C_n)$$



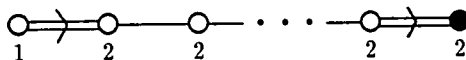
$$e_6^{(2)} \equiv \bar{D}^T(F_4) \equiv F_4^{(2)}$$



$$d_4^{(3)} \equiv \bar{D}^T(G_2) \equiv G_2^{(3)}$$



$$a_{2n}^{(2)} \equiv GD(H_n) \equiv BC_n$$



$$a_2^{(2)} \equiv GD(BD)$$

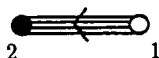
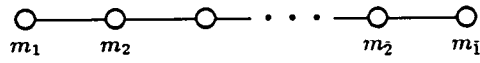
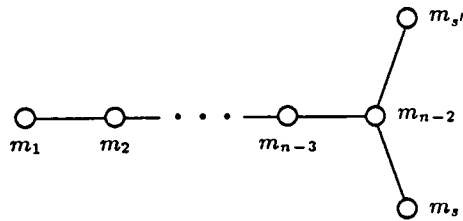


Table 6
Twisted affine Dynkin diagrams

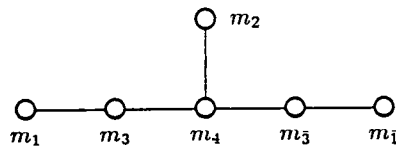
$a_n^{(1)}$:



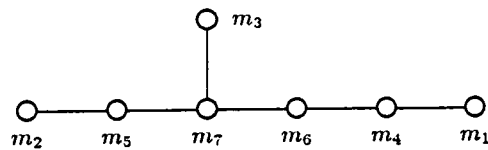
$d_n^{(1)}$:



$e_6^{(1)}$:



$e_7^{(1)}$:



$e_8^{(1)}$:

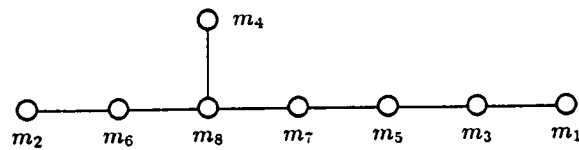
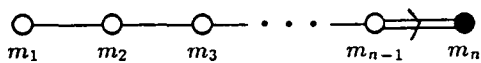


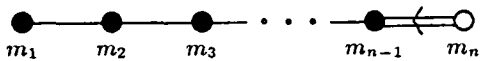
Table 7

Assignments of masses to Dynkin diagrams for the simply-laced theories

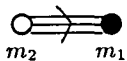
$b_n^{(1)}$:



$c_n^{(1)}$:



$g_2^{(1)}$:



$f_4^{(1)}$:

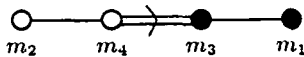


Table 7, continued

Assignments of masses to Dynkin diagrams for the
untwisted non simply-laced theories

$$A_n \begin{pmatrix} \gamma_s^1 \\ \gamma_s^2 \\ \vdots \\ \gamma_s^{\bar{2}} \\ \gamma_s^{\bar{1}} \end{pmatrix} = \begin{pmatrix} \sin \theta_s \\ \sin 2\theta_s \\ \vdots \\ \sin(n-1)\theta_s \\ \sin n\theta_s \end{pmatrix} \quad D_n \begin{pmatrix} \gamma_s^1 \\ \gamma_s^2 \\ \vdots \\ \gamma_s^{n-2} \\ \gamma_s^s \\ \gamma_s^{s'} \end{pmatrix} = \begin{pmatrix} 2 \cos(n-2)\theta_s \\ 2 \cos(n-3)\theta_s \\ \vdots \\ 2 \cos \theta_s \\ 1 \\ 1 \end{pmatrix}, \begin{pmatrix} 0 \\ 0 \\ \vdots \\ 0 \\ 1 \\ -1 \end{pmatrix}$$

$$E_6 \begin{pmatrix} \gamma_s^1 \\ \gamma_s^3 \\ \gamma_s^4 \\ \gamma_s^{\bar{3}} \\ \gamma_s^{\bar{1}} \\ \gamma_s^2 \end{pmatrix} = \begin{pmatrix} \sin \theta_s \\ \sin 2\theta_s \\ \sin 3\theta_s \\ \sin 10\theta_s \\ \sin 11\theta_s \\ \sin 8\theta_s - \sin 2\theta_s \end{pmatrix} \quad E_7 \begin{pmatrix} \gamma_s^1 \\ \gamma_s^4 \\ \gamma_s^6 \\ \gamma_s^7 \\ \gamma_s^5 \\ \gamma_s^2 \\ \gamma_s^3 \end{pmatrix} = \begin{pmatrix} \sin \theta_s \\ \sin 2\theta_s \\ \sin 3\theta_s \\ \sin 4\theta_s \\ \sin 7\theta_s - \sin 3\theta_s \\ \sin 6\theta_s - \sin 4\theta_s \\ \frac{1}{2}(\sin 9\theta_s - \sin 7\theta_s + \sin 5\theta_s - \sin \theta_s) \end{pmatrix}$$

$$E_8 \begin{pmatrix} \gamma_s^1 \\ \gamma_s^3 \\ \gamma_s^5 \\ \gamma_s^7 \\ \gamma_s^8 \\ \gamma_s^6 \\ \gamma_s^2 \\ \gamma_s^4 \end{pmatrix} = \begin{pmatrix} \sin \theta_s \\ \sin 2\theta_s \\ \sin 3\theta_s \\ \sin 4\theta_s \\ \sin 5\theta_s \\ \sin 8\theta_s - \sin 4\theta_s \\ \sin 7\theta_s - \sin 5\theta_s \\ \sin 14\theta_s - \sin 8\theta_s \end{pmatrix}$$

Table 8

Cartan matrix eigenvectors with eigenvalue $2 - 2 \cos \theta_s$, $\theta_s = \frac{\pi}{h}s$, s an exponent
(second vector for D_n is $\theta_s = \frac{\pi}{2}$, $s = n - 1$)

	1	$\bar{1}$	2	3	$\bar{3}$	4
1	(8) (6) (2)	-(10) (6) (4)	[9] [7]	(11) (5) [9] [7]	(7) (1) [9] [7]	[10] [8] ² [6]
$\bar{1}$		(8) (6) (2)	[9] [7]	(7) (1) [9] [7]	(11) (5) [9] [7]	[10] [8] ² [6]
2			-[10] [8] [6]	[10] [8] ² [6]	[10] [8] ² [6]	[11] [9] ² [7] ³
3	(11) (7)			(8) (6) (2) [10] [8] ² [6]	-(10) (6) (4) [10] [8] ² [6]	[11] [9] ³ [7] ⁴
$\bar{3}$	(5) {11}	{1} {7}			(8) (6) (2) [10] [8] ² [6]	[11] [9] ³ [7] ⁴
4	4	4	1 5			-[10] ³ [8] ⁵ [6] ³
3	{4} {6} {10}	{2} {6} {8}	3 5	{1} {3} {5} {7} ² {9}		
$\bar{3}$	{2} {6} {8}	{4} {6} {10}	3 5	{3} {5} ² {7} {9} {11}	{1} {3} {5} {7} ² {9}	
4	3 5	3 5	2 4 6	2 4 ² 6	2 4 ² 6	1 3 ² 5 ³

Table 9a : $e_6^{(1)}$ minimal and full S-matrix elements

1	2	3	4	5	6	7
2 ⁻ 4 ⁻	1 ⁻ 3	2 4 5	1 ⁻ 3 6	3 6	4 5 7	6
10 2	13 7	14 10 6	17 11 3	14 8	16 12 4	15
	2 ⁻ 4 ⁻ 5 ⁻	1 3 ⁻ 6 ⁻	2 ⁻ 5 ⁻	2 ⁻ 4 ⁻ 7 ⁻	3 ⁻	5 ⁻ 7
	12 8 2	15 11 5	14 8	17 13 3	15	16 10
		2 ⁻ 7 ⁻	1	1 6	2 ⁻ 5 7	3 ⁻ 6
		14 2	15	16 10	16 12 8	17 13
1			4 ⁻ 5 7 ⁻	2 ⁻ 4 7	1 6	4 ⁻ 5
2	2 4 5		12 10 4	15 13 7	17 11	16 14
3		2 4 5 7		5	1 3	2 ⁻ 4 7 ⁻
4	1 3 6			12	16 14	17 15 11
5	2 4 5		2 4 ² 5 7		4 7 ⁻	1 3 6 ⁻
6		2 4 5 7		2 4 ² 5 ²	14 10	17 15 13
7	3 6	1 3 6	2 4 5 ² 7	7 ²		2 5 ⁻ 7
	4 5 7	2 4 5 7		1 3 6 ²	2 4 ² 5 ²	16 14 12
		3 6	4 5 7 ³	2 4 5 ²	7 ³	
	6			7 ³	1 3 6 ³	2 4 ³ 5 ³
		3 6				7 ⁷

Table 10 : $e_7^{(1)}$ couplings and Clebsch-Gordon series

	1	2	3	4	5	6	7
1	[10] [2]	[5] [7]	[14] [10] [6]	[9] [11] [1] [3]	[2] [4] [10] ²	[16] [14] [8] ² [6]	[15] [13] ² [11] ² [9]
2		-[12] [10] [2]	[15] [13] [11] [9]	[8] [6] ² [4]	[13] [11] ² [9] [3] [1]	[15] [13] ² [11] ² [9]	[14] ² [10] ³ [6] ² [2]
3			[10] ² [6] ² [4] [2]	[15] [9] [7] ² [5] ²	[16] [14] ² [12] ² [10] ³	[8] ³ [6] ³ [4] ² [2]	[11] ⁴ [8] ² [5] ³ [3] ² [1]
4				-[16] ² [12] [8] ³ [4]	[13] ³ [9] [7] ³ [3]	[17] [15] ² [9] ² [7] ³ [5] ²	[14] ³ [10] ⁴ [6] ⁴ [2]
5	1 [9]	1 7			-[14] ² [12] ³ [10] ⁴ [2] ²	[16] [14] ³ [12] ⁴ [10] ⁴	[15] ³ [11] ⁵ [9] ³ [5] ⁴ [1]
6	6	4 8	1 5 7 [9]			[8] ⁵ [6] ⁴ [4] ³ [2] ²	[9] ³ [7] ⁶ [5] ⁵ [3] ³ [1]
7	2 8	5 7	4 6 8	1 3 7 9			-[16] ³ [12] ⁷ [8] ⁸ [4] ⁵
1					1 3 5 7 ² 9		
2				4 6 ² 8			
3			3 5 7 9	2 4 6 8 ²	3 5 ² 7 ² 9	1 3 5 ² 7 ² [9] ³	
4				3 5 ² 7 ² 9	2 4 ² 6 ² 8 ³		
5		2 6 8					
6	3 7 [9]	4 6 8	3 5 7 ² [9]	2 4 6 8 ²	3 5 ² 7 ² 9		
7	4 6 8	3 5 7 9	2 4 6 ² 8 ²	3 5 ² 7 ² 9	2 4 ² 6 ² 8 ³	1 3 5 ² 7 ² 9 ²	1 3 ² 5 ³ 7 ⁴ 9 ²

Table 10a : $e_7^{(1)}$ minimal and full S-matrix elements

	1	2	3	4	5	6	7	8
1	1 ⁻ 2 3 ⁻ 20 12 2	1 2 ⁻ 3 4 ⁻ 24 18 14 8	1 ⁻ 2 4 5 29 21 13 3	2 ⁻ 3 4 ⁻ 5 ⁻ 6 25 21 17 11 7	3 4 ⁻ 6 7 ⁻ 28 22 14 4	4 5 7 25 19 9	5 ⁻ 6 8 27 23 5	7 8 26 10
2	1 ⁻ 2 4 5 6 ⁻ 24 20 14 8 2	1 3 6 25 19 9	2 3 5 6 7 22 20 14 12 4	1 ⁻ 2 7 27 23 5	2 6 26 16	2 ⁻ 3 5 7 8 29 25 19 13 3	4 6 7 ⁻ 8 27 21 17 11	6 7 28 22
3				1 5 26 16	1 3 4 7 8 29 23 21 13 5	2 3 6 8 26 24 18 8	3 5 28 22	5 6 8 ⁻ 27 25 17
4	1 2 3 1 2 3	1 2 3 4 5 6		1 ⁻ 4 ⁻ 6 7 ⁻ 8 ⁻ 26 20 16 12 2	1 ⁻ 3 5 ⁻ 8 27 23 19 9	1 4 28 22	2 4 ⁻ 7 8 ⁻ 28 24 18 14	4 ⁻ 5 7 ⁻ 29 25 21
5	1 2 3 4 5 1 2 3 4 5 6	1 2 3 ² 4 5 6	1 2 ² 3 ² 4 ² 5 ³ 6 7		4 ⁻ 5 8 ⁻ 22 20 12	1 2 7 ⁻ 27 25 17	1 ⁻ 3 6 ⁻ 29 25 21	3 4 5 ⁻ 8 ⁻ 28 26 24 18
6	2 3 4 5 6 3 4 5 6 7	1 2 3 4 5 6 7	1 2 3 ² 4 ² 5 ³ 6 ³ 7 ³ 8	1 2 3 ² 4 ² 5 ³ 6 ³ 7 ³ 8		3 6 ⁻ 8 ⁻ 24 20 14	1 2 5 ⁻ 8 ⁻ 28 26 22 16	2 3 6 ⁻ 7 ⁻ 29 27 23 21
7	4 5 6 7 5 6 7 8	2 3 4 5 ² 6 7	1 2 3 ² 4 ² 5 ³ 6 ³ 7 ³ 8	1 2 3 ² 4 ² 5 ³ 6 ³ 7 ³ 8	1 2 ² 3 ³ 4 ³ 5 ⁶ 6 ⁶ 7 ⁶ 8 ³		2 ⁻ 4 7 ⁻ 26 24 20	1 2 4 ⁻ 6 ⁻ 8 29 27 25 23 19
8	4 5 6 7 8 7 8	4 5 6 7 ² 8	2 3 4 ² 5 ³ 6 ³ 7 ³ 8	1 2 3 4 5 ³ 6 ³ 7 ⁴ 8 ⁴	1 2 3 ² 4 ³ 5 ⁶ 6 ⁶ 7 ⁶ 8 ⁶	1 2 ² 3 ³ 4 ³ 5 ⁶ 6 ⁶ 7 ⁷ 8 ⁶	1 2 ² 3 ⁴ 4 ⁴ 5 ¹⁰ 6 ¹⁰ 7 ¹⁷ 8 ²²	1 3 ⁻ 5 ⁻ 7 8 28 26 24 22 20
			5 6 7 ³ 8 ⁶	4 5 6 ² 7 ⁴ 8 ⁶	3 4 5 ³ 6 ⁵ 7 ⁹ 8 ¹⁷	2 3 4 ² 5 ⁵ 6 ⁶ 7 ¹¹ 8 ¹⁷	1 2 3 ³ 4 ⁴ 5 ⁹ 6 ¹¹ 7 ²² 8 ³⁶	1 2 ³ 3 ⁵ 4 ⁶ 5 ¹⁷ 6 ¹⁷ 7 ³⁶ 8 ¹⁰

Table 11 : $e_8^{(1)}$ couplings and Clebsch-Gordan series

	1	2	3	4	5	6	7	8
1	-[20] [12] [2]	[24] [18] [14] [8]	[29] [21] [13] [3] [11] ²	[25] [21] [17] [11] [7] [15]	[28] [22] [14] [4] [10] ² [12] ²	[25] [19] [9] [15] [7] ² [13] ²	[27] [23] [5] [15] [9] ² [11] ² [13] ²	[26] [16] ³ [6] ² [10] ² [12] ²
2		-[24] [20] [14] [8] [2] [12] ²	[25] [19] [9] [15] [7] ² [13] ²	[27] [23] [5] [15] [19] ² [9] ² [13] ²	[26] [16] ³ [6] ² [8] ² [10] ²	[29] [25] [19] ² [13] ² [3] [9] ² [15] [7] ²	[27] [21] ³ [7] ² [17] ³ [11] ³ [15] ² [5] ²	[28] [22] ³ [14] ⁴ [12] ⁴ [10] ⁴ [4] ²
3			-[22] [20] ² [14] [28] ² [12] ² [4] [28] ²	[26] [16] ³ [20] ² [12] ² [6] ² [8] ²	[29] [23] [21] ³ [5] [15] [3] ² [11] ⁴	[26] [24] ³ [18] ³ [8] ³ [14] ⁴ [10] ²	[28] [22] ² [24] ² [12] ⁴ [10] ⁴ [14] ⁴	[27] [25] ³ [17] ⁵ [15] ³ [11] ⁴ [9] ⁴ [7] ⁴
4				-[26] [20] ³ [16] ³ [12] ³ [2] [6] ² [8] ²	[27] [23] ³ [19] ³ [9] ³ [13] ⁴ [15] ² [5] ²	[28] [22] ² [20] ⁴ [18] ⁴ [16] ⁴ [6] ² [4] ²	[28] [24] ³ [18] ⁵ [14] ⁵ [22] ⁴ [10] ⁴ [4] ²	[29] [25] ² [21] ⁵ [27] ² [15] ³ [13] ³ [11] ³ [7] ⁴
5					-[22] ³ [20] ⁵ [12] ⁵ [16] ⁴ [6] ² [4] ² [2] ²	[27] [25] ³ [17] ⁵ [15] ³ [11] ⁴ [9] ⁴ [7] ⁴	[29] [25] ³ [21] ⁵ [27] ² [23] ⁴ [19] ³ [15] ³ [13] ³	[28] [26] ³ [24] ⁵ [18] ⁵ [20] ³ [22] ³ [16] ³
6						-[24] ³ [20] ⁵ [14] ⁵ [28] ² [26] ² [12] ³ [8] ⁴	[28] [26] ³ [22] ⁵ [24] ⁵ [20] ³ [16] ³ [12] ³	[29] [27] ³ [23] ⁵ [21] ⁵ [17] ⁵ [15] ⁴
7							-[26] ³ [24] ⁵ [20] ⁷ [28] ² [22] ³ [16] ³ [12] ³	[29] [27] ³ [25] ⁵ [21] ⁵ [17] ⁵ [15] ⁴
8								-[28] ² [26] ³ [24] ⁷ [22] ⁴ [20] ⁴ [18] ¹² [16] ¹²
1								
2								
3								
4								
5								
6								
7								
8								

Table 11a : $e_8^{(1)}$ minimal and full S-matrix elements

References

- [1] A. B. Zamolodchikov, "Integrable Field Theory from Conformal Field Theory", Proceedings of the Taniguchi Symposium, Kyoto (1988).
- [2] A. B. Zamolodchikov, *Int. J. Mod. Phys. A* **4** (1989) 4235.
- [3] T. Eguchi and S-K Yang, *Phys. Lett.* **B224** (1989) 373.
- [4] V. A. Fateev and A. B. Zamolodchikov, *Int. J. Mod. Phys.* **A5** (1990) 1025.
- [5] T. J. Hollowood and P. Mansfield, *Phys. Lett.* **B226** (1989) 73.
- [6] H. W. Braden, E. Corrigan, P. E. Dorey and R. Sasaki, *Nucl. Phys* **B338** (1990) 689.
- [7] H. W. Braden, E. Corrigan, P. E. Dorey and R. Sasaki, *Phys. Lett.* **B227** (1989) 441.
- [8] H. W. Braden, E. Corrigan, P. E. Dorey and R. Sasaki, "Aspects of perturbed conformal field theory, affine Toda field theory and exact S-matrices", to appear in the proceedings of the XVIII International Conference on Differential Geometric Methods in Theoretical Physics: Physics and Geometry, Lake Tahoe, USA 2-8 July 1989.
- [9] H. W. Braden, E. Corrigan, P. E. Dorey and R. Sasaki, "Aspects of affine Toda field theory", preprint UDCPT 90-19.
- [10] P. Christe, preprint "S-matrices of the tri-critical Ising model and Toda systems", to appear in the proceedings of the XVIII International Conference on Differential Geometric Methods in Theoretical Physics: Physics and Geometry, Lake Tahoe, USA 2-8 July 1989.
- [11] P. Christe and G. Mussardo, *Nucl. Phys.* **B330** (1990) 465.
- [12] P. Christe and G. Mussardo, preprint "Elastic S-matrices in (1+1) dimensions and Toda field theories", UCSBTH-89-44.
- [13] C. Destri and H. J. de Vega, *Phys. Lett.* **B233** (1989) 336.
- [14] T. R. Klassen and E. Melzer, *Nucl. Phys.* **B338** (1990) 485.
- [15] G. Mussardo, preprint "Away from criticality: some results from the S-matrix approach", to appear in proceedings of the XVIII International Conference on Differential Geometric Methods in Theoretical Physics: Physics and Geometry, Lake Tahoe, USA 2-8 July 1989.

- [16] G. Mussardo and G. Sotkov, preprint "Bootstrap program and minimal integrable models" UCSBTH-89-64/ISAS-117-89.
- [17] See for example A. M. Polyakov, *Gauge Fields and Strings* (Harwood 1987).
- [18] See for example R. Baxter, *Exactly Solved Models in Statistical Mechanics* (Academic Press 1982).
- [19] K. Wilson and J. Kogut, *Phys. Rep.* **12C** (1974) 75.
- [20] P. Pfeuty and G. Toulouse, *Introduction to the Renormalization Group and to Critical Phenomena* (Wiley 1977).
- [21] G. Parisi, *Statistical Field Theory* (Addison-Wesley 1988).
- [22] S-K Ma, *Modern Theory of Critical Phenomena* (Benjamin 1976).
- [23] A. Z. Patashinskii and V. I. Pokrovskii, *Fluctuation Theory of Phase Transitions* (Pergamon 1979).
- [24] S. Shenker, in *Les Houches XXXIX - Recent Advances in Field Theory and Statistical Mechanics* (1982).
- [25] A. M. Polyakov, *JETP Letters* **12** (1970) 381.
- [26] A. A. Belavin, A. M. Polyakov and A. B. Zamolodchikov, *Nucl. Phys.* **B241** (1984) 333.
- [27] J. Cardy, in *Les Houches XLIX - Champs, Cordes et Phénomènes Critiques* (1988).
- [28] Vl. Dotsenko, *Advanced Studies in Pure Mathematics* **16** (1988) 123.
- [29] S. L. Lukyanov and V. A. Fateev, Lectures given in second Spring School 'Contemporary Problems in Theoretical Physics', Kiev 1988, preprints ITF-88-74P, 88-75P and 88-76P.
- [30] P. Ginsparg, in *Les Houches XLIX - Champs, Cordes et Phénomènes Critiques* (1988).
- [31] A. B. Zamolodchikov, "Exact Solutions of Conformal Field Theory in Two Dimensions and Critical Phenomena", Kiev IMP preprint 87-65P (1987).
- [32] S. Fubini, A. Hanson and R. Jackiw, *Phys. Rev.* **D7** (1973) 1732.
- [33] A. B. Zamolodchikov, *Teor. Mat. Fiz.* **65** (1985) 347.
- [34] D. Gepner and E. Witten, *Nucl. Phys.* **B278** (1986) 493.
- [35] P. Goddard, A. Kent and D. Olive, *Phys. Lett.* **B152** (1985) 88; *Comm. Math. Phys.* **103** (1986) 105.

- [36] F. A. Bais, P. Bouwknegt, M. Surridge and K. Schoutens, *Nucl. Phys.* **B304** (1988) 348, 371.
- [37] A. B. Zamolodchikov, *JETP Letters* **43** (1986) 730.
- [38] P. Bowcock and P. Goddard, *Nucl. Phys.* **B285** (1987) 651.
- [39] A. B. Zamolodchikov, *Int. J. Mod. Phys.* **A3** (1988) 743.
- [40] A. Cappelli, C. Itzykson and J-B Zuber, *Comm. Math. Phys.* **113** (1987) 1.
- [41] G. Watts, *Phys. Lett.* **B245** (1990) 65.
- [42] A. B. Zamolodchikov and Al. B. Zamolodchikov, *Ann. Phys.* **120** (1979) 253.
- [43] A. B. Zamolodchikov, *Sov. Sci. Rev., Physics*, **v.2** (1980).
- [44] R. Shankar and E. Witten, *Phys. Rev.* **D17** (1978) 2134.
- [45] See for example several of the articles in: C. N. Yang and M. L. Ge, *Braid Group, Knot theory and Statistical mechanics*, (World Scientific 1989).
- [46] R. J. Eden, P. V. Landshoff, D. I. Olive and J. C. Polkinghorne, *The Analytic S-matrix*, (Cambridge University Press 1966).
- [47] M. Karowski, *Nucl. Phys.* **B153** (1979) 244.
- [48] A. N. Leznov and M. V. Saveliev, *Group methods for the integration of nonlinear dynamical systems* (Moscow Nauka 1985).
- [49] A. V. Mikhailov, M. A. Olshanetsky and A. M. Perelomov, *Comm. Math. Phys.* **79** (1981) 473.
- [50] G. Wilson, *Ergod. Th. and Dynam. Sys.* **1** (1981) 361.
- [51] V. G. Drinfel'd and V. V. Sokolov, *J. Sov. Math.* **30** (1984) 1975.
- [52] S. Helgason, *Differential geometry, Lie groups, and symmetric spaces* (Academic Press Inc. 1978).
- [53] P. Mansfield, *Nucl. Phys.* **B222** (1983) 419.
- [54] J-L. Gervais and A. Neveu, *Nucl. Phys.* **B224** (1983) 329.
- [55] D. I. Olive and N. Turok, *Nucl. Phys.* **B215** (1983) 470.
- [56] E. Ogievetsky and P. Wiegmann, *Phys. Lett.* **B168** (1986) 360.
- [57] H. Braden, private communication.

- [58] R. Sasaki, private communication.
- [59] V. Pasquier, *Nucl. Phys.* **B285** (1987) 162.
- [60] R. Köberle and J. A. Swieca, *Phys. Lett.* **B86** (1979) 209.
- [61] A. E. Arinshtein, V. A. Fateev and A. B. Zamolodchikov, *Phys. Lett.* **B87** (1979) 389.
- [62] E. K. Sklyanin, *Nucl. Phys.* **B326** (1989) 719.
- [63] C. J. Goebel, *Prog. Theor. Phys. Suppl.* **86** (1986) 261.
- [64] S. Coleman, *Aspects of Symmetry*, (Cambridge University Press 1985).
- [65] S. Coleman, *Phys. Rev.* **D11** (1975) 2088.
- [66] S. Coleman and H. Thun, *Comm. Math. Phys.* **61** (1978) 31.
- [67] S. Coleman and R. Norton, *Nuovo Cimento* **38** (1965) 438.
- [68] R. Brunskill and A. Clifton-Taylor, *English Brickwork* (Hyperion 1977).
- [69] E. Corrigan, private communication.
- [70] A. B. Zamolodchikov, "Thermodynamic Bethe Ansatz in Relativistic Models. Scaling 3-state Potts and Lee-Yang Models", Moscow ITEP preprint (1989).
- [71] D. Amit, Y. Goldschmidt and G. Grinstein, *J. Phys.* **A13** (1980) 585.
- [72] M. Grisaru, A. Lerda, S. Penati and D. Zanon, "Renormalization Group Flows in Generalized Toda Field Theories", MIT preprint CTP #1850 (1990).
- [73] A. B. Zamolodchikov, Talk given in Oxford, January 1989.

